INITIALIZATION OF A 5-LEVEL GLOBAL ATMOSPHERIC GENERAL CIRCULATION MODEL USING A STAGGERED, SPHERICAL SPHERICAL, SIGMA COORDINATE SYSTEM

James Michael McCullough

Naval Postgraduate School
Monterey, California

March 1974

SECURITY CLASSIFICATION OF THIS PAGE (When Data Entered)

REPORT DOCUMENTATION PAGE

READ INSTRUCTIONS BEFORE COMPLETING FORM

1. REPORT NUMBER	2. GOVT ACCESSION NO.	3. RECIPIENT'S CATALOG NUMBER
		AD 776 321

4. TITLE (and Subtitle)
Initialization of a 5-Level Global Atmospheric General Circulation Model Using a Staggered, Spherical, Sigma Coordinate System

5. TYPE OF REPORT & PERIOD COVERED
Master's Thesis; March 1974

6. PERFORMING ORG. REPORT NUMBER

7. AUTHOR(s)
James Michael McCollough

8. CONTRACT OR GRANT NUMBER(s)

9. PERFORMING ORGANIZATION NAME AND ADDRESS
Naval Postgraduate School
Monterey, California 93940

10. PROGRAM ELEMENT, PROJECT, TASK AREA & WORK UNIT NUMBERS

11. CONTROLLING OFFICE NAME AND ADDRESS
Naval Postgraduate School
Monterey, California 93940

12. REPORT DATE
March 1974

13. NUMBER OF PAGES
99

14. MONITORING AGENCY NAME & ADDRESS(if different from Controlling Office)
Naval Postgraduate School
Monterey, California 93940

15. SECURITY CLASS. (of this report)
Unclassified

15a. DECLASSIFICATION/DOWNGRADING SCHEDULE

16. DISTRIBUTION STATEMENT (of this Report)
Approved for public release; distribution unlimited.

17. DISTRIBUTION STATEMENT (of the abstract entered in Block 20, if different from Report)

18. SUPPLEMENTARY NOTES

19. KEY WORDS (Continue on reverse side if necessary and identify by block number)

Numerical	Staggered Grid	Initialization
Atmospheric	Spherical Coordinates	Balance Equation
Global	Sigma Coordinate System	
Baroclinic	Primitive Equation	

20. ABSTRACT (Continue on reverse side if necessary and identify by block number)

Initialization of a five-level global baroclinic primitive equation model was examined using real data. Experiments were conducted using a Robert (1965) time frequency filter, Euler backward time integration, and an iterative initialization scheme to determine the effect of each on the generation of inertial-gravity waves resulting from an improper balance between initial mass and wind fields. In addition, a global

DD FORM 1 JAN 73 1473 EDITION OF 1 NOV 65 IS OBSOLETE
S/N 0102-014-6601

1a

SECURITY CLASSIFICATION OF THIS PAGE (When Data Entered)

(20. ABSTRACT continued)

sigma-surface linear balance equation solution was examined for the purpose of determining initial winds. Although all forecast fields were meteorological, certain undesirable features were generated in the polar and equatorial regions.

Initialization of a 5-Level Global Atmospheric General Circulation Model Using a Staggered, Spherical, Sigma Coordinate System

by

James Michael McCollough
Lieutenant, United States Navy
A.B., Indiana University, 1967

Submitted in partial fulfillment of the requirements for the degree of

MASTER OF SCIENCE IN METEOROLOGY

from the

NAVAL POSTGRADUATE SCHOOL
March 1974

Author James M. McCollough

Approved by: G. J. Haltiner
Thesis Advisor

G. J. Haltiner
Chairman, Department of Meteorology

Academic Dean

ABSTRACT

Initialization of a five-level global baroclinic primitive equation model was examined using real data. Experiments were conducted using a Robert (1965) time frequency filter, Euler backward time integration, and an iterative initialization scheme to determine the effect of each on the generation of inertial-gravity waves resulting from an improper balance between initial mass and wind fields. In addition, a global sigma-surface linear balance equation solution was examined for the purpose of determining initial winds. Although all forecast fields were meteorological, certain undesirable features were generated in the polar and equatorial regions.

TABLE OF CONTENTS

LIST OF CHARTS

LIST OF FIGURES

LIST OF SYMBOLS AND ABBREVIATIONS

A	- Constant in the sigma coordinate linear balance equation
B	- Constant in the sigma coordinate linear balance equation
a	- Earth's radius
C_P	- Specific heat for dry air at constant pressure
D	- Lateral diffusion for the quantity indicated by the subscript
D_T	- Lateral diffusion of heat
D_q	- Lateral diffusion of specific humidity
D_m	- Lateral diffusion of momentum
FNWC	- Fleet Numerical Weather Central
$\vec{F}$	- Frictional stress
f	- Coriolis parameter
H	- Diabatic heating
i	- Grid index in the x-direction (east-west)
j	- Grid index in the y-direction (north-south)
mb	- Millibars
NPS	- Naval Postgraduate School
P	- Pressure
Q	- Moisture source/sink term
q	- Specific humidity
R	- Specific gas constant for dry air
t	- Time
T	- Temperature
u	- Zonal wind
v	- Meridional wind

$\vec{V}$ - Horizontal vector velocity - (u,v)

w - Measure of vertical velocity, positive upward
$w = -\dot{\sigma} = -d\sigma/dt$

Δt - Time increment

Δx - Distance increment in the x-direction
$a \Delta\lambda \cos\theta$

α - Specific volume

α - Robert time frequency parameter

δ_m - Phase angle for wave number m

θ - Latitude, positive northward from south pole

$\Delta\theta$ - Distance increment in the latitudinal direction

λ - Longitude, positive eastward from Greenwich

π - Terrain pressure parameter

σ - Dimensionless vertical coordinate, $0 \leq \sigma \leq 1$, increasing downward

$\dot{\sigma}$ - Measure of vertical velocity - $\frac{d\sigma}{dt}$, -w

ϕ - Geopotential

ψ - Stream function

∇ - Del operator (horizontal)

∇^2 - Laplacian operator (horizontal)

ACKNOWLEDGEMENTS

The author wishes to express his thanks to Dr. G. J. Haltiner for his encouragement and guidance throughout this project, and to Lt. W. T. Elias of FNWC for his assistance with the prediction model and balance equation programs.

In addition, the author wishes to express his appreciation to the staff of the W. R. Church Computer Center at the Naval Postgraduate School for their assistance in the completion of this project.

I. INTRODUCTION

The proposed FNWC five-level, global, weather prediction model using a spherical, staggered, sigma coordinate system is currently under development at FNWC to augment or replace FNWC Northern Hemispheric model on an operational basis. The model was converted to operate on the IBM 360 at the W. R. Church Computer Center for continued student and faculty research at the Naval Postgraduate School.

The purpose of this particular study was to examine various schemes for initialization of the model using real data from FNWC objective analyses. A previous study by Elias (1973) and a current study by Mihok (1974) utilized analytically derived fields to examine the model characteristics. The use of real data permitted real, operational type problems to be present and examined in the model initialization.

The objective was to determine the best method of controlling inertial-gravity waves generated by the initial imbalance between the mass and wind fields with the aim of improving the model in the early stages of a forecast. These spurious disturbances normally diminish due to the "geostrophic adjustment" mechanism inherent in the model so that the 24-hour forecasts and longer are not seriously affected. However, as satellite data, which are essentially continuous in time, are increasingly used on a regular basis between synoptic times to update numerical predictions, it

will be highly desirable to suppress this inertial-gravity "noise" resulting from the introduction of new data.

A procedure was developed to obtain initial balanced wind fields on sigma surfaces for comparison with the balanced winds on pressure surfaces.

In addition, tests were made with various combinations of the Robert time frequency filter, periodic usage of an Euler backward time step, the sigma-surface balanced winds, and a dynamic balancing scheme suggested by Temperton (1973) in order to determine the best method of controlling the initial trauma.

II. BAROCLINIC PRIMITIVE EQUATION MODEL

The governing equations in the model (Elias, 1973) are given below. These equations are similar to those used by Smagorinsky, et al. (1965), Arakawa, et al. (1969) and Kesel and Winninghoff (1972). A brief description of the physics of the model may be found in detailed form in Kesel and Winninghoff (1972). Mihok (1974) lists a complete set of finite difference equations in spherical form used in the current model. Appendix A contains the finite difference forms of the sigma coordinate linear balance equation, the vector form is given below.

A. PRIMITIVE EQUATIONS

The vector form of the equations of motion in the sigma coordinate system are as follows:

Momentum equation

$$\frac{\partial}{\partial t}(\pi\vec{V}) + (\nabla\cdot\pi\vec{V})\vec{V} + \pi\frac{\partial}{\partial\sigma}(\dot{\sigma}\vec{V}) + f(\vec{K}X\pi\vec{V}) + \pi\nabla\phi + \sigma\pi\alpha\nabla\pi = \vec{F} + \vec{D}_m$$

Thermodynamic equation

$$\frac{\partial}{\partial t}(\pi T) + \nabla\cdot(\pi T\vec{V}) + \pi\frac{\partial}{\partial\sigma}(T\dot{\sigma}) - \frac{\pi\alpha}{C_p}(\sigma\frac{\partial\pi}{\partial t} + \sigma\vec{V}\nabla\pi + \pi\dot{\sigma}) = \pi H + D_T$$

Mass continuity equation

$$\frac{\partial \pi}{\partial t} + \nabla \cdot (\pi \vec{V}) + \pi \frac{\partial \dot{\sigma}}{\partial \sigma} = 0$$

Moisture continuity equation

$$\frac{\partial}{\partial t}(\pi q) + \nabla \cdot (\pi q \vec{V}) + \pi \frac{\partial}{\partial \sigma}(q \dot{\sigma}) = \pi Q + D_q$$

Hydrostatic equation

$$\frac{\partial \phi}{\partial \sigma} + \pi \alpha = 0$$

Equation of state

$$\alpha P = RT$$

The vertical coordinate sigma (σ) is related to pressure (P) and surface pressure (π) by the equation

$$\sigma = P/\pi$$

The terms and symbols are identical to those used in Kesel and Winninghoff (1972). A List of Symbols and Abbreviations appears on page 6 of this paper.

B. GRID

The grid used by the model is a staggered, spherical, five-degree, latitude-longitude grid. Mass variables

(ϕ, T, q, w) are carried at 10-degree intervals over the globe and at the poles. Motion variables (u,v) are carried at alternate 10-degree intervals over the globe. Figure 1 depicts the grid configuration.

C. VERTICAL LAYERS

Figure 2 depicts the five layers vertically distributed in the model and the variables associated with each layer. Specific humidity (q) is carried in only the three lowest layers, at the .9, .7, and .5 sigma levels. The remaining variables u, v, T, and ϕ are carried at the .9, .7, .5, .3, and .1 sigma levels. The vertical motion variable, w, is calculated diagnostically from the continuity equation at layer interfaces, the .8, .6, .4, and .2 sigma levels.

D. TIME DIFFERENCING

The two basic difference schemes followed are the centered difference scheme (leapfrog) and the Euler backward difference scheme. The centered difference form is

$$F(t + \Delta t) = F(t - \Delta t) + 2\Delta t \frac{\partial F(t)}{\partial t}$$

Since this difference form is of higher order than that of the differential equation a computational mode exists and solution separation at even and odd time steps will develop, perhaps even leading to a type of instability (Haltiner, 1971). In addition, the leapfrog method cannot be used on the first time step.

To eliminate the solution separation and also to initiate the integration procedure the Euler backward scheme is used:

$$F^* = F(t) + \Delta t \frac{\partial F(t)}{\partial t}$$

$$F(t + \Delta t) = F(t) + \Delta t \frac{\partial F^*}{\partial t}$$

The Euler backward scheme is applied at six-hour intervals in most of the experiments conducted, however where indicated the scheme was applied more often.

A time step of ten minutes was used in all experiments. In order to insure linear computational stability (Haltiner, 1971), a much shorter time step would have to be taken in a latitude-longitude grid where for a fixed longitude increment the east-west distance between grid points decreases toward the poles. To avoid the shorter time step the model employs the Arakawa (Gates, 1971) technique of filtering or damping short waves that would lead to instability near the poles thus allowing the 10-minute time step throughout. Specifically a weighted average is taken of those longitudinal derivatives that are involved in gravity wave propagation with increasing smoothing toward the poles. This technique appears to be superior to decreasing the time step or skipping grid points toward the poles.

The heating package is called every six time steps while lateral diffusion, friction, convective adjustment, convective

condensation, and large scale condensation are computed every time step.

III. INITIALIZATION

A. DATA INPUT

The real data used in the experiments was provided on magnetic tape by FNWC from objective analyses on the Northern Hemisphere 63 x 63 point grid.

The model interpolates the 63 x 63 data to a latitude-longitude grid of five-degree intersections in the Northern Hemisphere. The grid interpolation values are then reflected in the Southern Hemisphere to allow the model to integrate over the globe. FNWC is currently converting the model to read data directly on the global latitude-longitude grid with real input to the Southern Hemisphere.

In all tests data consisted of 12 constant-pressure level temperature analyses, 10 height analyses, 4 moisture analyses, sea-level pressure and sea-surface temperature analyses. The date of the data for the experiments is 12 Z 10 May 1972.

The terrain height provided to the model is an unsmoothed "gross" terrain. In addition the interpolation to the latitude-longitude grid yields an unrealistic height for the interpolated grid point. The conversion to global input should eliminate this problem.

B. LINEAR BALANCE ON PRESSURE SURFACES

The stream function field is derived from the solution to the linear balance equation

$$\nabla^2\psi = -\frac{1}{f}\nabla\psi\cdot\nabla f + \frac{1}{f}\nabla^2\phi \qquad (1)$$

using height values horizontally interpolated from the polar stereographic 63 x 63 grid to the spherical grid. Equation (1) was solved using the over-relaxation, iterative technique (Haltiner, 1971) with a modified coriolis parameter in the equatorial region. The wind fields were then derived from the computed stream function field as follows:

$$u = -\frac{1}{a}\frac{\partial\psi}{\partial\theta} \qquad (2)$$

$$v = \frac{1}{a\cos\theta}\frac{\partial\psi}{\partial\lambda} \qquad (3)$$

After the u and v components have been computed on the pressure surface spherical coordinate system, the components are then interpolated vertically to the sigma coordinate system through a logarithmic interpolation scheme. The u and v wind fields are then reflected to the Southern Hemisphere.

C. LINEAR BALANCE ON SIGMA SURFACES

Sundquist (1973) stated that the interpolation process described in the previous section by the very process of interpolation further stimulates the inertial-gravity oscillations in the early stages of the integration. By

balancing the mass and stream function fields directly on the model sigma surfaces inertial-gravity waves were suppressed (Sundquist, 1973). The non-linear balance equation (Sundquist, 1973) is:

$$\nabla\cdot(f\nabla\psi) - \{\frac{\partial}{\partial x}[\frac{\partial\psi}{\partial y}\frac{\partial}{\partial x}(\frac{1}{\pi}\frac{\partial\psi}{\partial y}) - \frac{\partial\psi}{\partial x}\frac{\partial}{\partial y}(\frac{1}{\pi}\frac{\partial\psi}{\partial y})]$$

$$+ \frac{\partial}{\partial y}[\frac{\partial\psi}{\partial x}\frac{\partial}{\partial y}(\frac{1}{\pi}\frac{\partial\psi}{\partial x}) - \frac{\partial\psi}{\partial y}\frac{\partial}{\partial x}(\frac{1}{\pi}\frac{\partial\psi}{\partial x})]$$

$$= \nabla\cdot[\pi\nabla\phi + RT\nabla\pi] \qquad (4)$$

Due to time limitations the complete balance equation was not tested; however the following linear form was solved over the entire globe:

$$f\nabla^2\psi + (\nabla\psi\cdot\nabla f) = \pi\nabla^2\phi + \nabla\pi\cdot\nabla\phi + R[T\nabla^2\pi + \nabla T\cdot\nabla\pi] \qquad (5)$$

The finite difference form of this equation is given in Appendix A. The Fortran program used to solve Equation (5) is on page 85.

The correct value of the coriolis parameter was used everywhere except in the equatorial region where two alternatives were tested to obtain convergence of the relaxation scheme. The initial guess for the ψ field was made with the coriolis parameter held constant from 10 degrees, in one case and 20 degrees in the other case, to the equator in both hemispheres. Elsewhere the correct value of the

coriolis parameter was used at both north and south latitudes, initially and during relaxation. This scheme yielded a positive stream function in Northern Hemisphere and a negative function in the Southern Hemisphere. During relaxation the value of ψ at the equator was obtained by averaging the values at 5N and 5S.

D. TIME FREQUENCY FILTER

The Robert (1965) time-frequency filter incorporated into the model utilizes the following averaging operator:

$$F(t)^* = F(t) + \alpha[F(t-1) + F(t+1) - 2F(t)] \quad (6)$$

where α is the filter parameter, t is time and F is the field being filtered. Different values of α were tested ranging from 0 (no filtering) to .5 (maximum filtering).

This filter tends to damp the inertial-gravity waves arising from the imbalance between the mass and wind fields, especially $2\Delta t$ periods, and also essentially eliminates solution decoupling (Robert, 1965).

E. ITERATIVE AVERAGING OF WIND COMPONENTS

An iterative scheme of averaging the u and v components of the wind field derived from both a forward and a backward integration of the model for specified periods of time such as 1, 3, and 6 hours was developed. The components derived from each set of forward and backward integrations were separately averaged to constitute new initial winds to begin

the integration from time zero. On the other hand, the mass and temperature fields were restored to their original values at time zero. This procedure was repeated two to six times.

The backward integration used a ten minute time step. Due to the non-reversibility of the heating routine, diabatic heating was not incorporated in the backward integration.

Winninghoff (1971) and Temperton (1973) have shown this type of procedure is quite effective in removing the imbalance between the initial mass and wind fields. The process, as they applied it, is too time consumming, however, when considered from an operational point of view.

IV. RESULTS

Eight experiments will be presented in this section. The first three experiments were performed to determine what filter parameter value would be used in subsequent experiments and how often the Euler backward time step would be used. Experiment IV consisted of two 12-hour forecasts using an iteration initialization scheme. Experiments V and VI involved a comparison of winds derived from a sigma-surface balance equation and winds derived from a pressure-surface balance equation both without terrain. Experiment VII introduced terrain into the sigma-surface balance scheme. Experiment VIII consisted of an 84-hour forecast using a filter parameter of 0.4.

In certain indicated experiments plots of terrain pressure versus forecast time for 12 hours were made at three latitudes, 20 N, 40 N, and 80 N on 110 E longitude. The small amplitude waves depicted are a reflection of the inertial-gravity waves generated by the lack of a proper balance between the mass and wind fields. As a consequence of the "geostrophic adjustment" mechanism inherent in the model the waves gradually tend to diminish. The degree of time smoothing has a noticeable effect on these initial oscillations. In addition, the iteration initialization scheme also has a damping effect on the initial oscillations, particularly on the longer periods. Although the initial

winds obtained from the sigma-surface linear balance equation were expected to help damp initial inertial-gravity wave oscillations, the results do not demonstrate the damping.

Chart A depicts the surface pressure objective analysis from FNWC magnetic tape used as initial input for the model. Chart B is also of the initial surface pressure but is a result of the model interpolating from the Northern Hemisphere 63 x 63 grid to the latitude-longitude grid and back to the 63 x 63. Some original detail in the surface pressure field is lost in the process.

1. Experiment I

Four 12-hour forecasts were made, each forecast using a different filter parameter. The Euler backward time step was used once every six hours in each case. The forecast surface pressure fields resulting from use of filter parameter values of 0.0, 0.3, 0.4, and 0.5 can be found on Charts C-F, respectively. Figures 3-5 show four curves per figure, each curve a plot of terrain pressure from each of the forecasts versus forecast time for the three latitude grid points previously mentioned. Curve 1 in each figure demonstrates the unfiltered case and, as a consequence, the most oscillations. Filtering very effectively damps short period oscillations, as is evident from Curves 2, 3, and 4 in each figure. In Figure 5, the terrain pressure at 80N tends to increase as the filtering is increased. A value

of $\alpha = 0.4$ was selected as a reasonable compromise with respect to limiting the rise of pressure at the poles and still accomplishing a significant damping of the inertial-gravity noise.

2. Experiment II

Three 12-hour forecasts were produced in this experiment using the Euler backward time step at 1, 2, and 3 hour intervals. The forecast surface pressure fields are depicted on Charts G-I. In addition Chart C depicts the surface-pressure forecast using the Euler backward time step every six hours. In this experiment the filter parameter α was set to zero so that no filtering was performed. Figures 6-8 show the terrain pressure versus forecast time for each forecast at the three latitudes selected. Curve 1 in each figure represents the case where $\alpha = 0.0$ and the Euler backward is used once every six hours. Curves 2, 3, and 4 represent the Euler step being used every one, two, and three hours, respectively. Although very short period oscillations are damped, the longer period oscillations that were significantly damped by the time frequency filter are not appreciably affected.

3. Experiment III

Combinations of a filter value $\alpha = 0.4$ and the Euler backward time step every one hour and every six hours were used to produce 12-hour forecasts. Figures 9-11 depict three curves each of terrain pressure versus forecast time; Curve 1 representing $\alpha = 0.4$ and 1 hour use of the

Euler step while Curve 2 represents $\alpha = 0.4$ and 6 hour use of the step. Curve 3 was added for comparison and represents $\alpha = 0.0$ or no filtering and the Euler backward time step used once every six hours. As can be readily seen at all three latitudes, increasing the use of the Euler backward time step does not appreciably alter the degree of damping of oscillations when used in conjunction with the filter parameter $\alpha = 0.4$.

4. Experiment IV

Two 12-hour forecasts were made utilizing an iteration initialization equivalent in model time to a 12-hour forecast. Chart J depicts the surface pressure forecast obtained using a one-hour forward/one-hour backward integration followed by averaging and repeated six times. Chart K demonstrates the surface pressure forecast obtained using the iteration scheme repeated twice for a three hour forward and three hour backward iteration. Both forecast procedures used a filter parameter of $\alpha = 0.4$ and the Euler backward time step once every six hours. Figures 12-14 show plots of terrain pressure versus forecast time, Curve 1 representing the one-hour scheme and Curve 2 the three-hour scheme. Curve 3 represents the plot obtained by using a normal non-iterative initialization with $\alpha = 0.4$ and the Euler backward step once every six hours. Both iteration schemes damp the longer period oscillations remaining after time filtering.

5. Experiment V

Initial winds derived from the linear balance equation solved on sigma surface without terrain were compared with initial winds computed on pressure surfaces. The initial winds obtained directly on sigma surfaces were used to integrate the model to seventy-nine hours. The 12-hour and 72-hour forecast surface pressure fields are shown on Charts X and Z to demonstrate the meteorological product. Chart Y depicts the 12-hour surface pressure forecast field obtained using initial winds derived from the linear balance equation solved on pressure surfaces and interpolated to sigma surfaces. Again terrain was not used in order to hopefully show similarity between the stream function fields produced.

Charts L and M show the initial stream function fields on the 0.9-sigma level and 925-mb level, respectively. Charts N and O show the final ψ fields for the two levels. Although the initial guess ψ fields are considerably different, the final fields show quite similar trough and ridge patterns. Charts P and Q show the isotach patterns for the 0.9-sigma level and 925-mb level, respectively. The magnitude of the winds on the sigma surface are 5 to 10 meters per second slower than those on the pressure surface.

Charts R-W show the same fields for the 0.5-sigma level and 500-mb level that Charts L-P did for the 0.9-sigma level and 925-mb level. Again the final ψ fields have similar trough and ridge patterns although the first guess

fields are different. Also the wind intensity on the 0.5-sigma surface is less than that on the 500-mb surface.

Figures 15-17 show two curves of terrain pressure versus forecast time for the two balance systems. Curve 1 represents the pressure case while Curve 2 represents the sigma case. In both cases $\alpha = 0.4$ was used with an Euler backward time step once every six hours.

In this particular test the initial guess for the ψ field in the sigma-surface balance program was made with a constant coriolis parameter from 10 degrees to the equator in both hemispheres. The correct coriolis value was used everywhere else, initially and during the relaxation.

At the equator where $f = 0$, the balance equation is no longer of the Poisson or Helmholtz type to which the relaxation scheme is applicable. To avoid the difficulty, the value of ψ at the equator was obtained by averaging the value at 5N and 5S during each pass in the relaxation scheme.

6. Experiment VI

Another initial guess for the stream function in the sigma-surface balance scheme was made in this experiment. The value of the coriolis parameters was held constant this time from 20 degrees to the equator in both hemispheres. Again, the correct coriolis parameter was used everywhere else initially and during relaxation.

The equator value of ψ was again obtained by averaging the values at 5N and 5S during the relaxation.

Chart AA depicts the .9-sigma level final stream function field. Chart BB shows the 12-hour forecast surface pressure field. Although Chart AA and N should be identical if convergence to the same solution was being accomplished, it is evident from Charts BB and X that the solution to the linear balance equation produced is sufficient to yield similar surface pressure forecasts.

7. Experiment VII

This experiment is identical in conditions to the sigma-surface balance part of Experiment V except that terrain was included. As previously stated, the terrain currently used in the model is an unsmoothed terrain. Although the introduction of terrain to a scheme that is intended to take advantage of the terrain in balancing the mass and wind fields is probably not the sole cause, the model immediately went unstable in 3 hours and a forecast was not obtained.

8. Experiment VIII

An 84-hour forecast was made with the model using a filter parameter $\alpha = 0.4$ and the Euler backward time step once every six hours. Charts CC and EE show the 72-hour and 84-hour forecast surface pressure fields and charts DD and FF show the FNWC verifying analyses. Of note are the extreme pressure gradients generated in the polar region.

VI. CONCLUSIONS

Various schemes for initializing a five-level, global, weather prediction model using a spherical, staggered, sigma coordinate system were examined in order to determine an optimum method for controlling inertial-gravity waves generated by the initial imbalance between the mass and wind fields.

The Robert (1965) time frequency filter was quite successful in damping the inertial-gravity waves, expecially the computational mode which has a period of approximately $2\Delta t$. Values of α from 0.0 to 0.5 were tried in early experiments. The value of $\alpha = 0.4$ appeared the best compromise between rising polar terrain pressure and damping and was used in subsequent experiments. Since the time frequency filter essentially eliminates solution decoupling, the need for restarting with the Euler backward time step is eliminated. It would still serve a useful purpose for the first one or two time steps. More frequent use does not seem warranted since damping due to use of the Euler scheme is minimal compared to the time frequency filter.

The iterative scheme (Temperton, 1973) of averaging the u and v components of the wind fields derived from a forward and backward integration of the model further damped the longer period oscillations already partially damped by the Robert filter.

Additional work and testing is required on the solution of the balance equation on sigma surfaces. Although convergence to the program criteria was indicated, simply changing the initial guess for the stream function field altered considerably the final field, implying that true convergence toward the correct solution was not accomplished by the program. Nevertheless the similarity between the final stream function fields produced on pressure surfaces and those produced without terrain on sigma surfaces warrants further program testing. Moreover, actual convergence of the iterative procedure to a correct solution of the balance equation may not be necessary or even desirable if several iterations will produce better initial winds than the pressure-surface balanced winds.

The inclusion of terrain in the sigma-surface balance scheme caused instability in the model very rapidly. As previously mentioned, the terrain used in the model is not smooth. Smoothing may reduce the trauma encountered with the sigma-surface balance program integration, but it is not conclusive at this time if terrain is the sole cause of instability.

Perhaps the solution of the full balance equation will reduce the inertial-gravity waves at the start of the integration as indicated by Sundquist (1973), although the linear balance version was not effective in these experiments.

The problems encountered with the linear balance equation in the equatorial regions where the coriolis parameter is negligible and pressure gradients are small could be resolved through another approach to the problem.* Using the FNWC objectively analyzed winds for the equatorial region for instance from 40S to 40N the vorticity at each grid point could be calculated using:

$$\zeta_{obs} = \frac{\partial v_{obs}}{\partial x} - \frac{\partial u_{obs}}{\partial y} + \frac{v_{obs}}{a} \tan \theta \qquad (7)$$

The stream function ψ could then be determined by solving the Poisson equation:

$$\nabla^2 \psi = \zeta_{obs} \qquad (8)$$

The calculated values of ψ, say at 20 or 30 N and S could then be used as boundary conditions to solve the non-linear balance equation for the stream function in the regions poleward of the selected latitudes from the analyzed geopotential fields in the standard manner. Continuity of the stream function between the equatorial belt and the regions poleward would be automatically satisfied. Finally, the mass field (ϕ) in the tropical belt should be obtained by solving the balance equation using the previously

---

*Haltiner, G. J., personal communication, 1973.

calculated stream function together with the objectively analyzed ϕ values at the boundaries. The u and v irrotational wind components are then derived from the final global stream function field.

The long term integration indicates a need for a review of the polar region finite differencing and the method of handling the pole points. Severe "noise" develops at the pole causing model instability at about 88 hours prognostic time.

Although it is evident that additional experimentation is desired for the purpose of removing initialization trauma, the reader should bear in mind that in these experiments the method of data input by interpolating to latitude-longitude grid points from a polar stereographic grid probably introduces further imbalance between mass and wind fields.

On the basis of these experiments a definite conclusion reached is that for the purpose of reducing inertial-gravity wave noise, a combination of the Robert time frequency filter (with $\alpha = 0.4$) and a forward and backward dynamic balancing scheme is quite effective and not overly time-consuming. Conversion to a global latitude-longitude grid data input system coupled with a full balance equation solved on sigma-surfaces may perhaps reduce the inertial trauma sufficiently to obviate the need for dynamic balancing by the Temperton (1973) method.

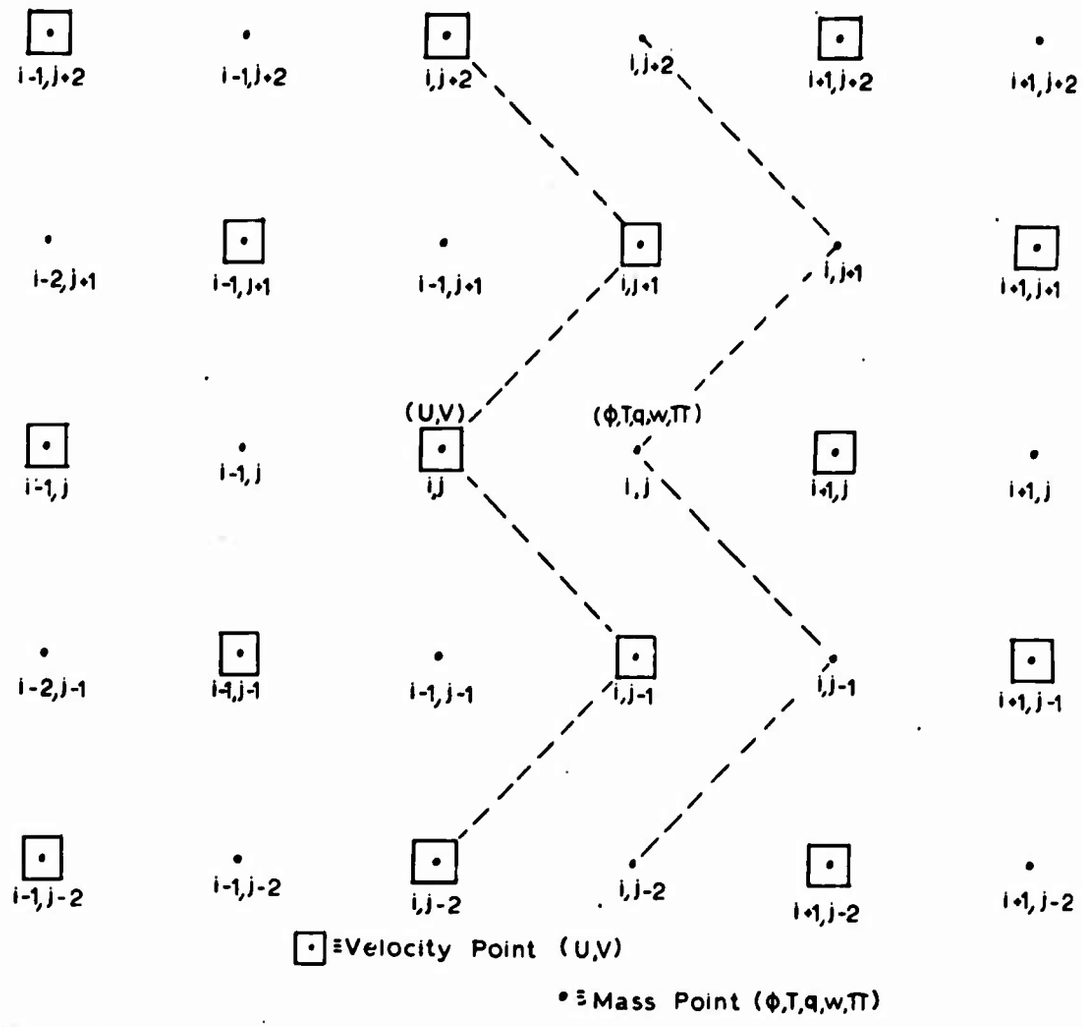

FIGURE 1. LOCATION OF VARIABLES.

i is the column counter and j is the row counter.
Point (1,1) is at 85S, 10E.

Pressure	Computed Variables (at each level)	Level (National Subscript)	Sigma (σ)
0.0	w = 0 UPPER BOUNDARY		0.0
.1 × π	u,v,T,ϕ	5	0.1
.2 × π	w	4	0.2
.3 × π	u,v,T,ϕ	4	0.3
.4 × π	w	3	0.4
.5 × π	u,v,T,ϕ,q	3	0.5
.6 × π	w	2	0.6
.7 × π	u,v,T,ϕ,q	2	0.7
.8 × π	w	1	0.8
.9 × π	u,v,T,ϕ,q	1	0.9
π	w = 0 LOWER BOUNDARY		1.0

FIGURE 2. VERTICAL LAYERING

In the above figure, sigma (σ) is the dimensionless vertical coordinate, u and v are the zonal and meridional wind components, respectively, q is the specific humidity, ϕ is the geopotential, π is the terrain pressure and w is the vertical velocity ($-\dot{\sigma}$).

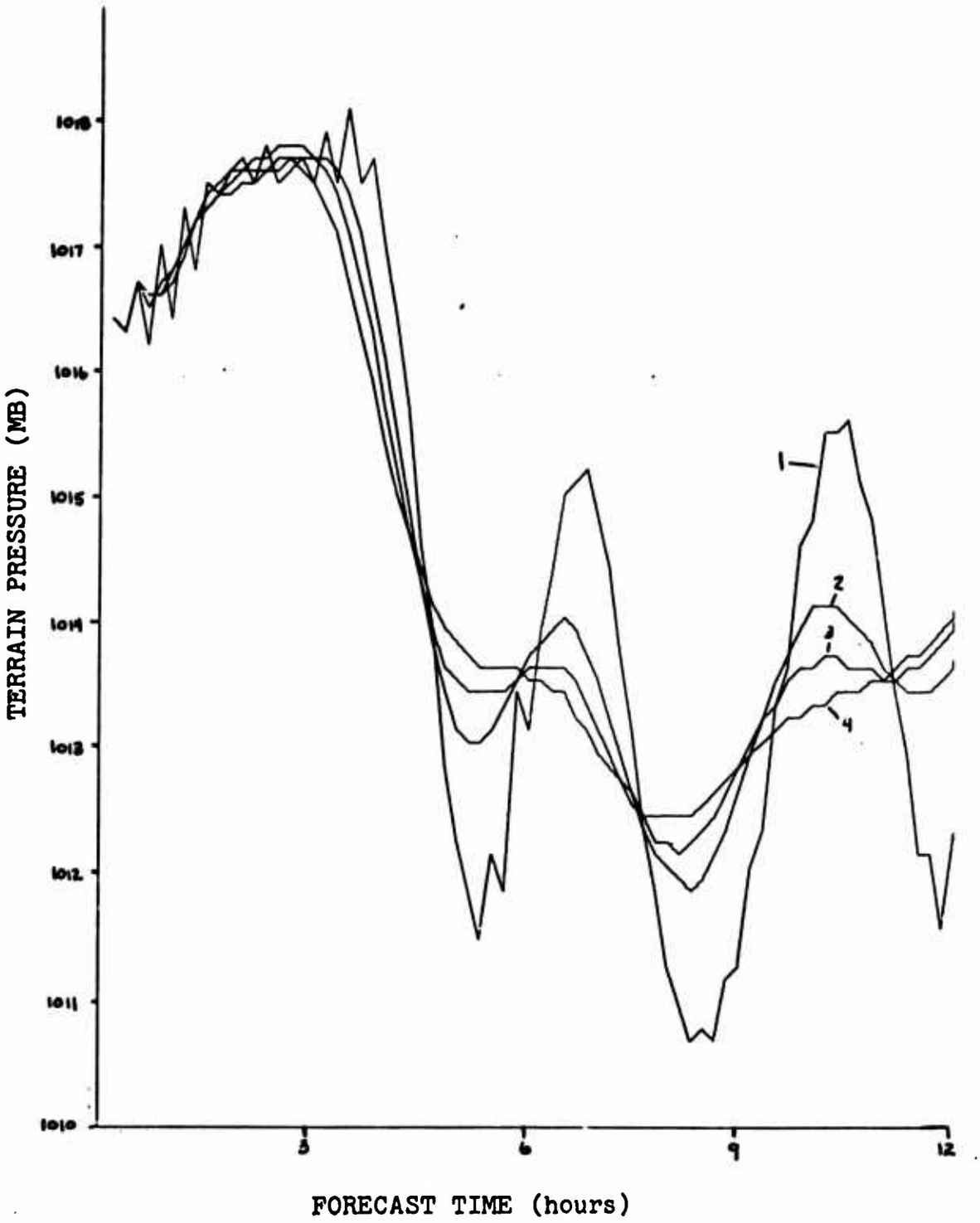

FIGURE 3. Plot of Terrain Pressure Versus Forecast Minute at 20N 110E (Experiment I).

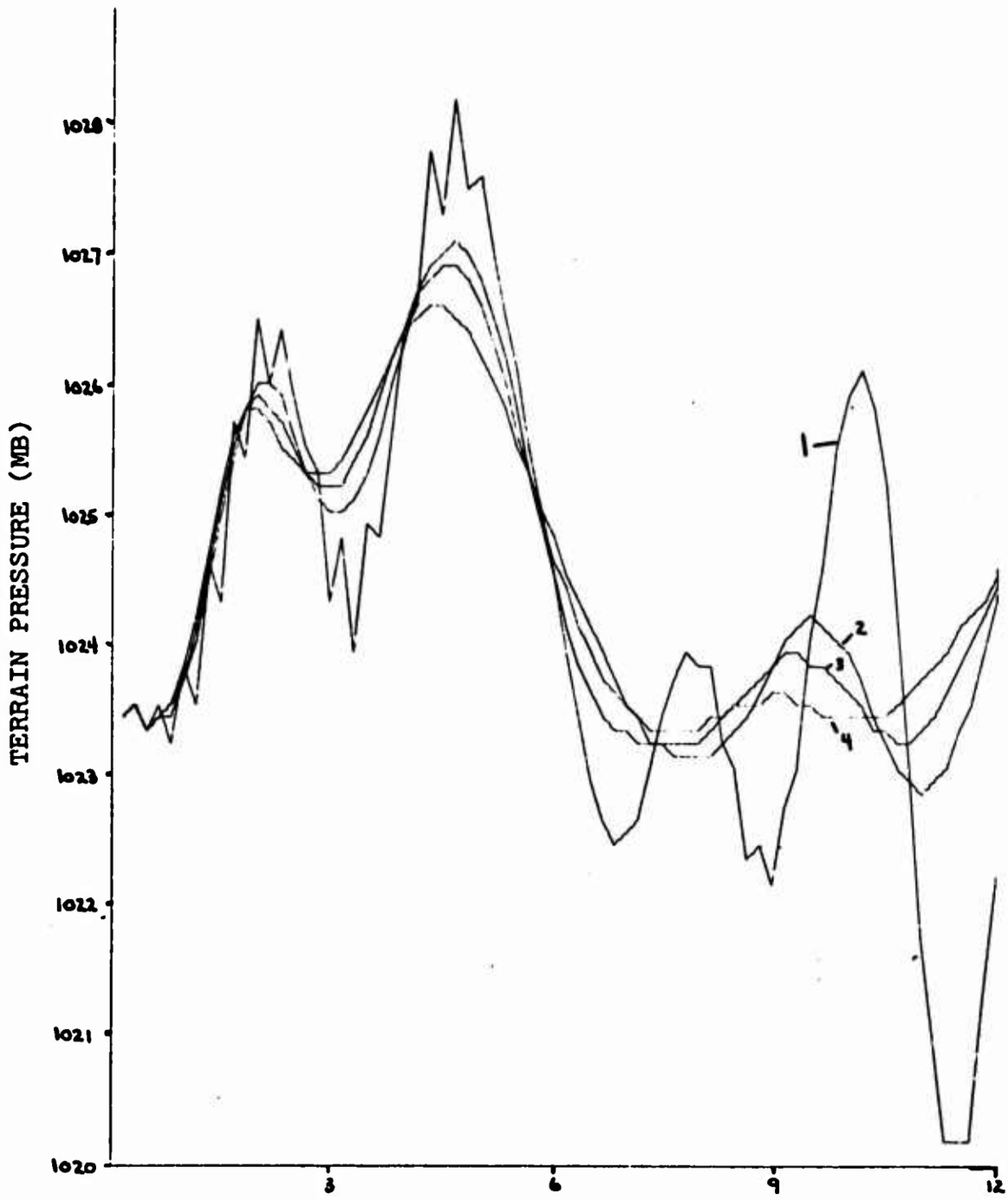

FIGURE 4. Plot of Terrain Pressure Versus Forecast Minute at 40N 110E (Experiment I)

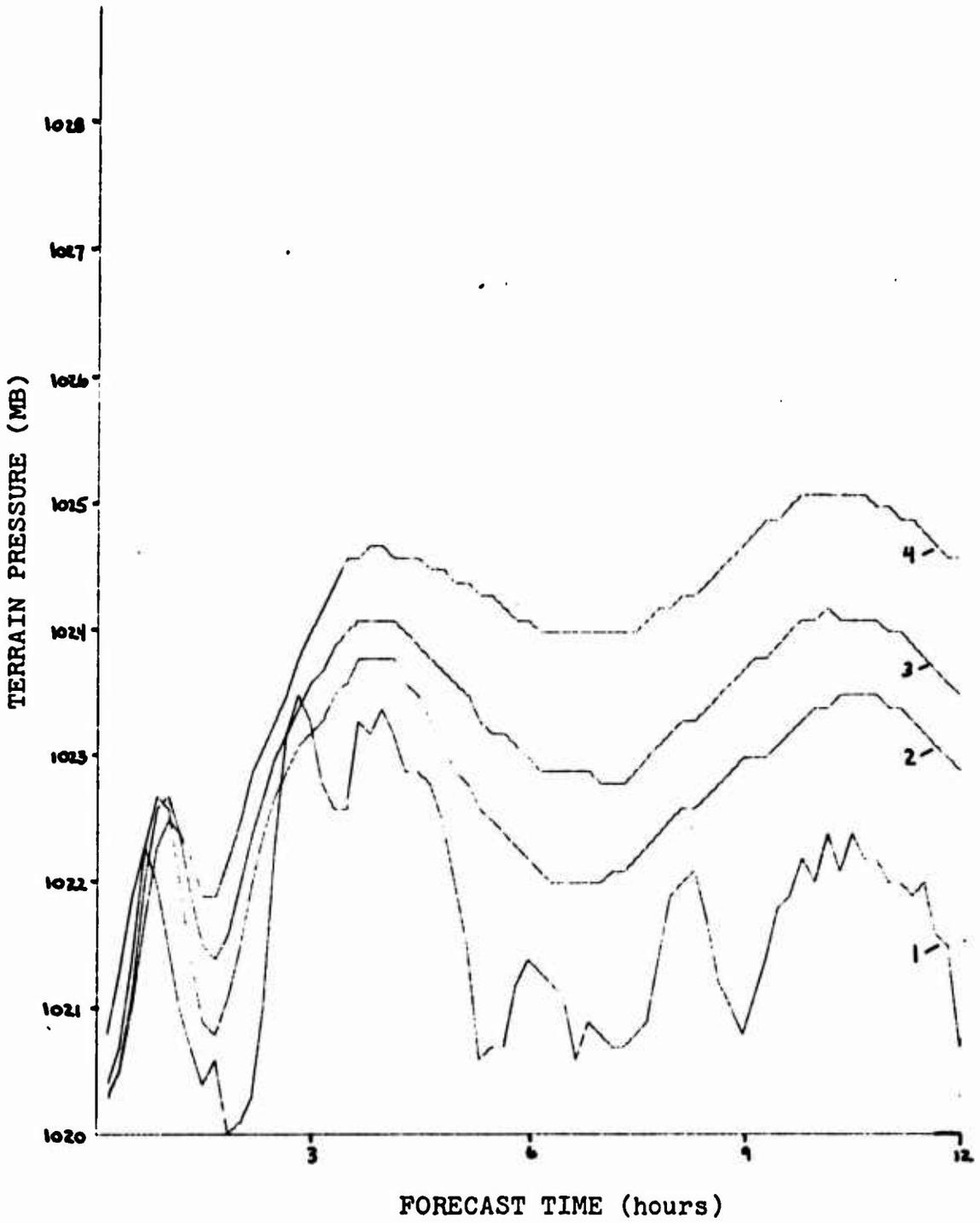

FIGURE 5. Plot of Terrain Pressure Versus Forecast Minute at 80N 110E (Experiment I)

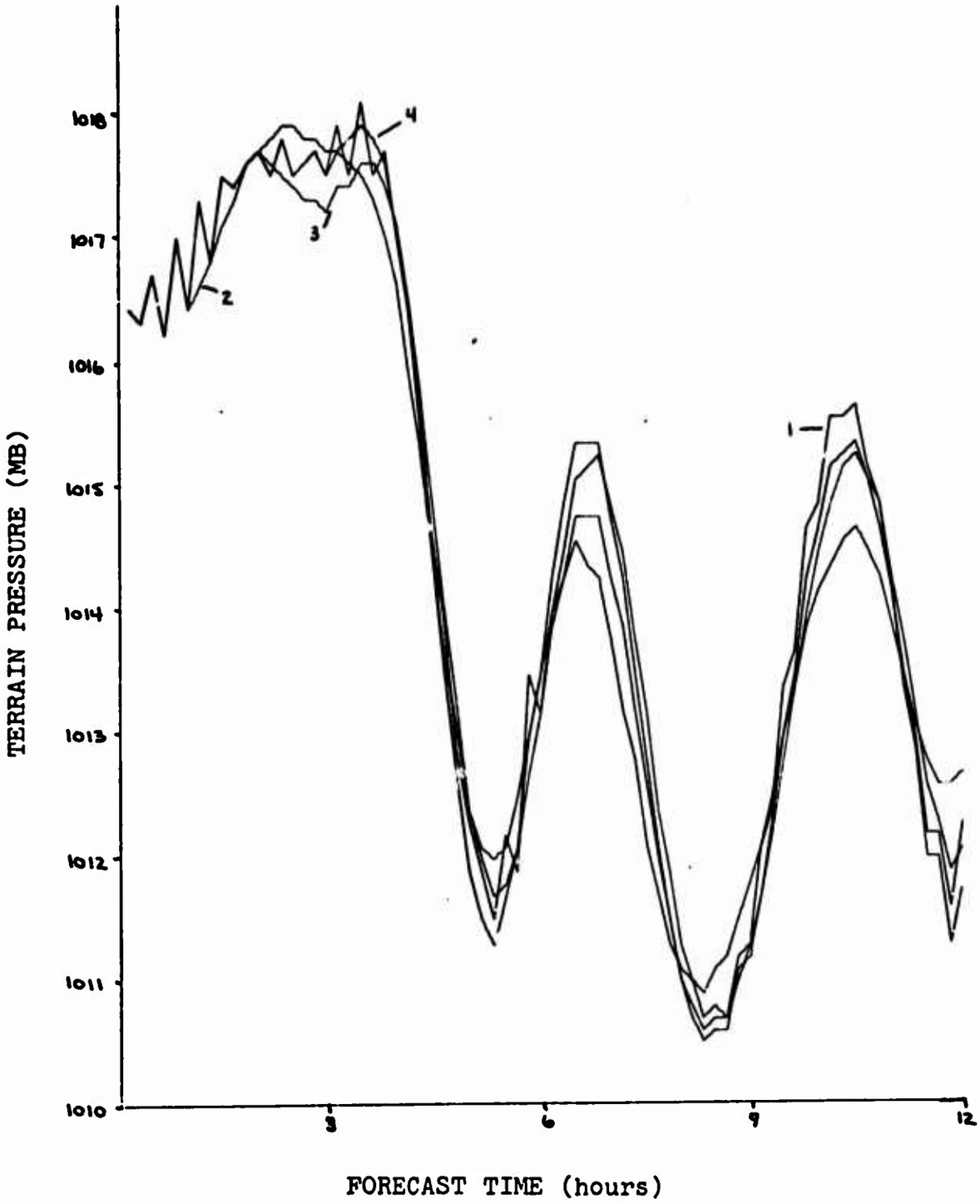

FIGURE 6. Plot of Terrain Pressure Versus Forecast Minute at 20N 110E (Experiment II)

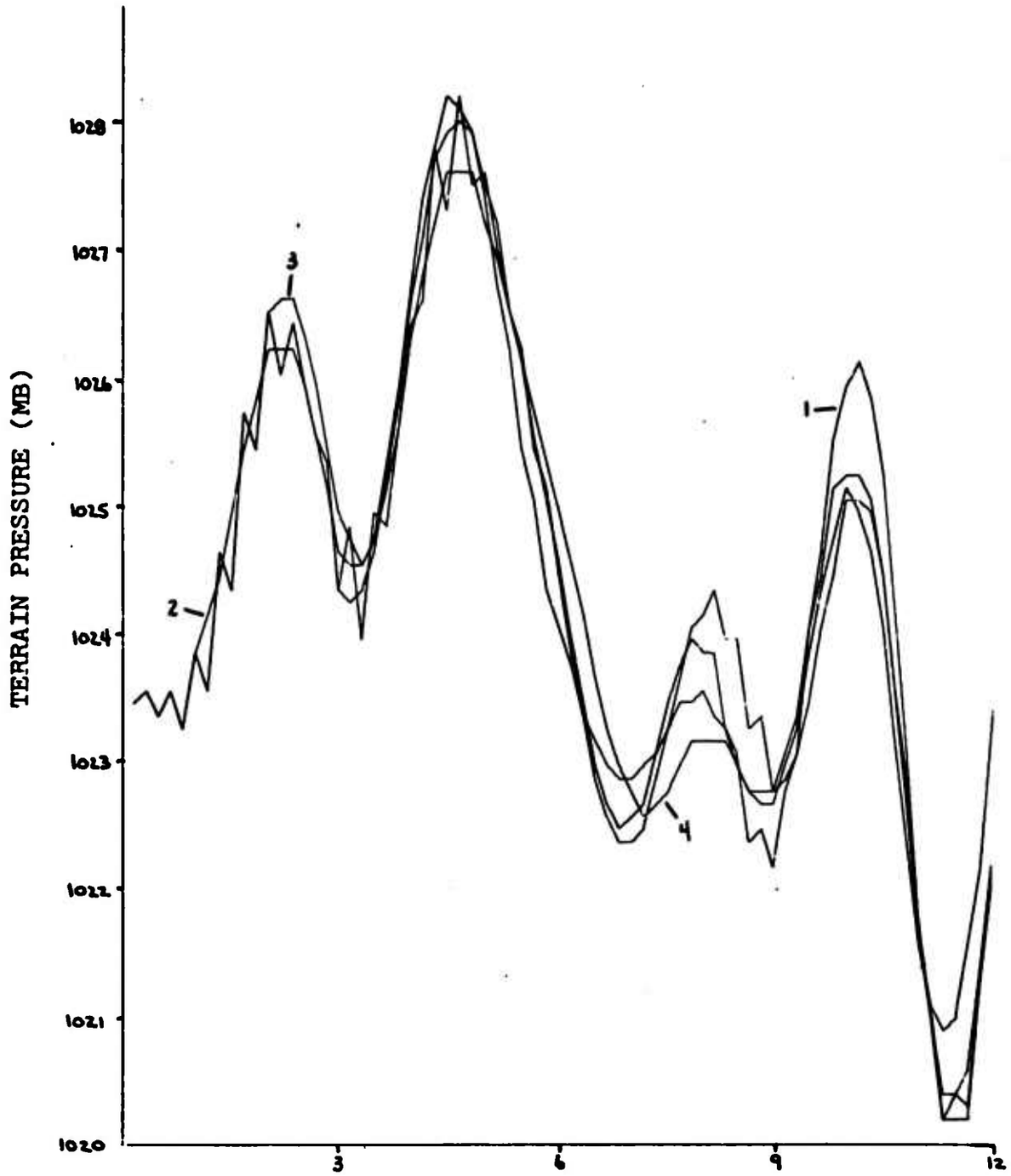

FIGURE 7. Plot of Terrain Pressure Versus Forecast Minute at 40N 110E (Experiment II)

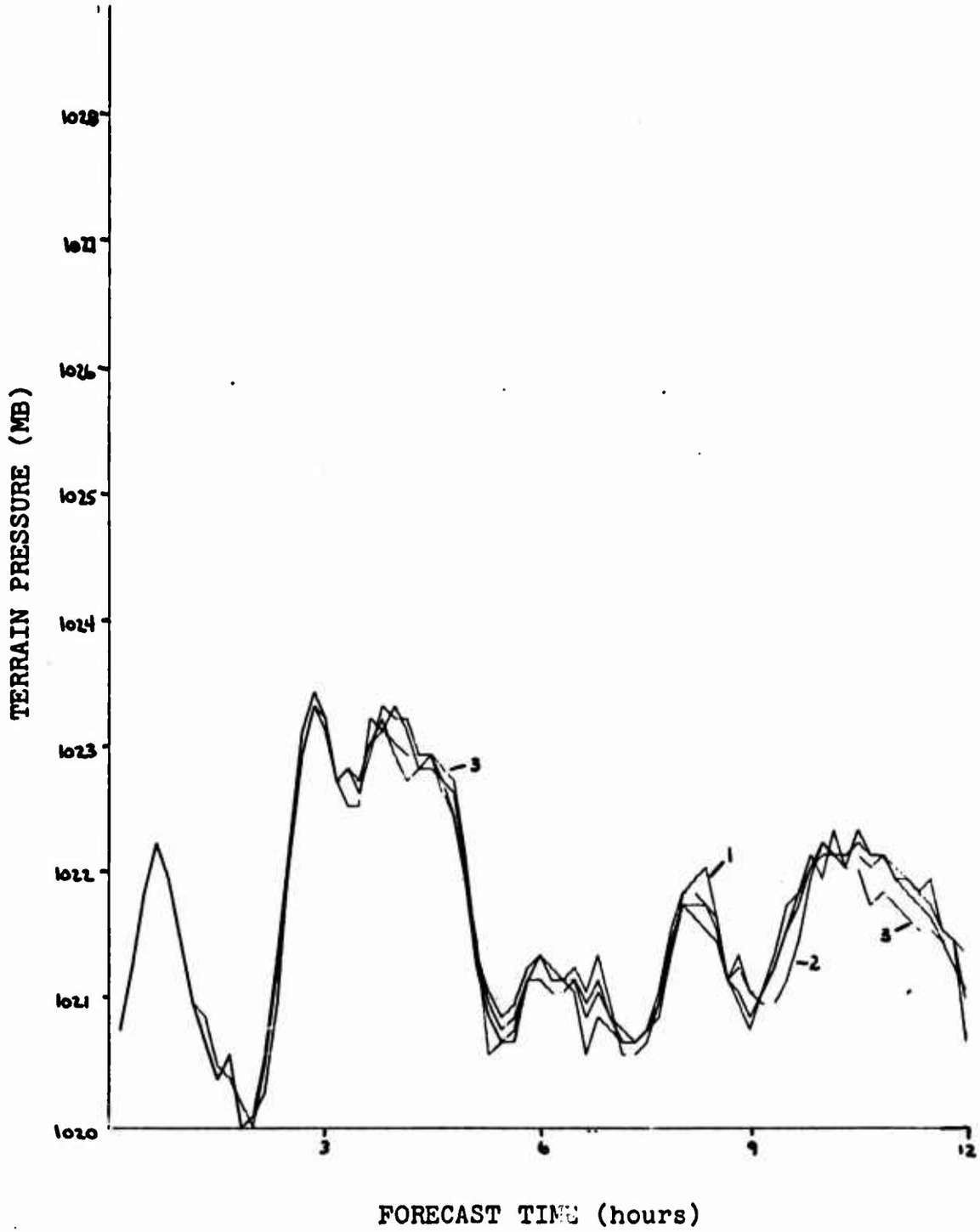

FIGURE 8. Plot of Terrain Pressure Versus Forecast Minute at 80N 110E (Experiment II)

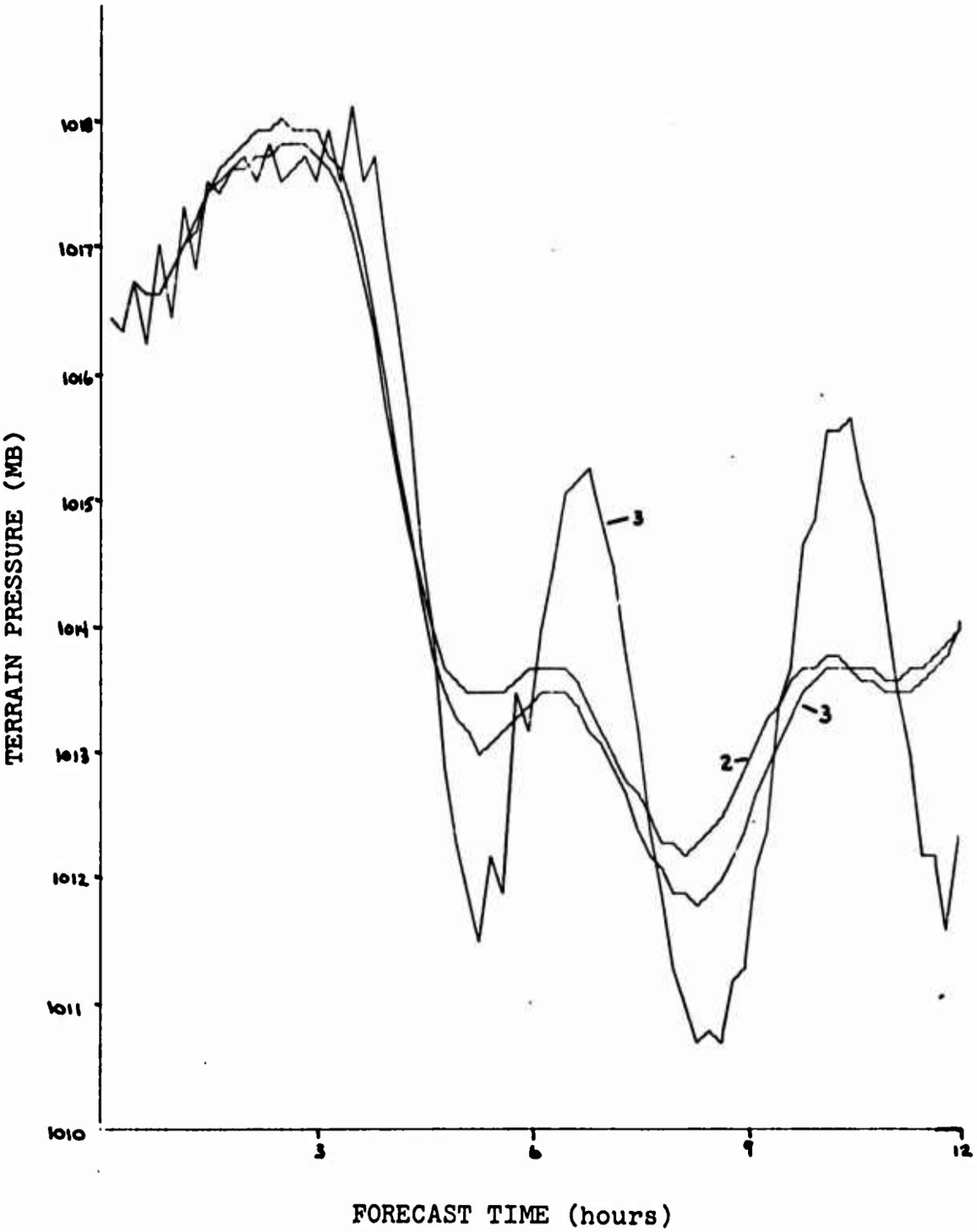

FIGURE 9. Plot of Terrain Pressure Versus Forecast Minute at 20N 110E (Experiment III).

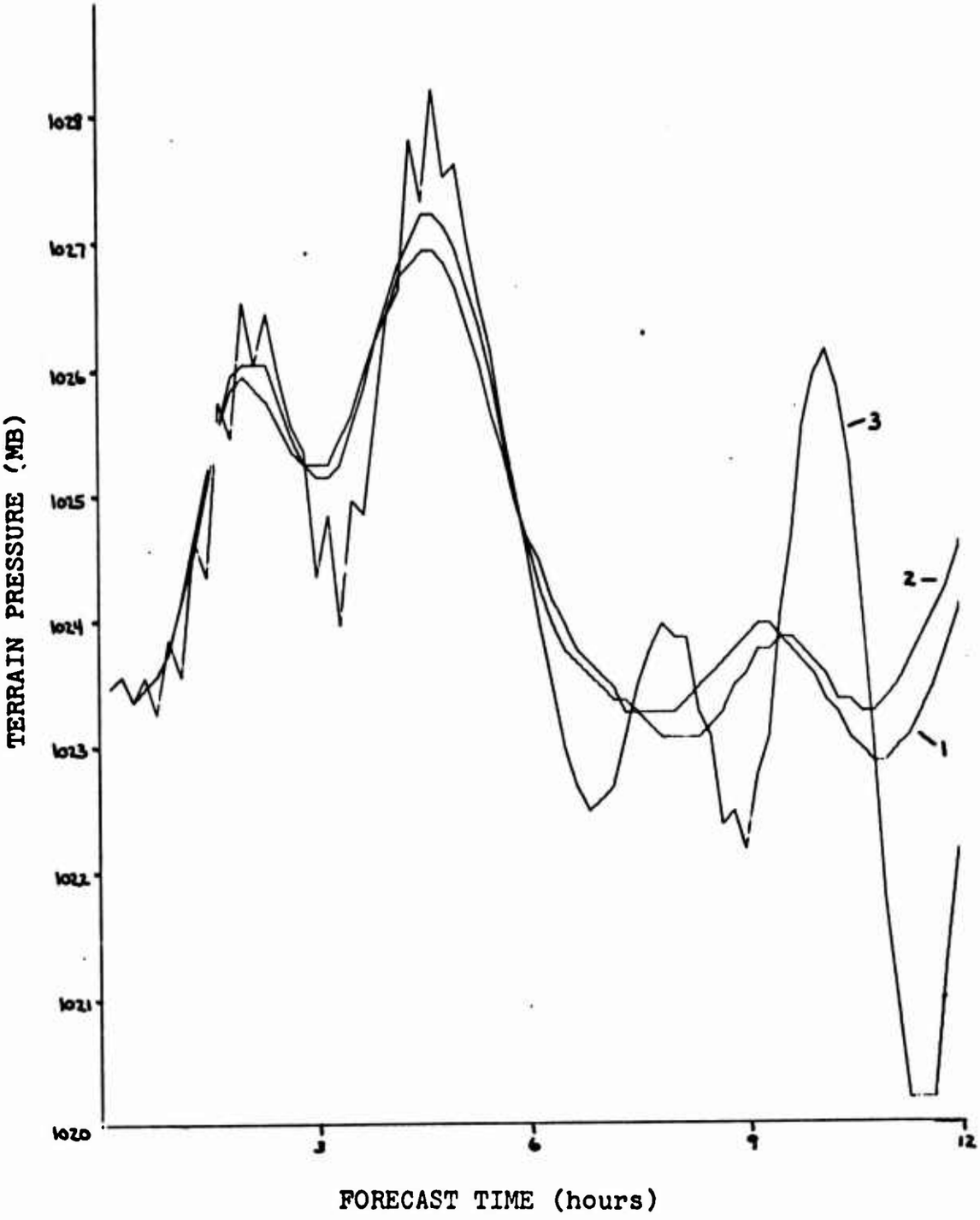

FIGURE 10. Plot of Terrain Pressure Versus Forecast Minute at 40N 110E (Experiment III)

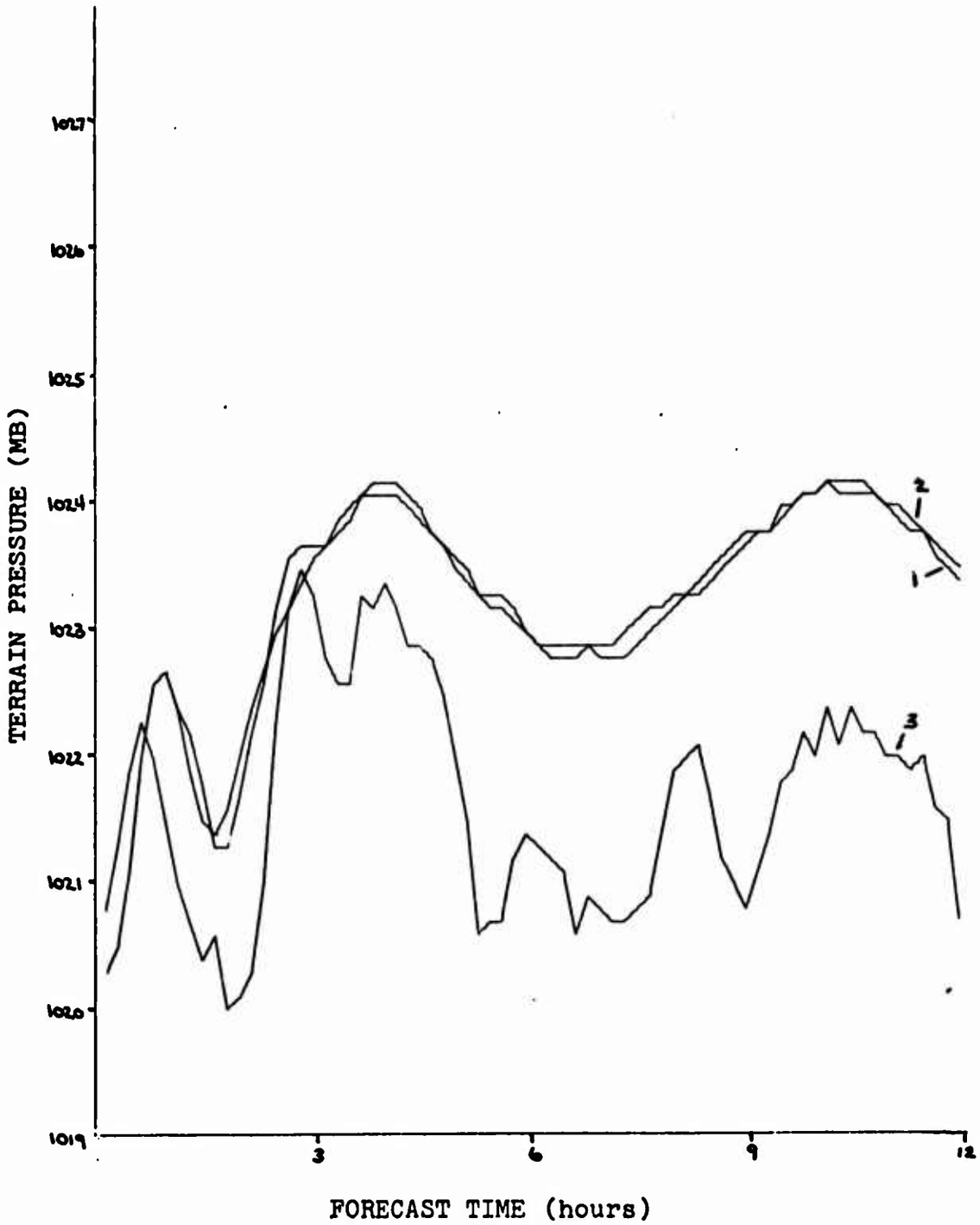

FIGURE 11. Plot of Terrain Pressure Versus Forecast Minute at 80N 110E (Experiment III)

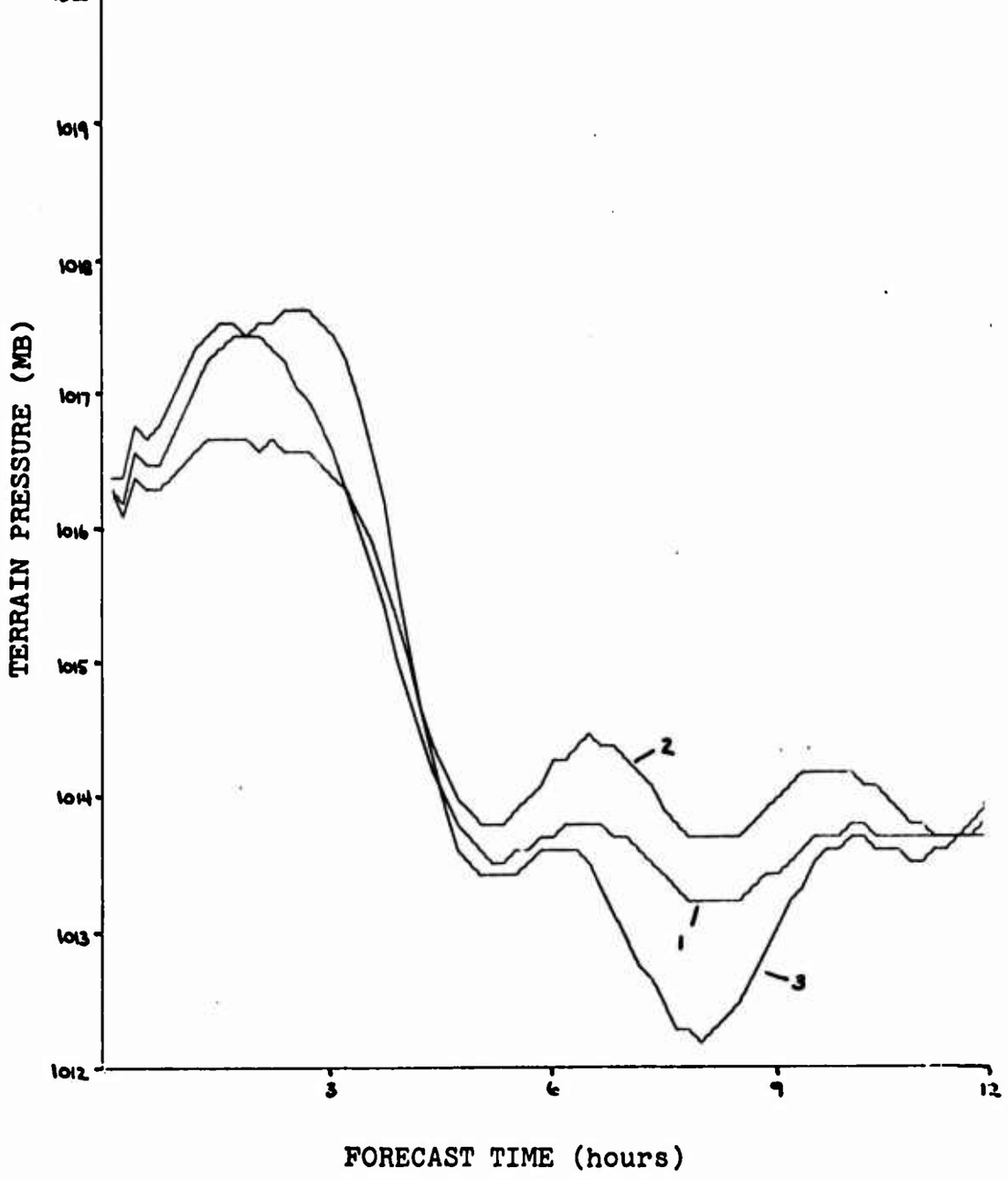

FIGURE 12. Plot of Terrain Pressure Versus Forecast Minute at 20N 110E (Experiment IV)

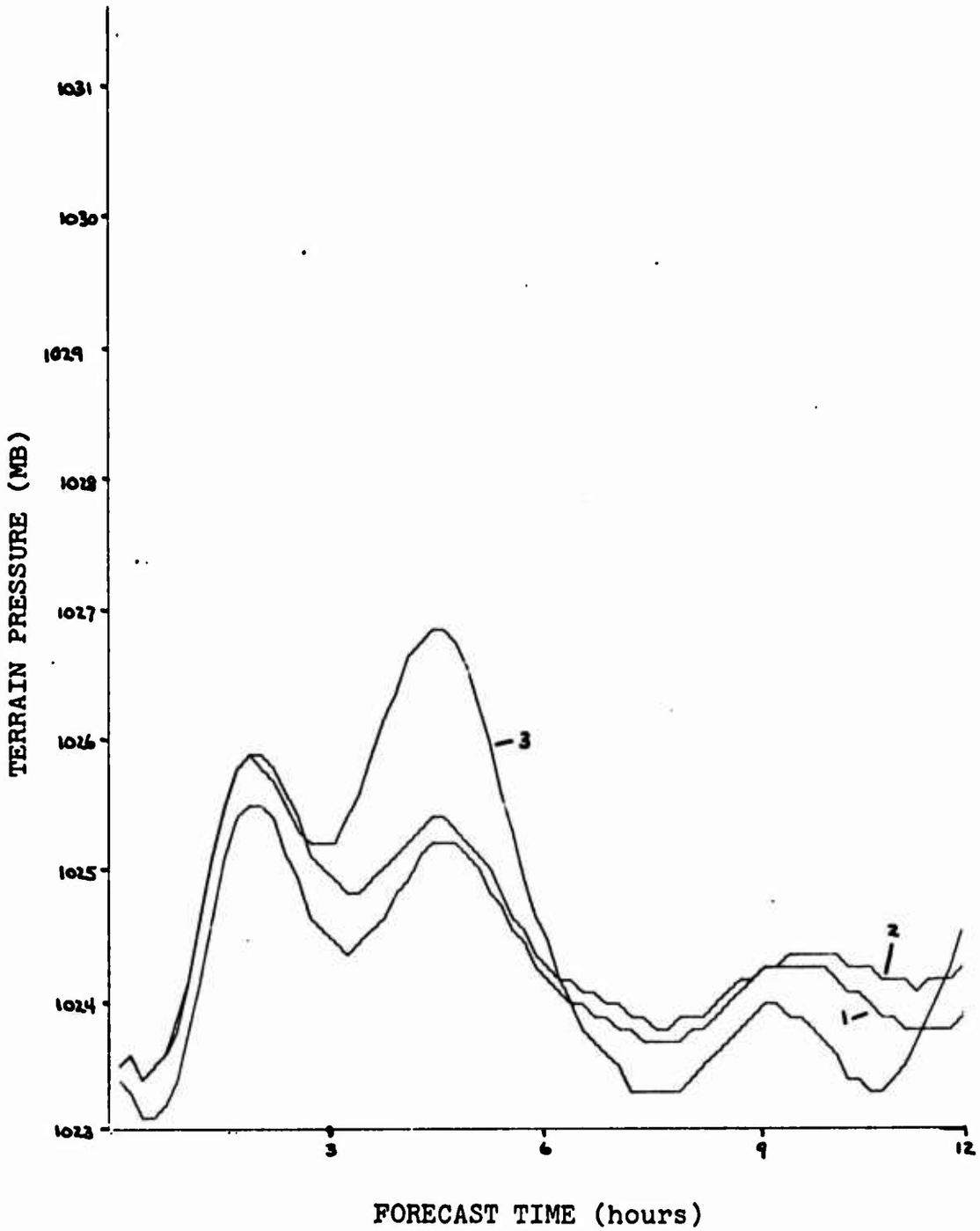

FIGURE 13. Plot of Terrain Pressure Versus Forecast Minute at 40N 110E (Experiment IV)

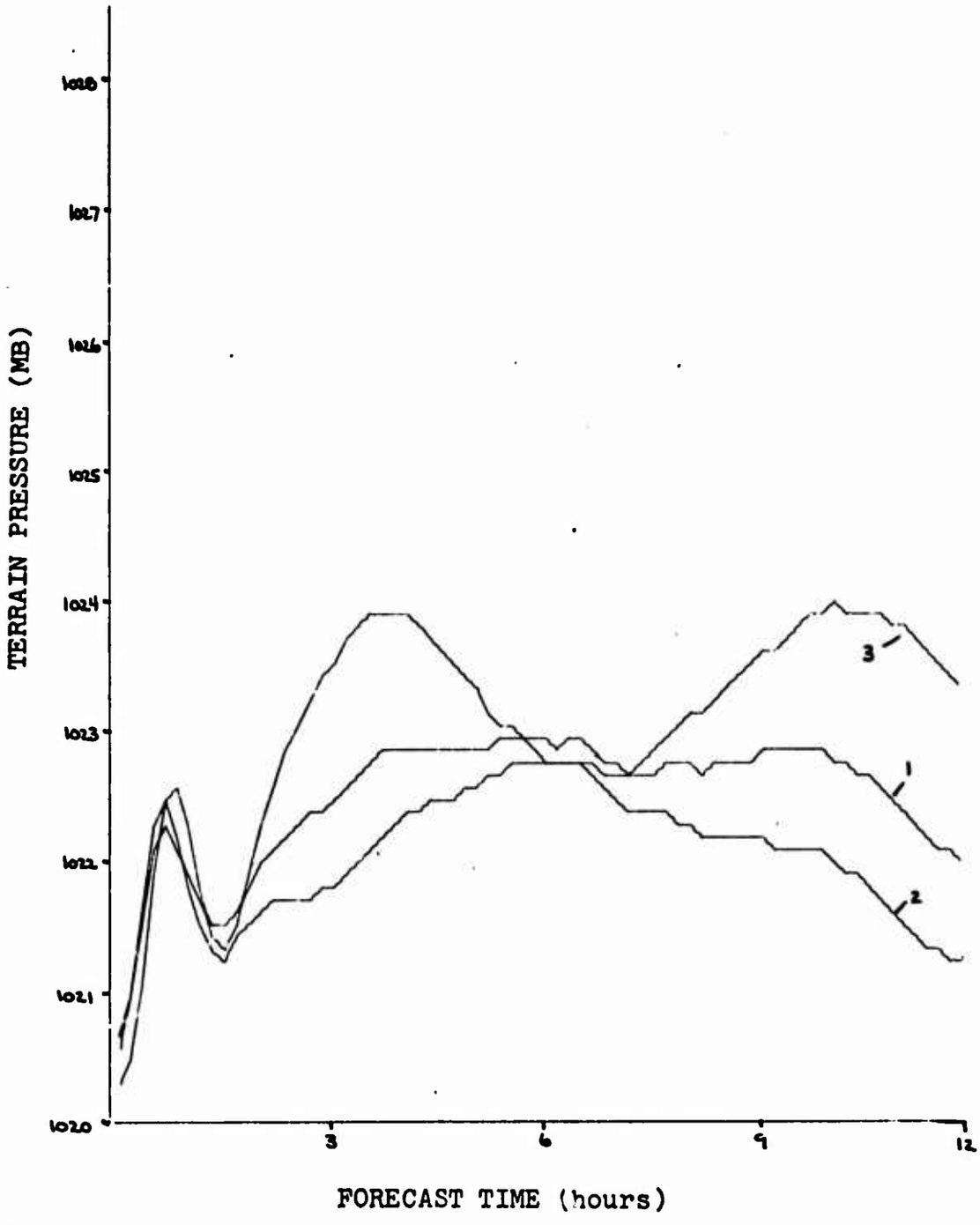

FIGURE 14. Plot of Terrain Pressure Versus Forecast Minute at 80N 110E (Experiment IV)

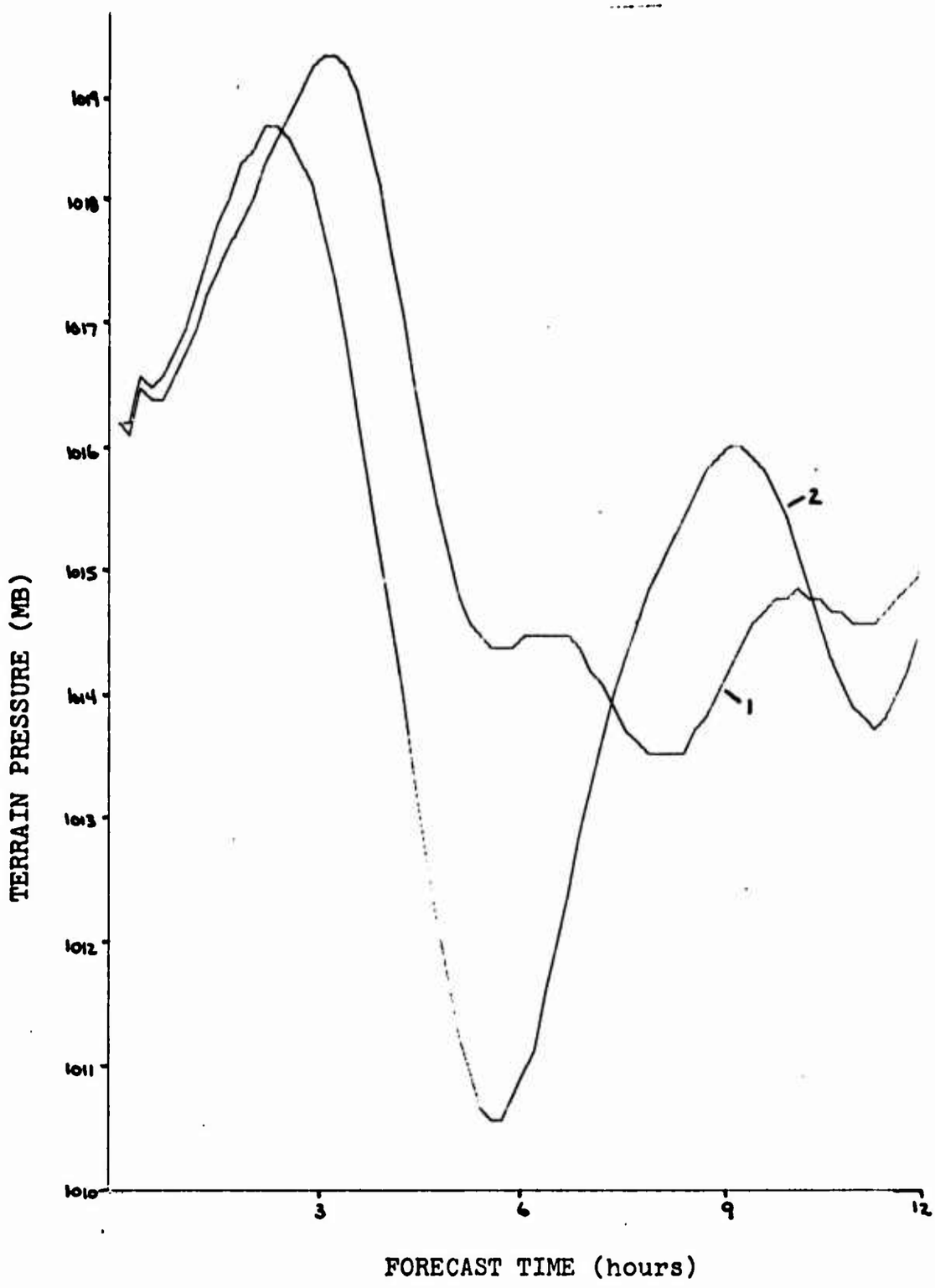

FIGURE 15. Plot of Terrain Pressure Versus Forecast Minute at 20N 110E (Experiment V)

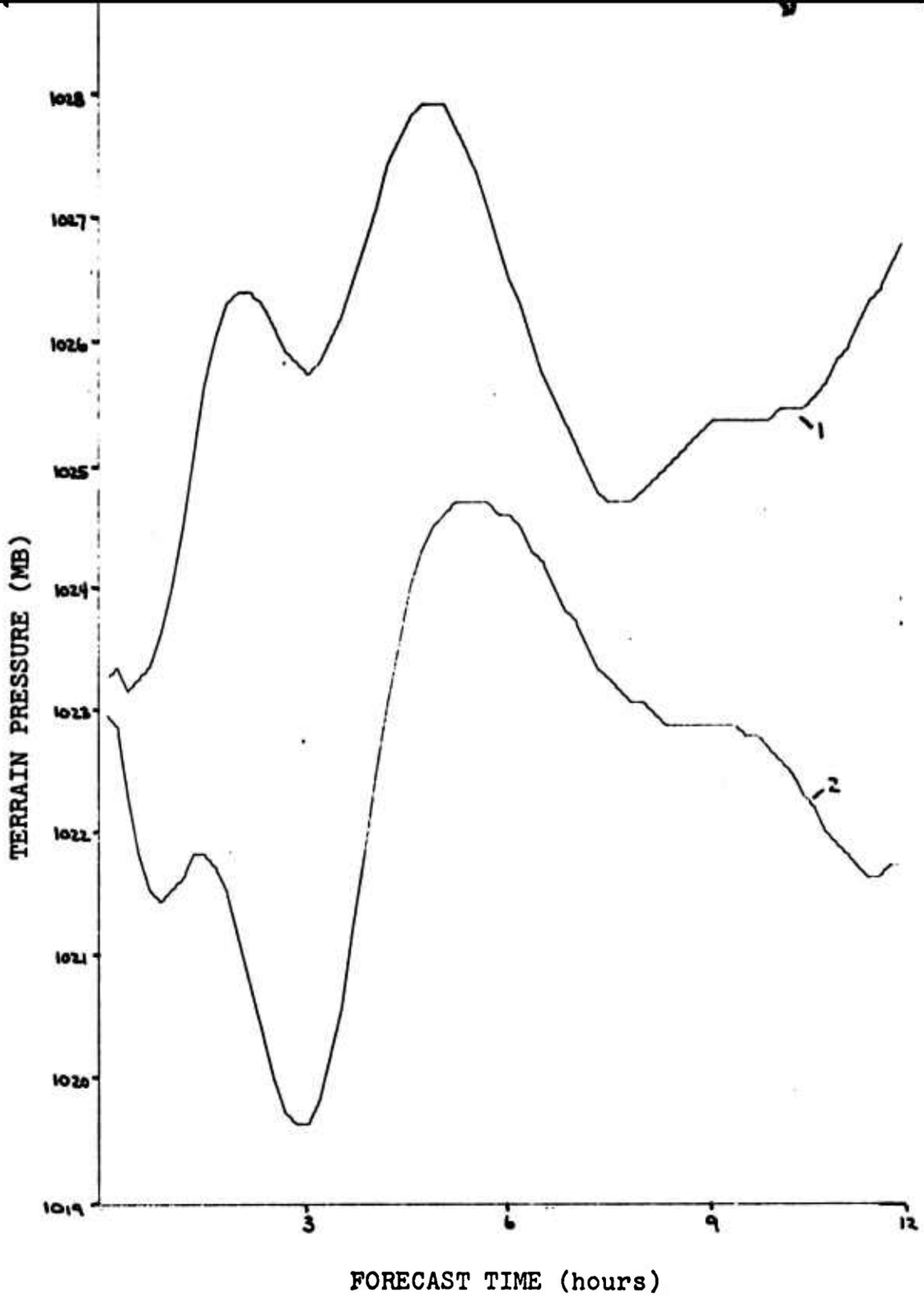

FIGURE 16. Plot of Terrain Pressure Versus Forecast Minute at 40N 110E (Experiment V)

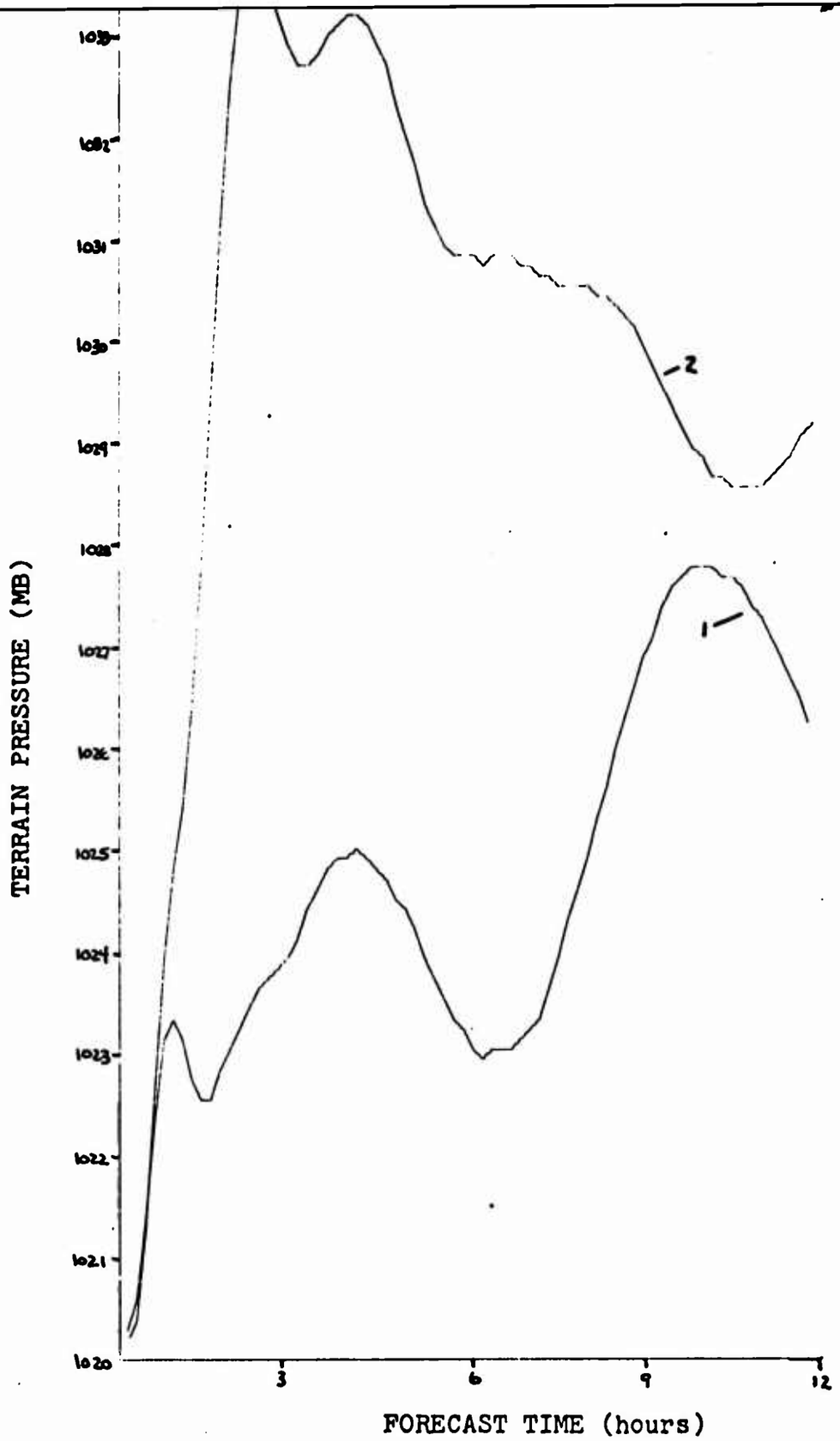

FIGURE 17. Plot of Terrain Pressure Versus Forecast Minute at 80N 110E (Experiment V)

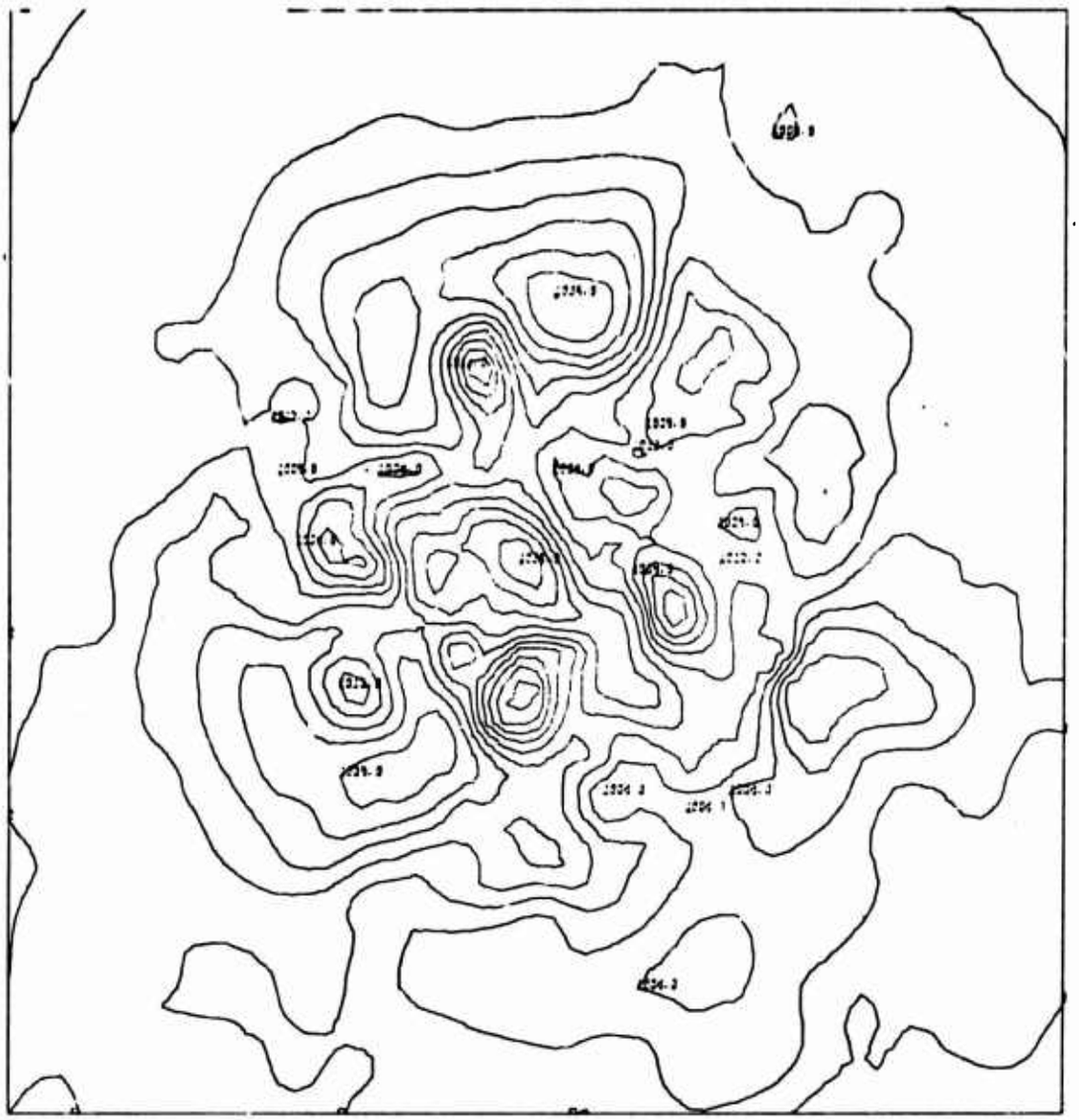

CHART A. Initial Surface Pressure Analysis From FNWC Tape. 12 Z 10 May 73

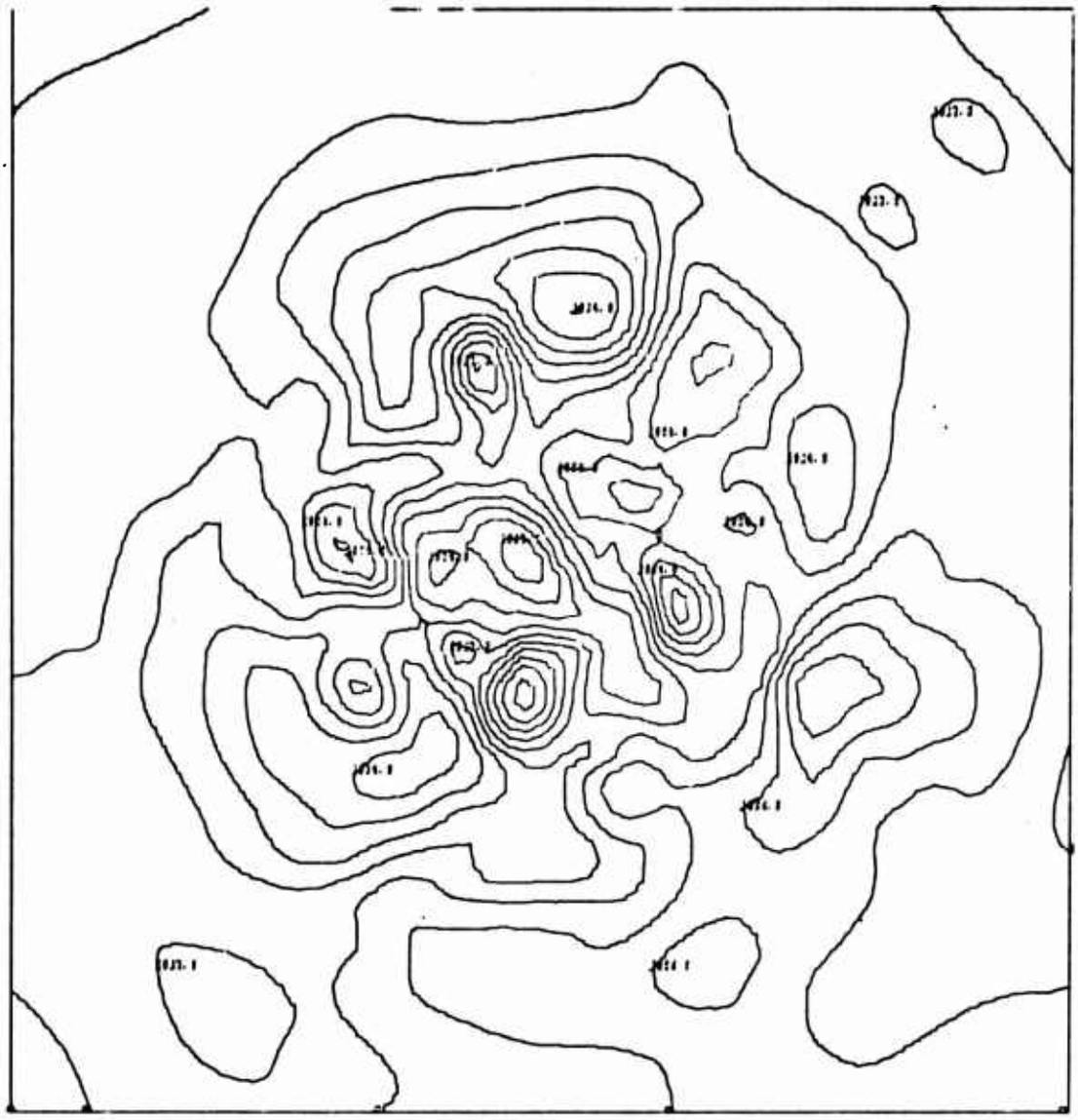

CHART B. Surface Pressure Analysis From Model Interpolation. 12 Z 10 May 73

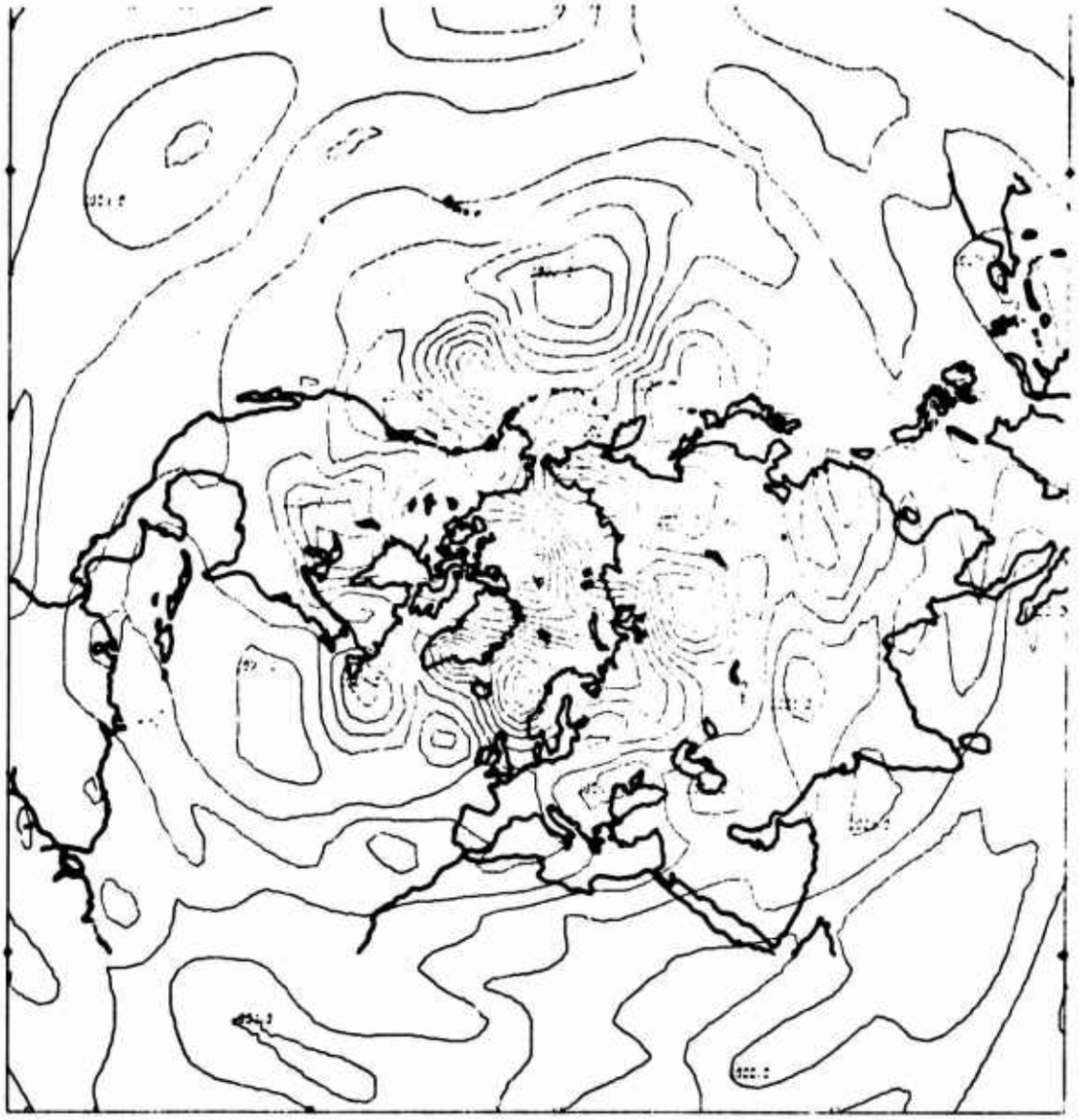

CHART C. 12-Hour Surface Pressure Forecast Using $\alpha = 0.0$ and Euler Backward Every 6 Hours. VT 00 Z 11 May 73 (Experiment I & II).

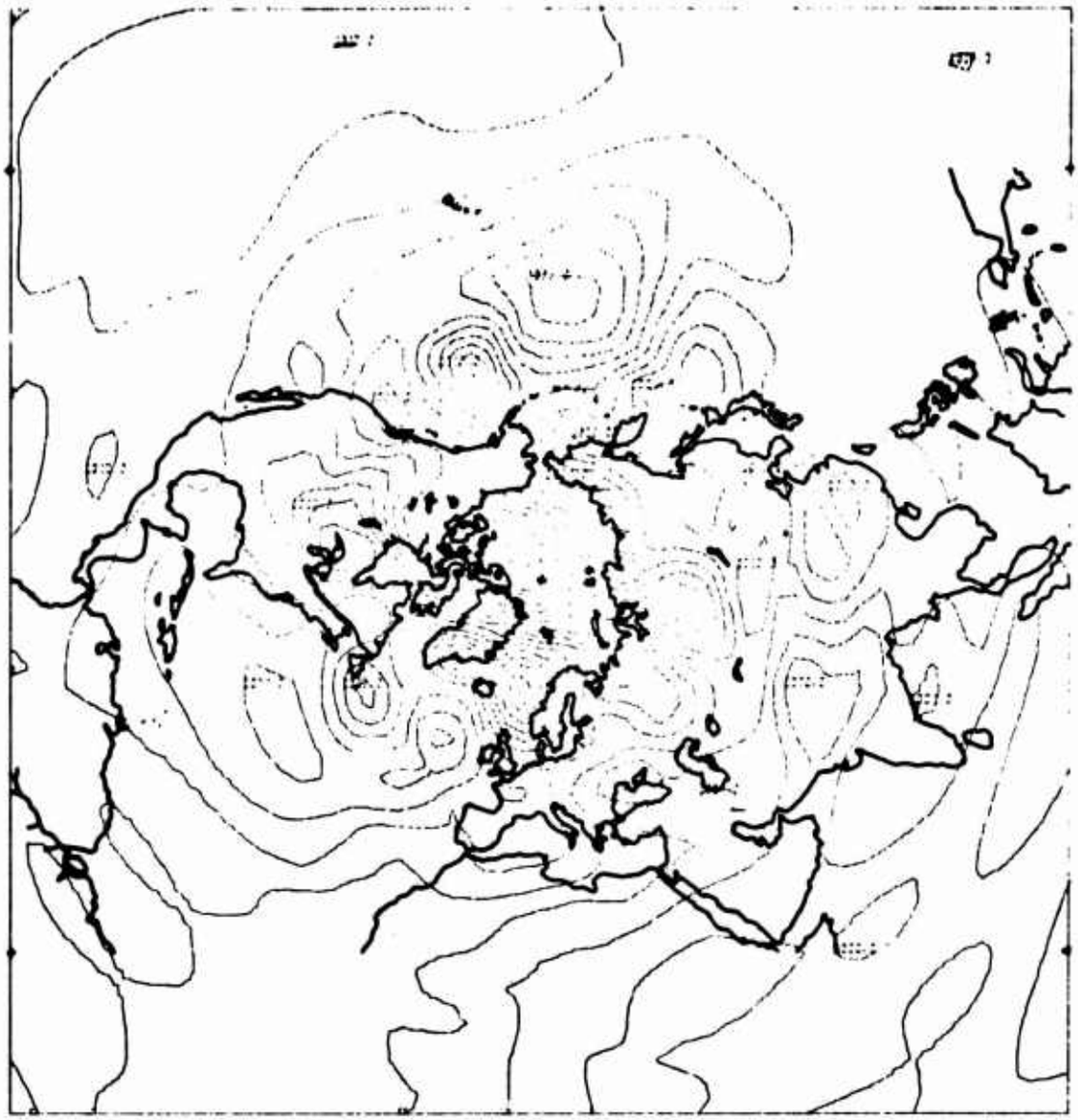

CHART D. 12-Hour Surface Pressure Forecast Using $\alpha = 0.3$ and Euler Backward Every 6 Hours. VT 00 Z 11 May 73 (Experiment I)

CHART E. 12-Hour Surface Pressure Forecast Using
$\alpha = 0.4$ and Euler Backward Every 6 Hours.
VT 00 Z 11 May 73 (Experiment I)

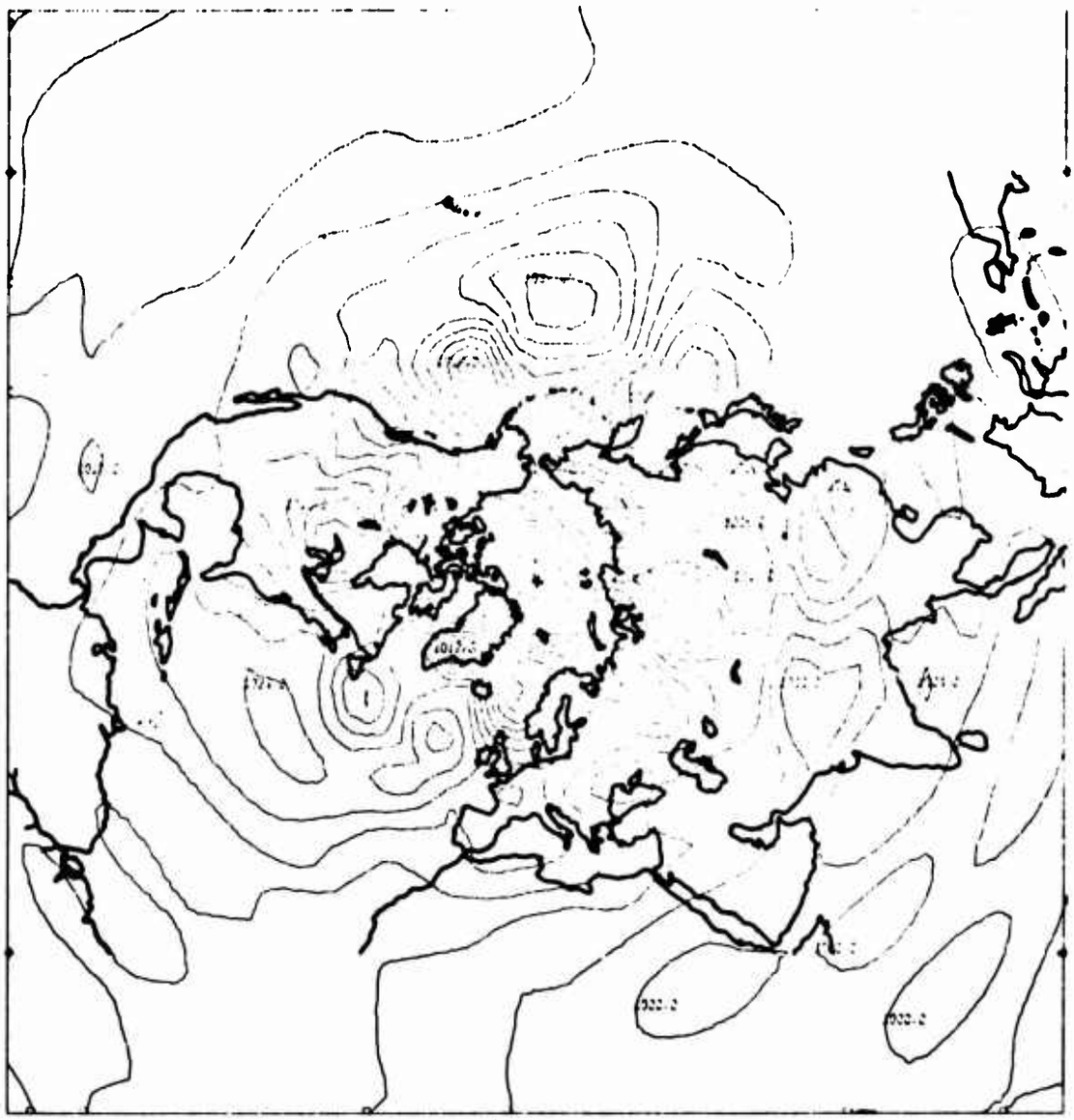

CHART F. 12-Hour Surface Pressure Forecast Using
$\alpha = 0.5$ and Euler Backward Every 6 Hours.
VT 00 Z 11 May 73 (Experiment I)

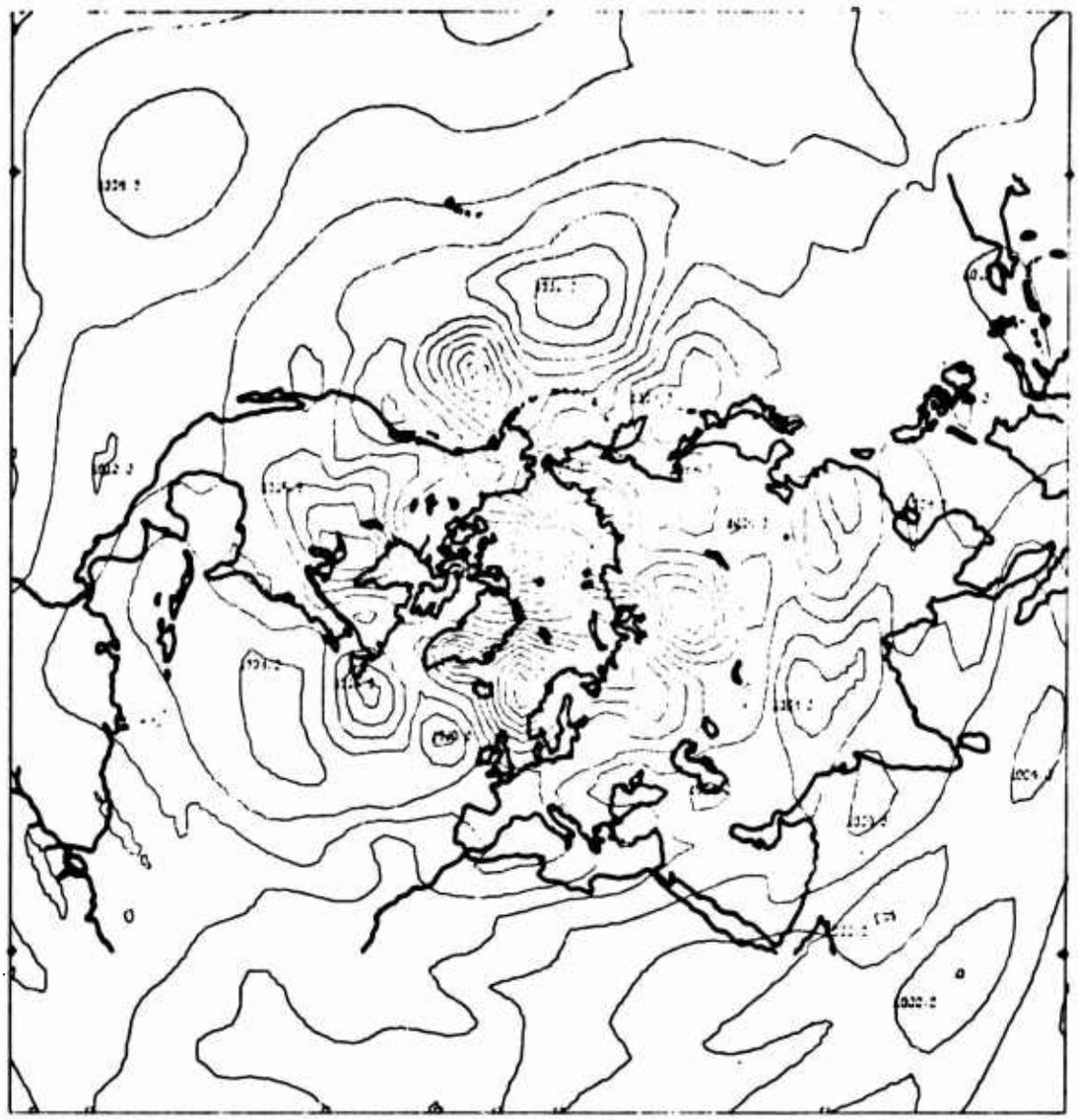

CHART G. 12-Hour Surface Pressure Forecast Using
α = 0.0 and Euler Backward Every 1 Hour.
VT 00 Z 11 May 73 (Experiment II)

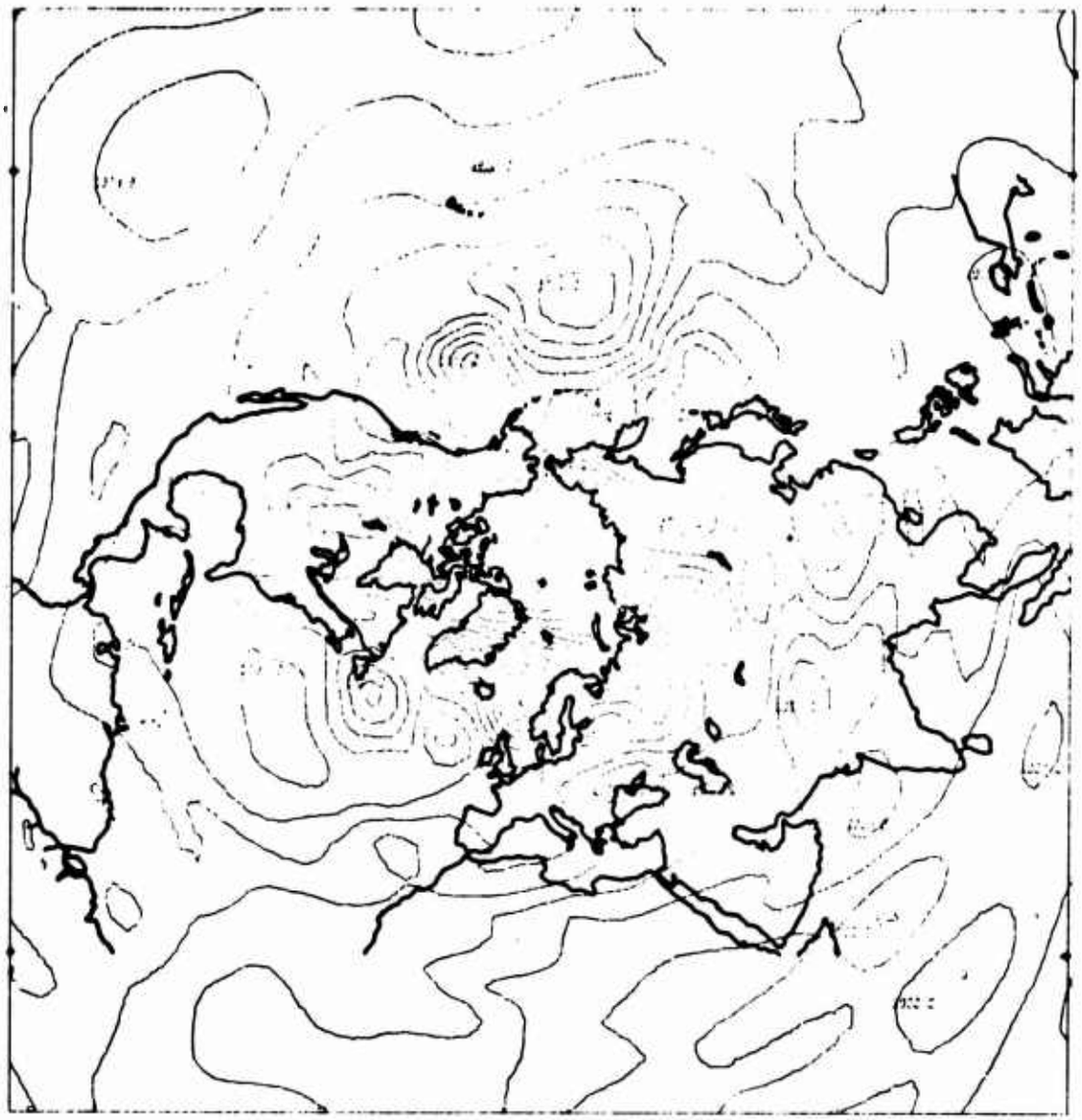

CHART H. 12-Hour Surface Pressure Forecast Using
α = 0.0 and Euler Backward Every 2 Hours.
VT 00 Z 11 May 73 (Experiment II)

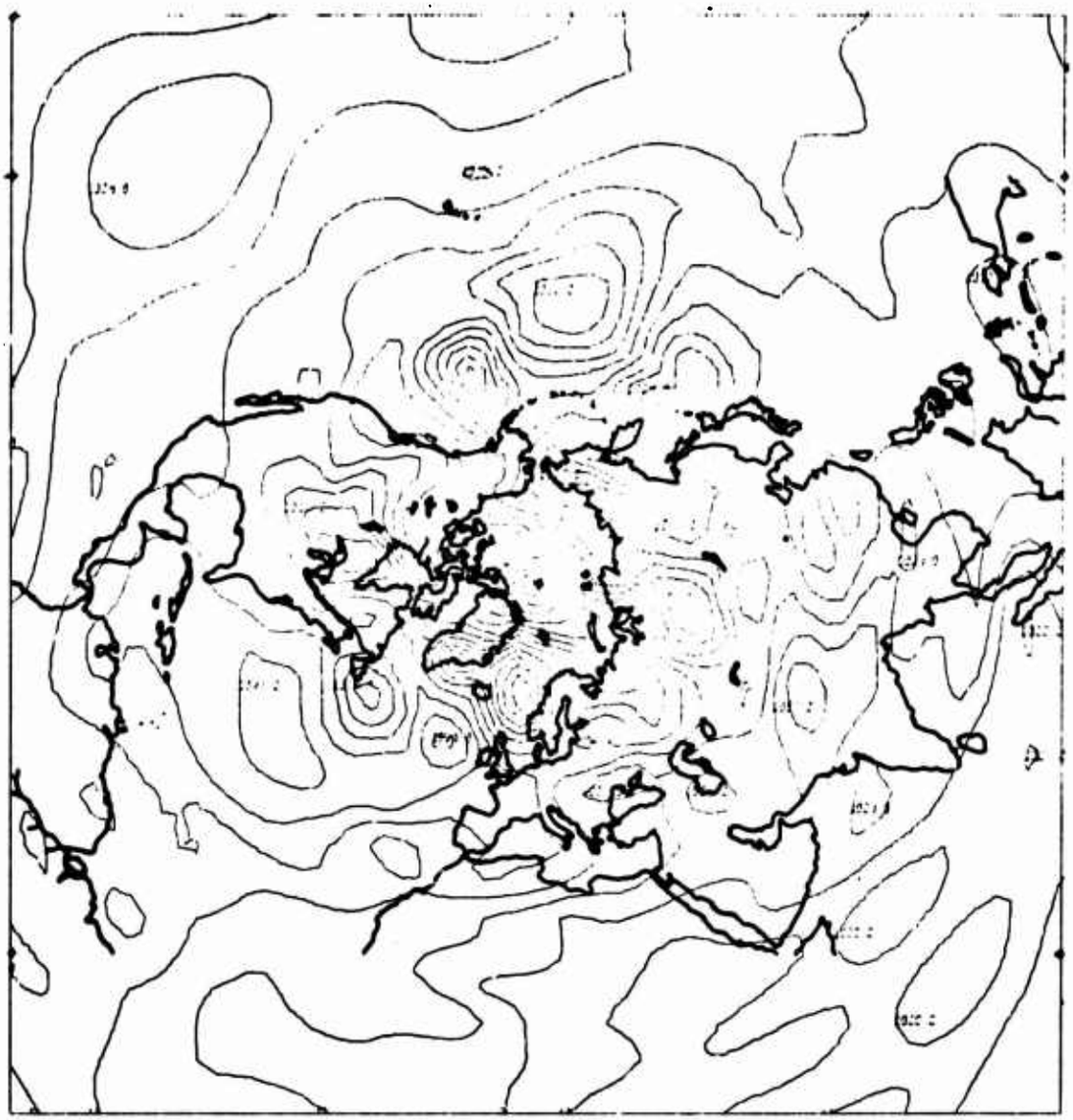

CHART I. 12-Hour Surface Pressure Forecast Using
$\alpha = 0.0$ and Euler Backward Every 3 Hours.
VT 00 Z 11 May 73 (Experiment II)

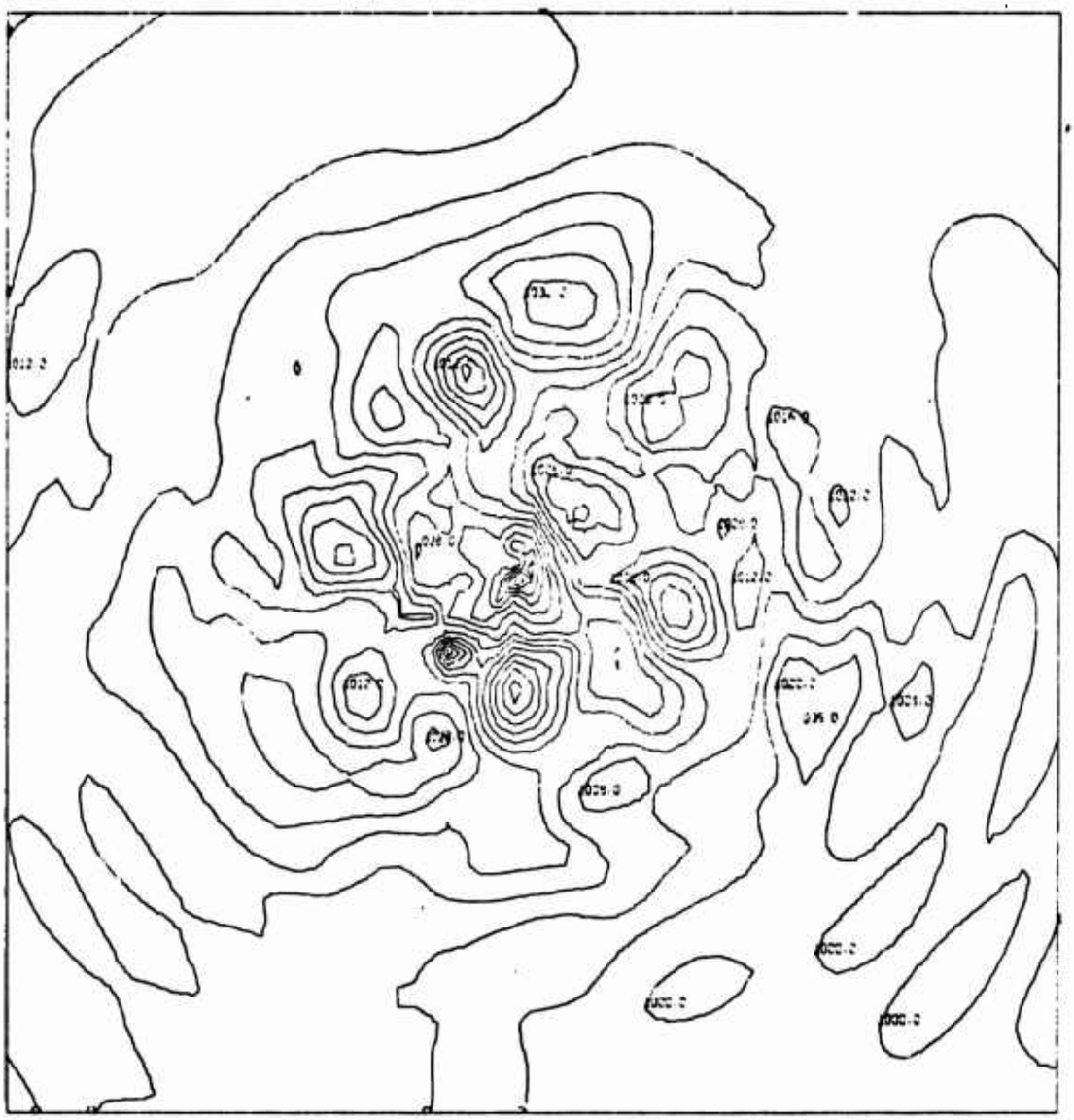

CHART J. 12-Hour Surface Pressure Forecast Using Iteration Initialization (One Hour) VT 00 Z 11 May 73 (Experiment IV)

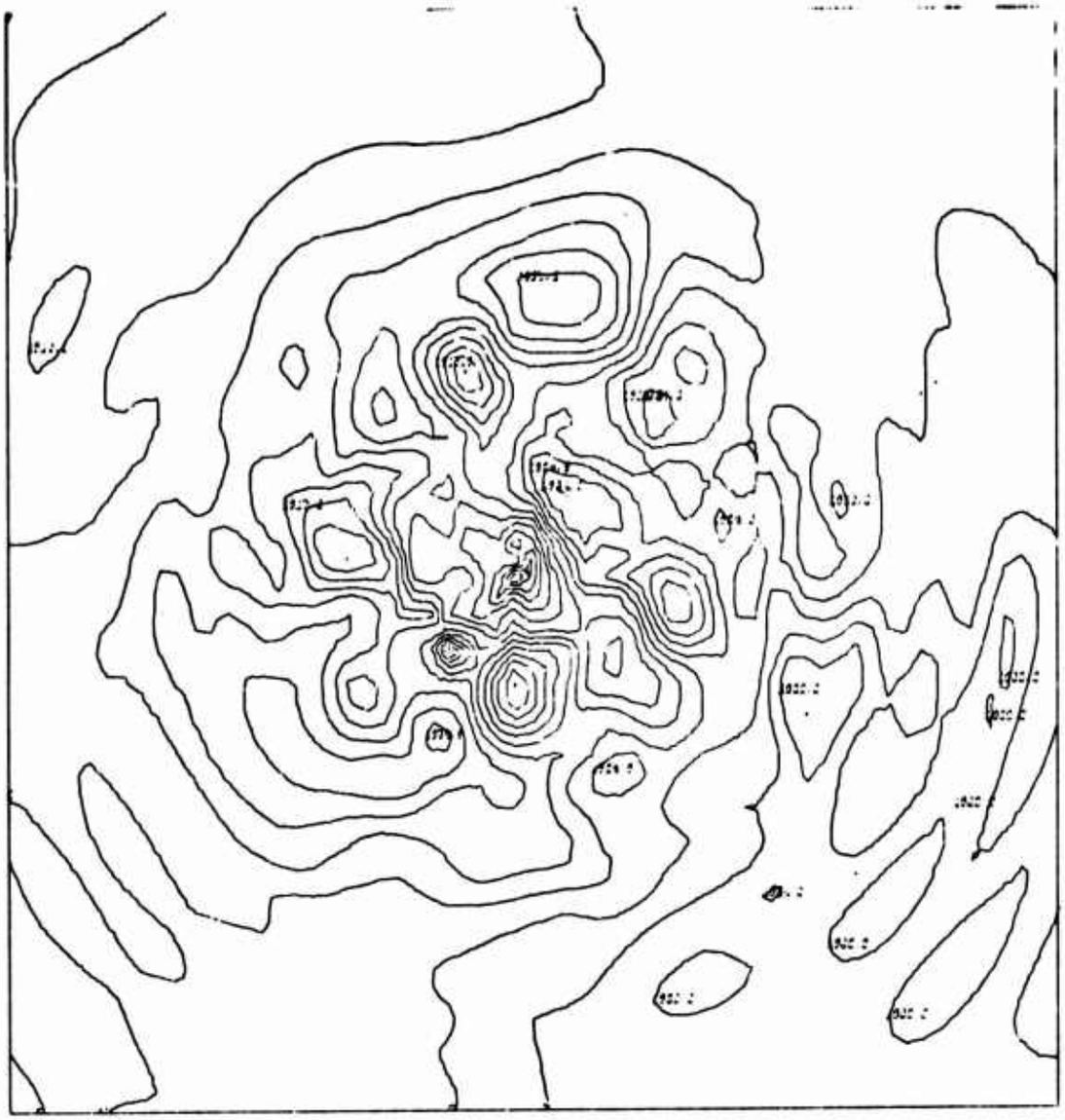

CHART K. 12-Hour Surface Pressure Forecast Using Iteration Initialization (Three Hours) VT 00 Z 11 May 73 (Experiment IV)

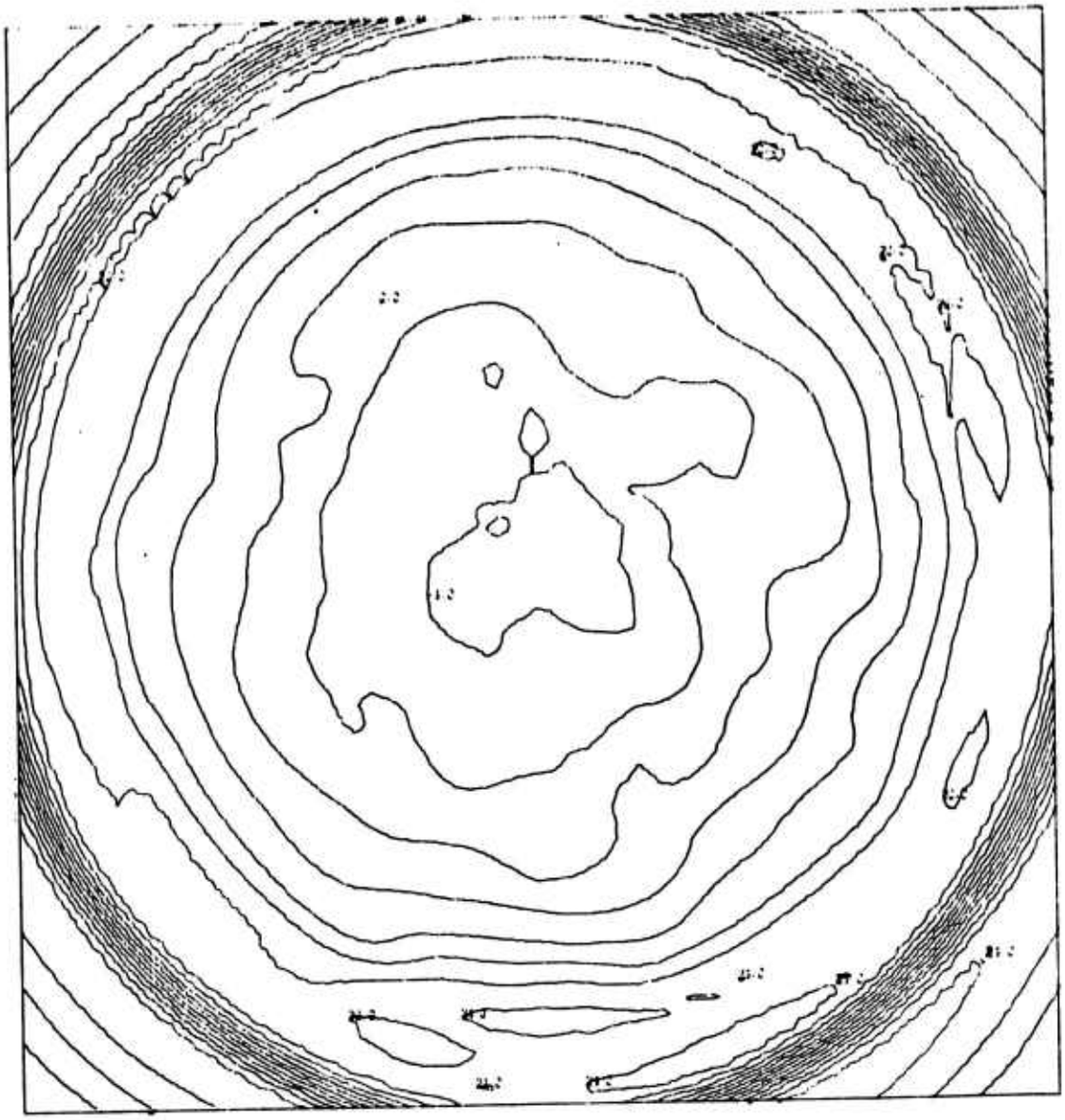

CHART L. 0.9 Sigma Level Initial Guess Stream Function Field (Experiment V)

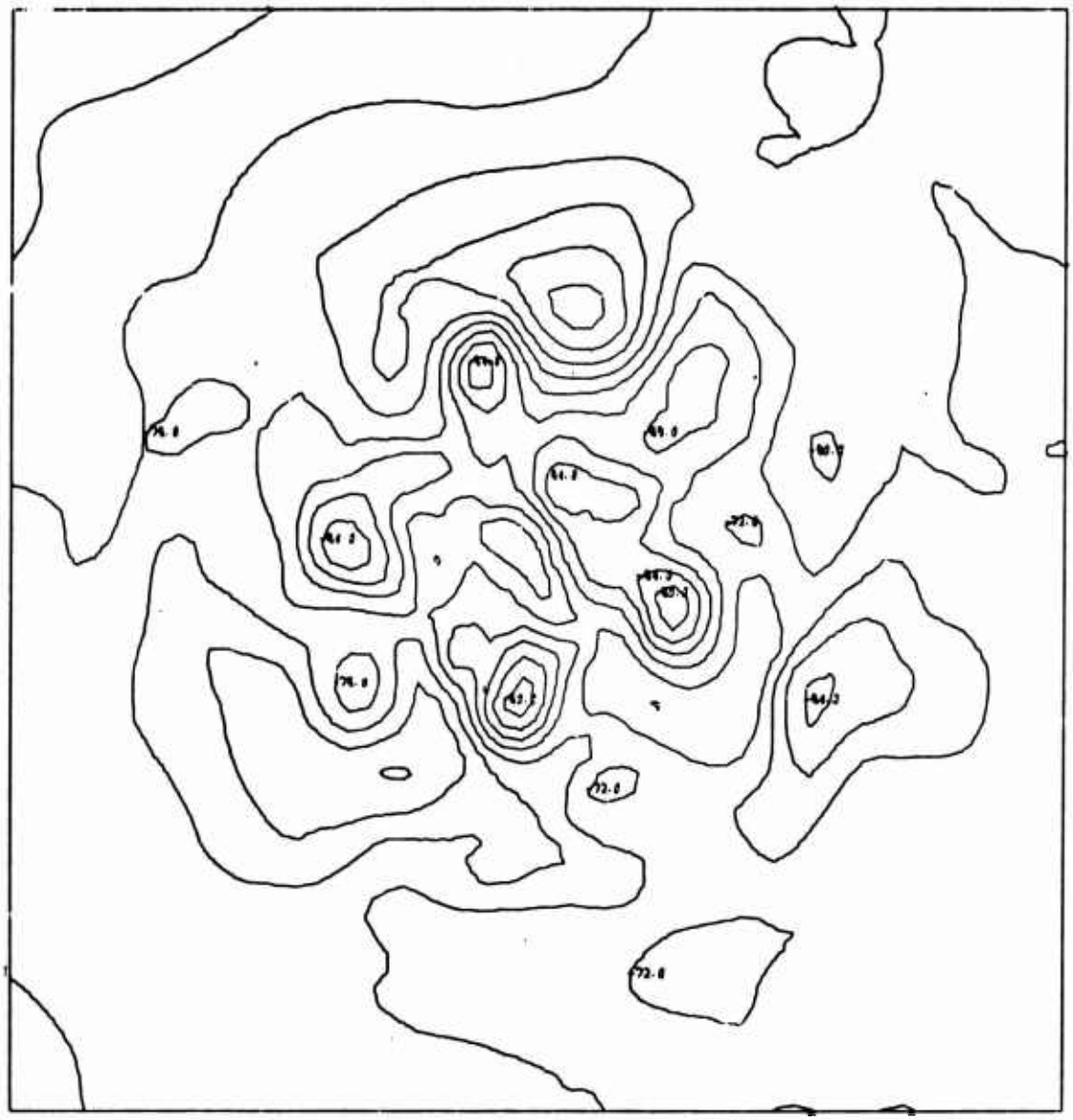

CHART M. 925 MB Level Initial Guess Stream Function Field (Experiment V)

CHART N. 0.9 Sigma Level Final Stream Function Field
(Experiment V)

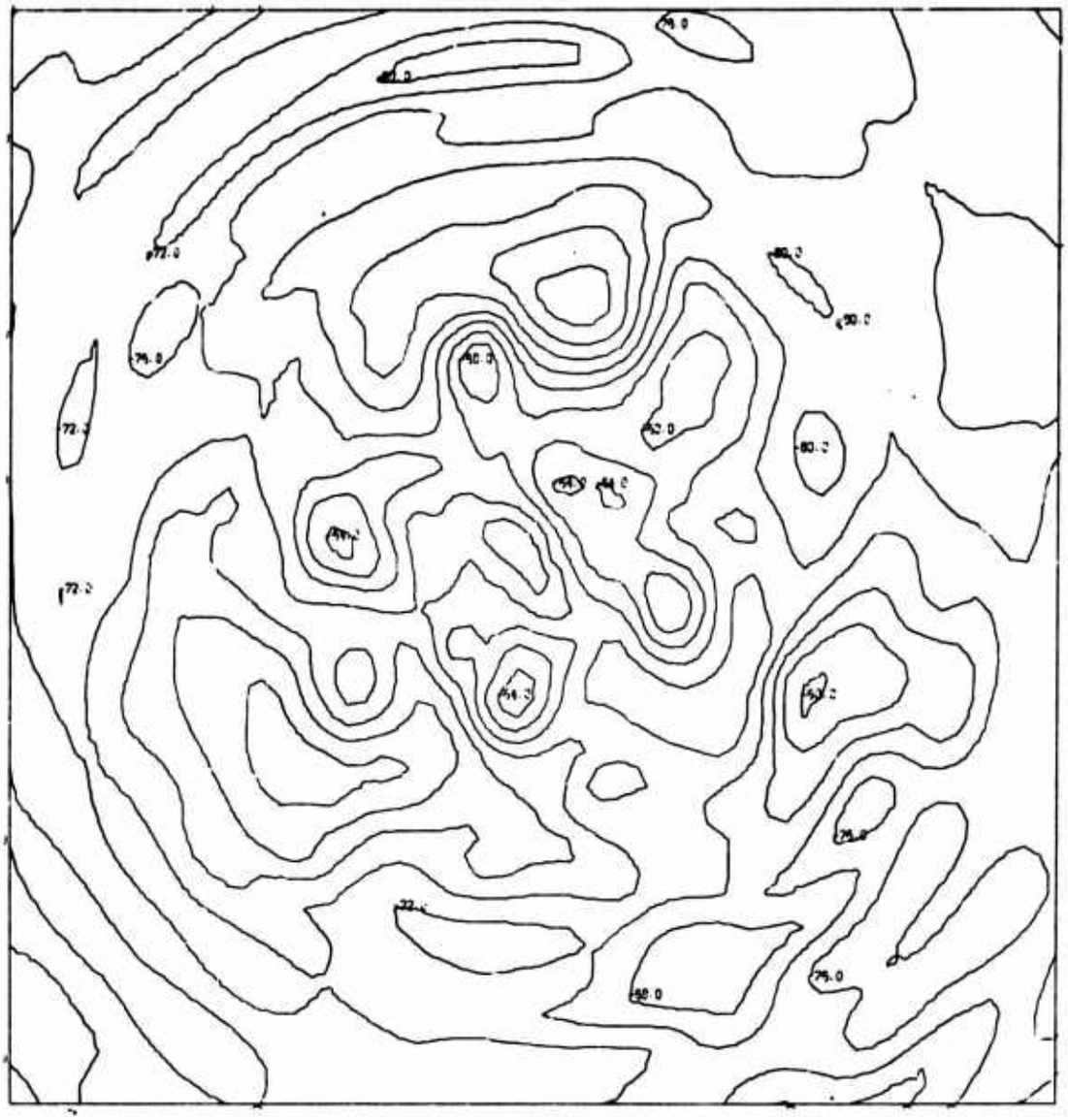

CHART O. 925 MB Level Final Stream Function Field
(Experiment V)

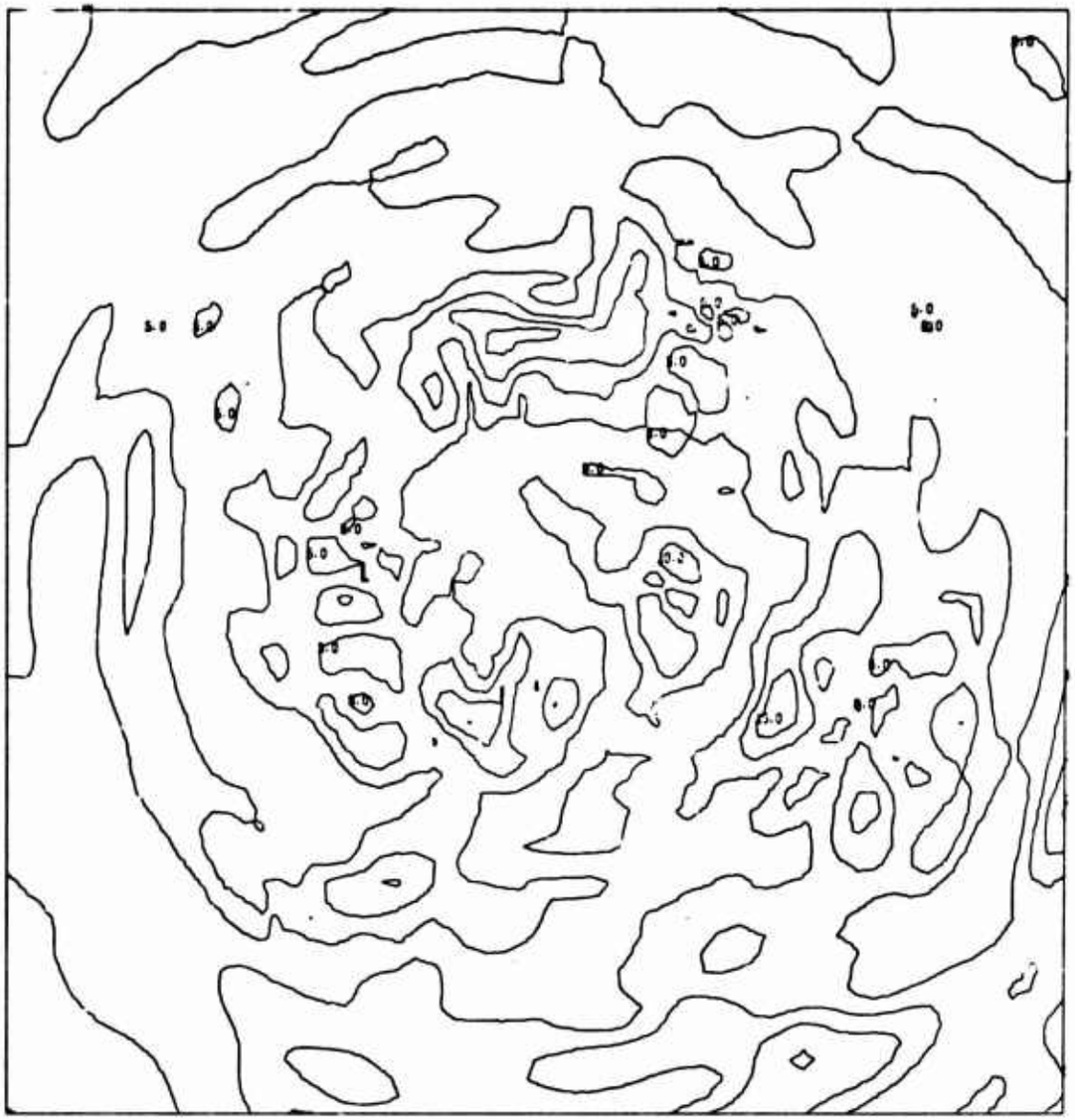

CHART P. 0.9 Sigma Level Isotach Field
(Experiment V)

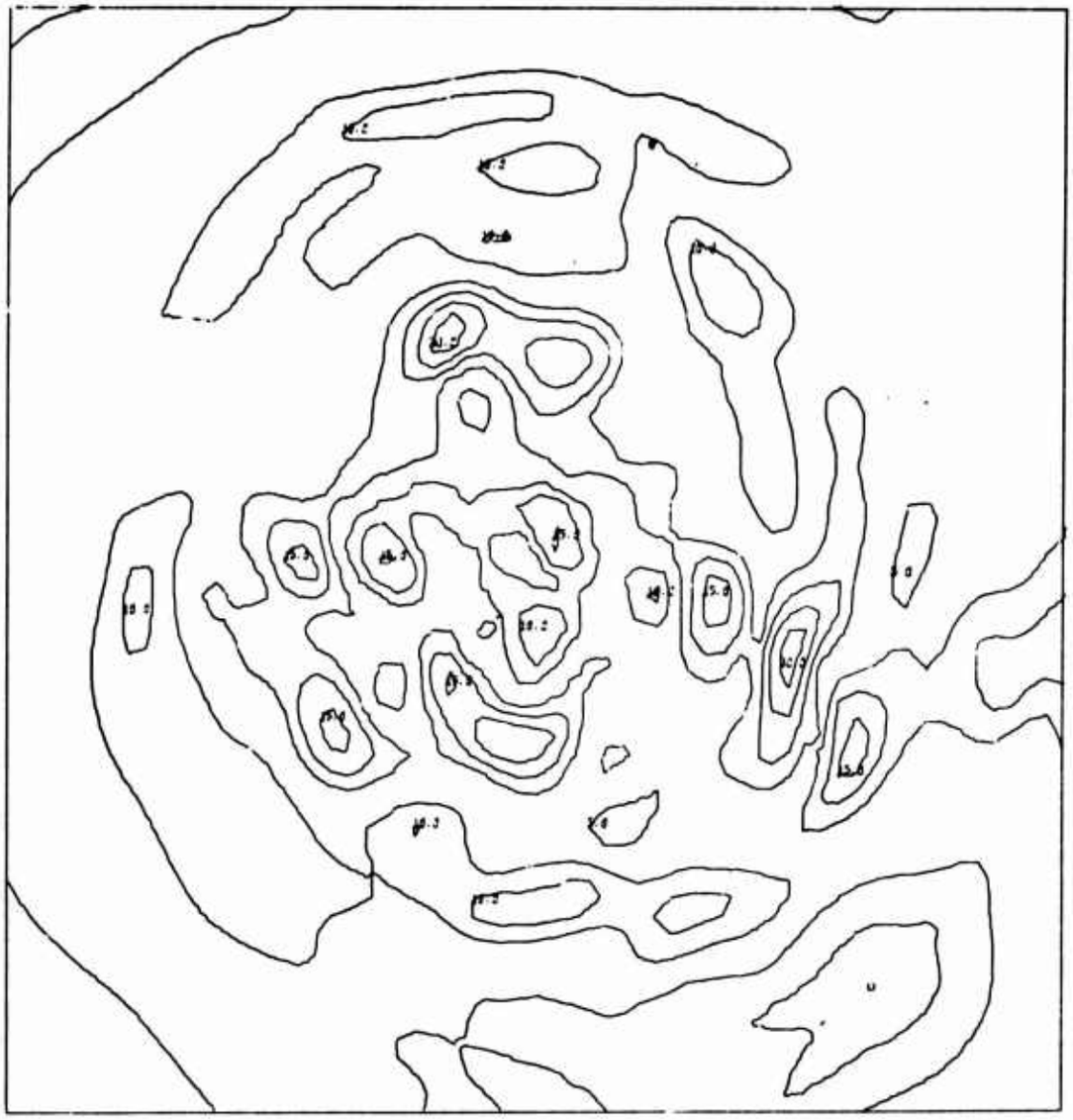

CHART Q. 925 MB Level Isotach Field
(Experiment V)

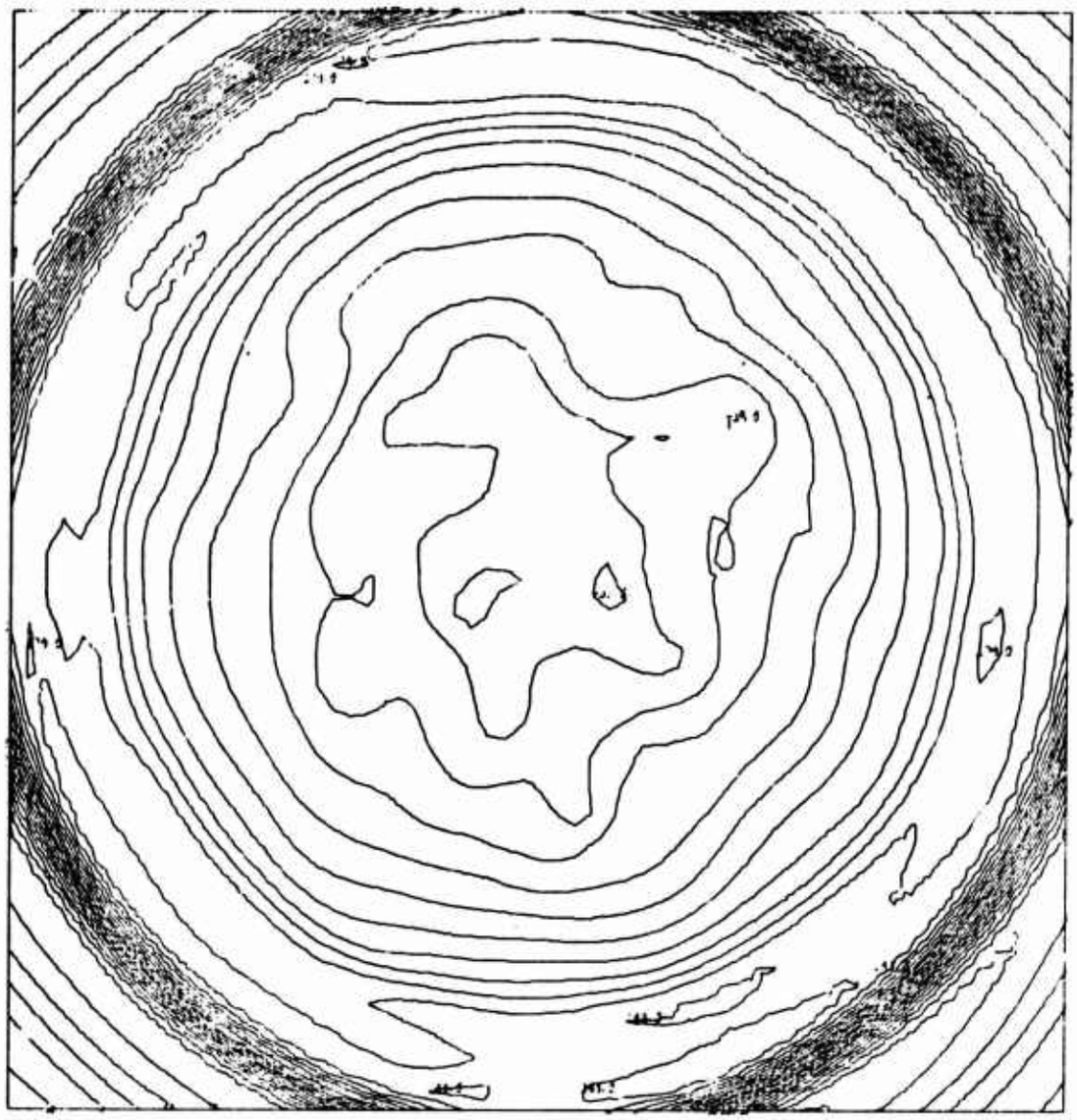

CHART R. 0.5 Sigma Level Initial Guess Stream Function Field (Experiment V).

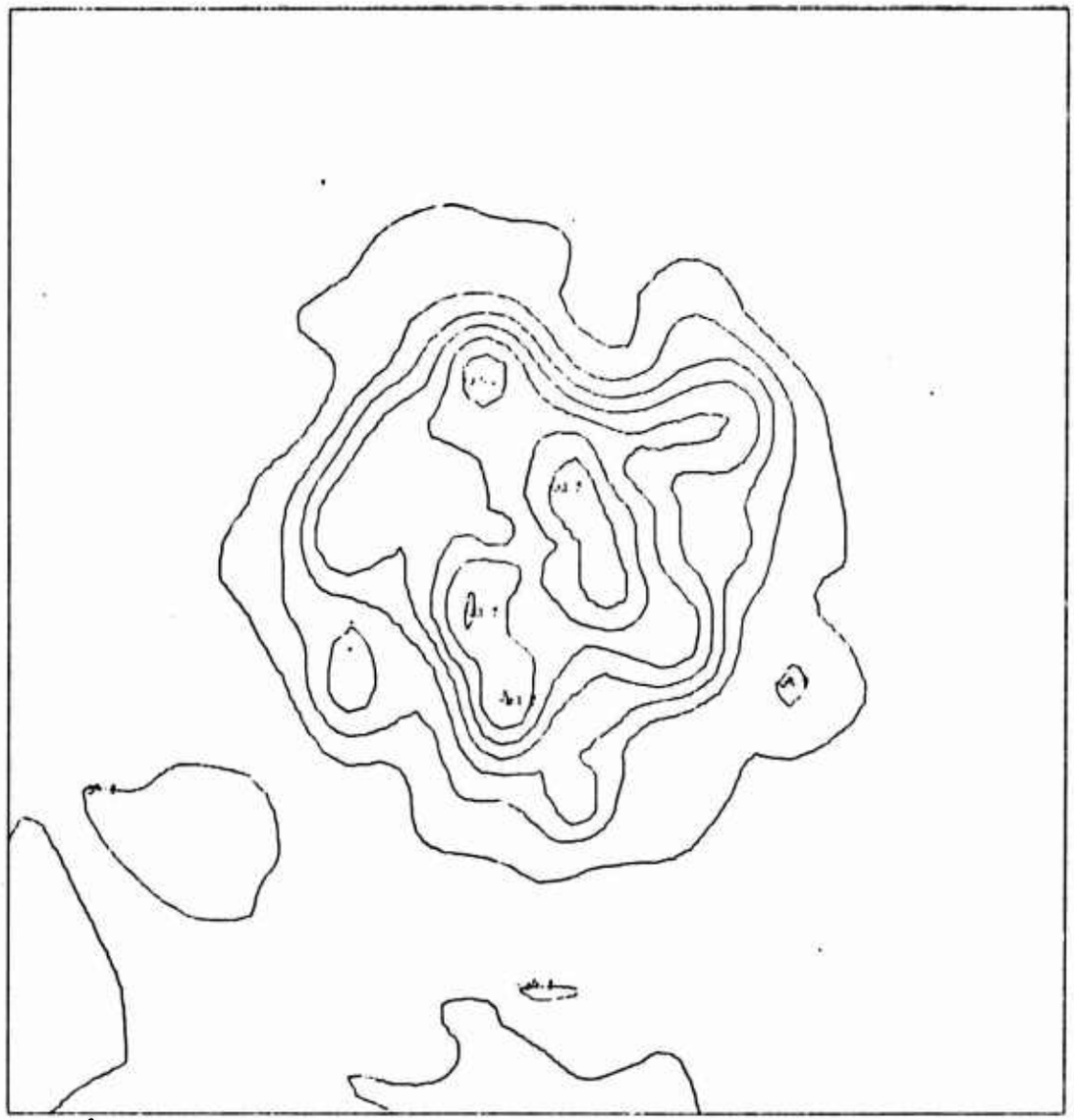

CHART S. 500 MB Level Initial Guess Stream Function Field (Experiment V)

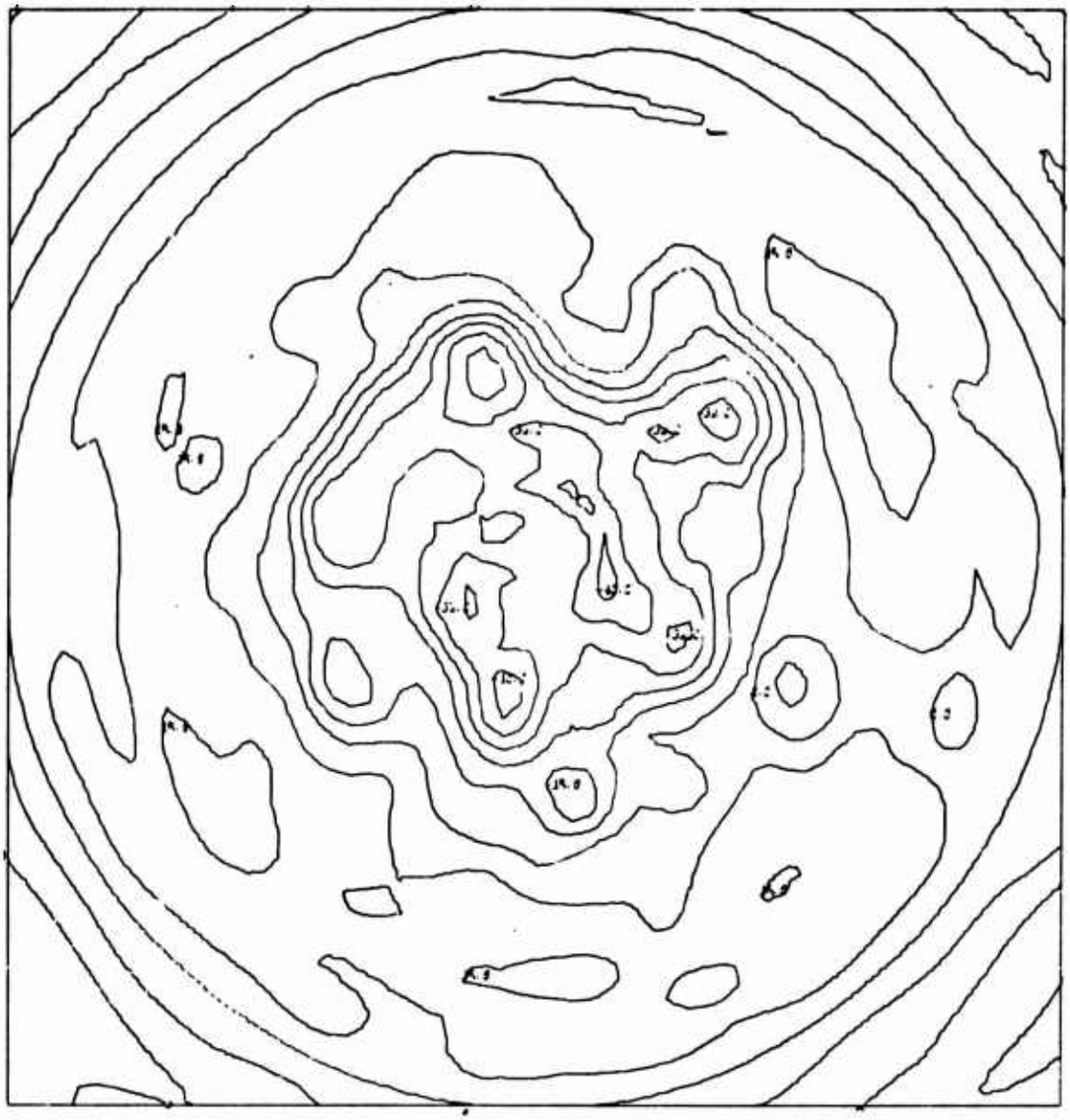

CHART T. 0.5 Sigma Level Final Stream Function Field (Experiment V)

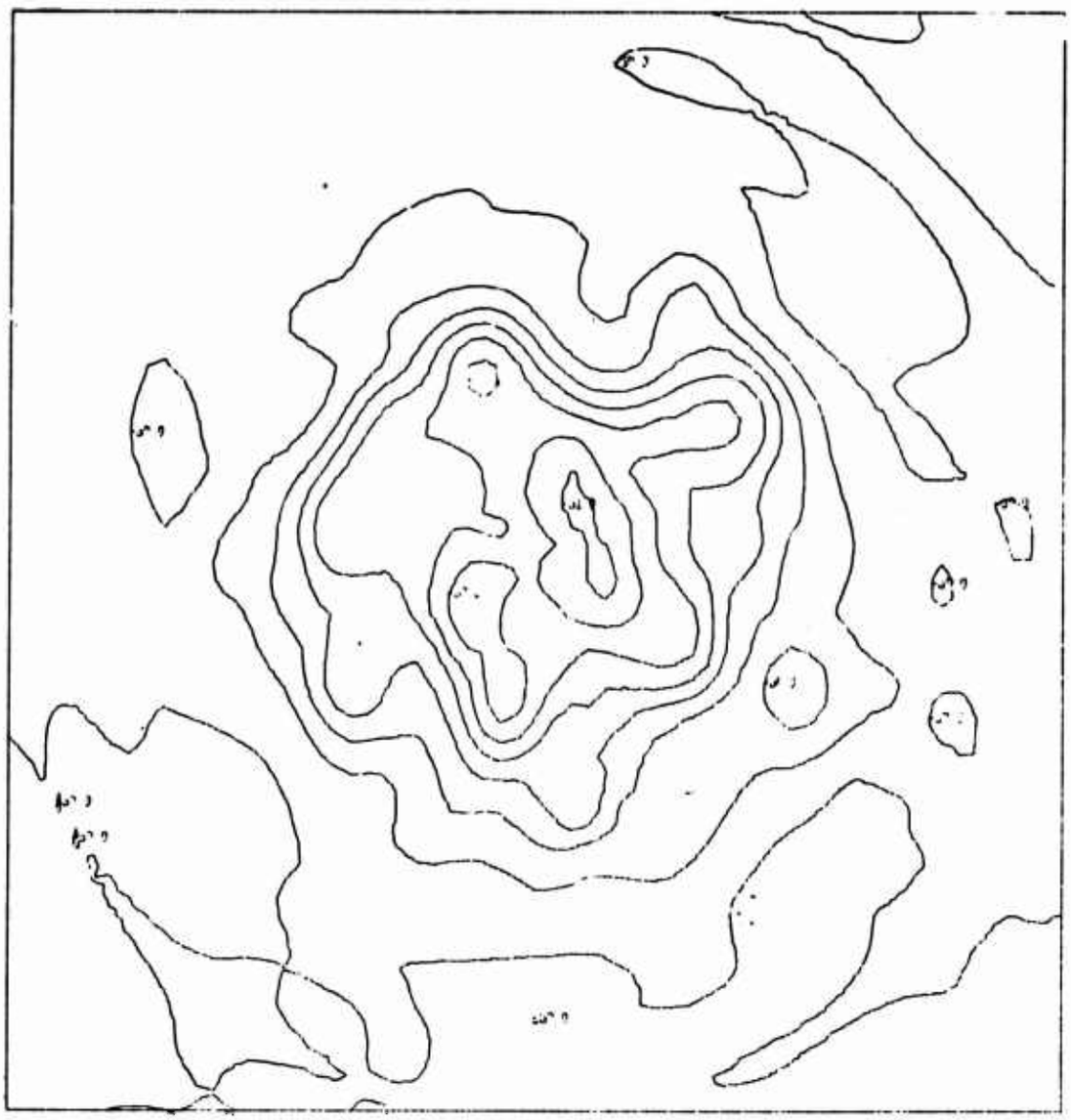

CHART U. 500 MB Level Final Stream Function Field (Experiment V)

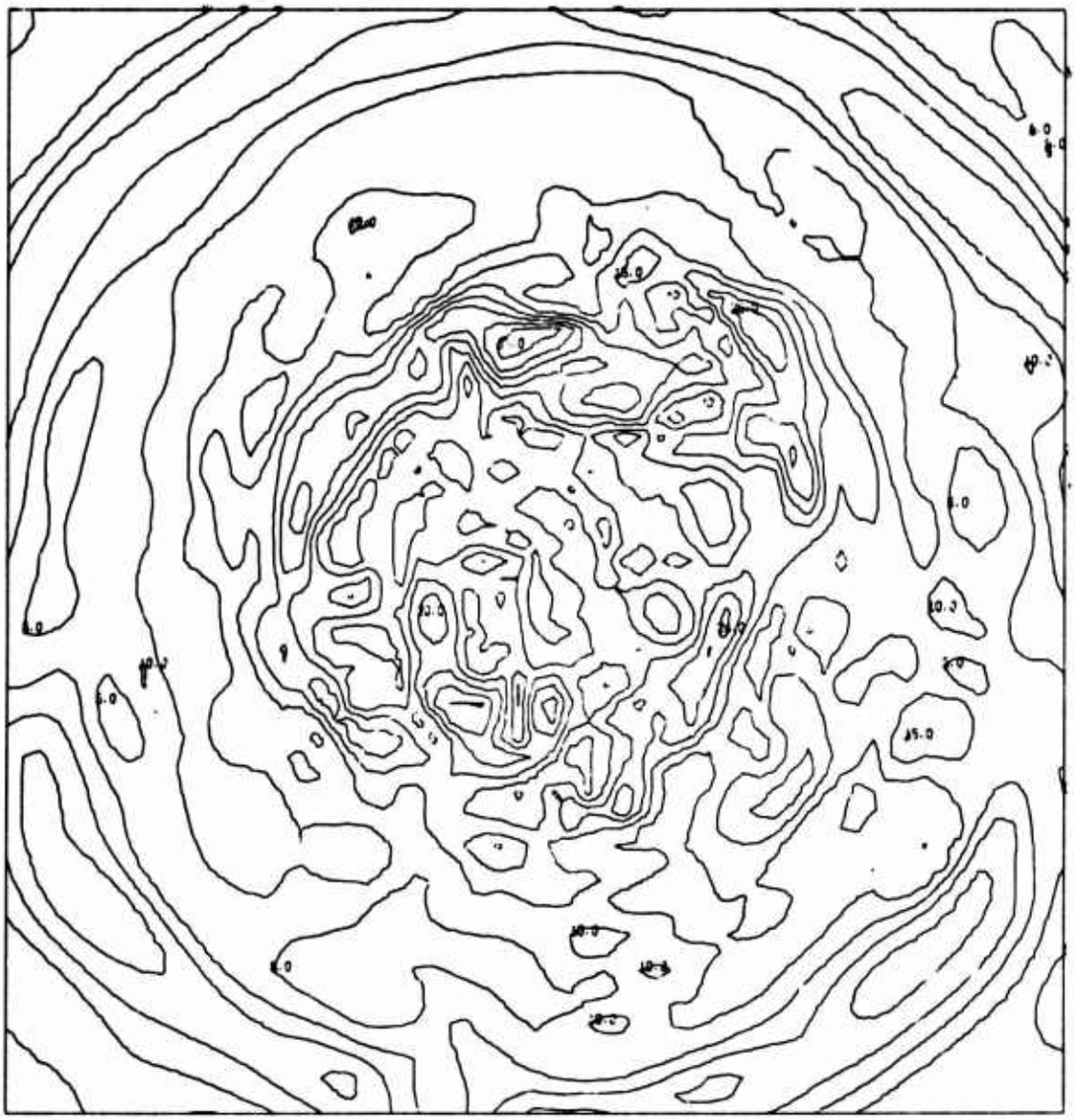

CHART V. 0.5 Sigma Level Isotach Field
(Experiment V)

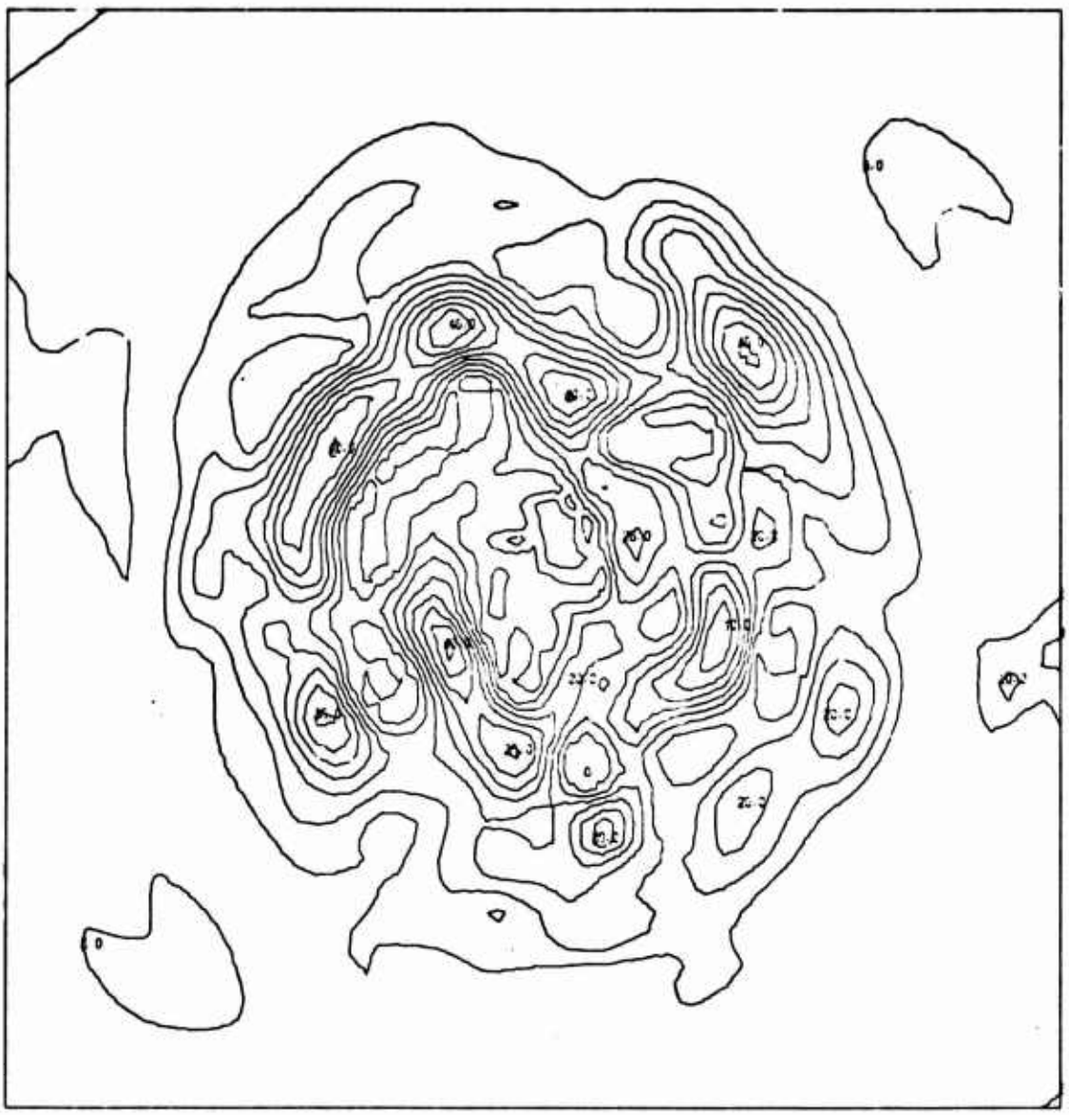

CHART W. 500 MB Level Isotach Field (Experiment V)

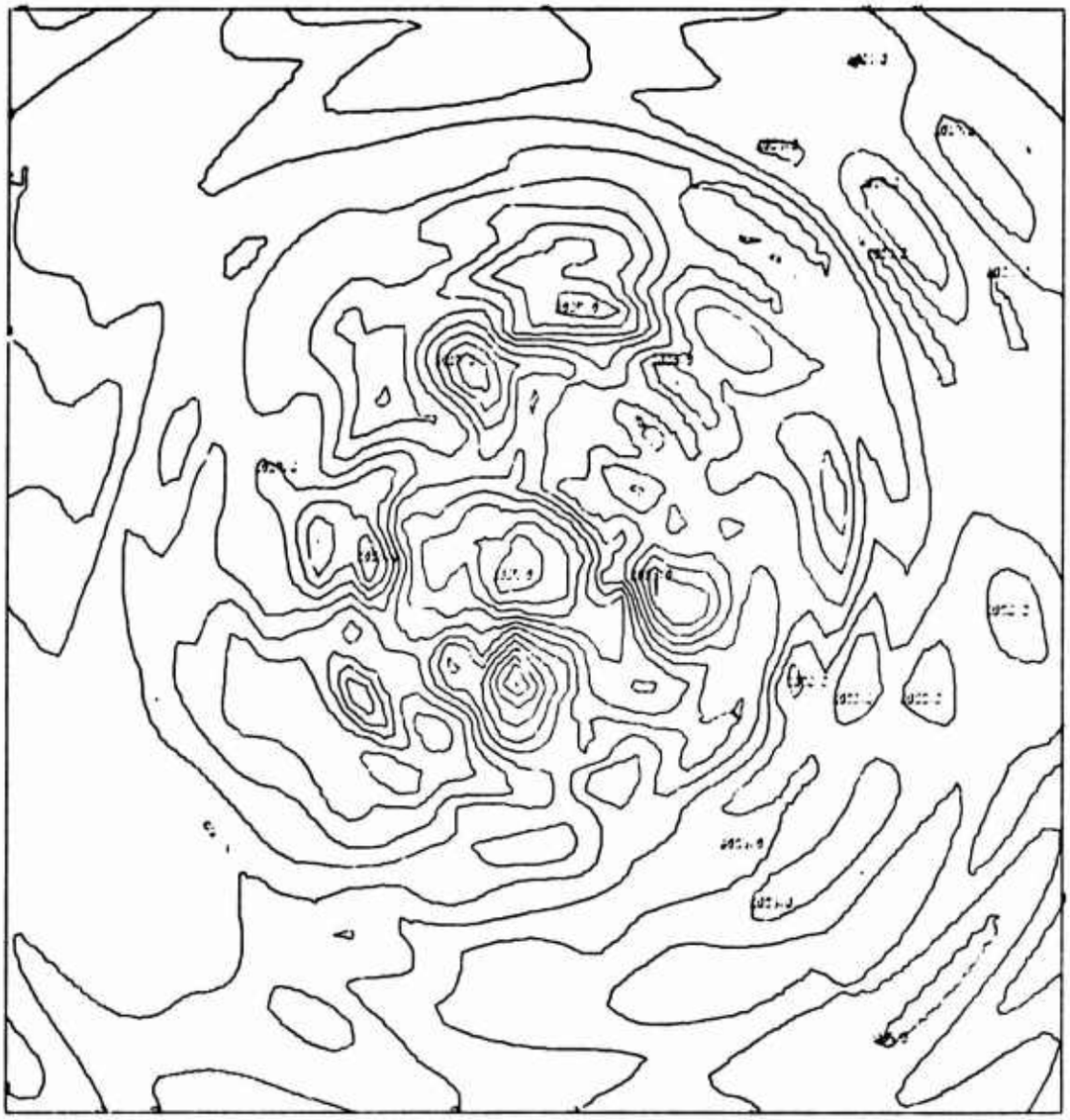

CHART X. 12-Hour Surface Pressure Forecast Without Terrain Using Sigma Surface Initialized Winds (Experiment V)

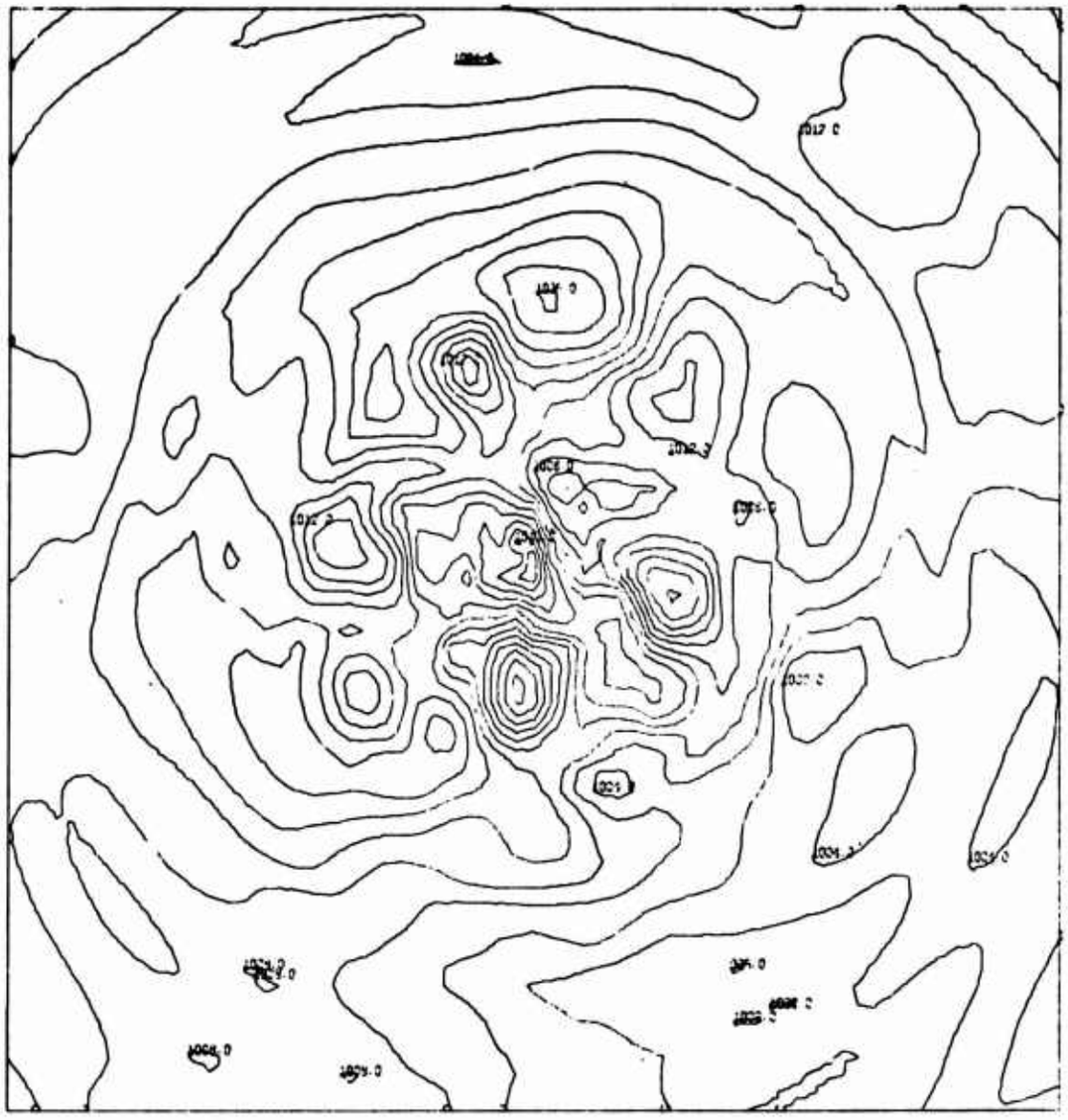

CHART Y. 12-Hour Surface Pressure Forecast Without Terrain Using Pressure Surface Initialized Winds (Experiment V)

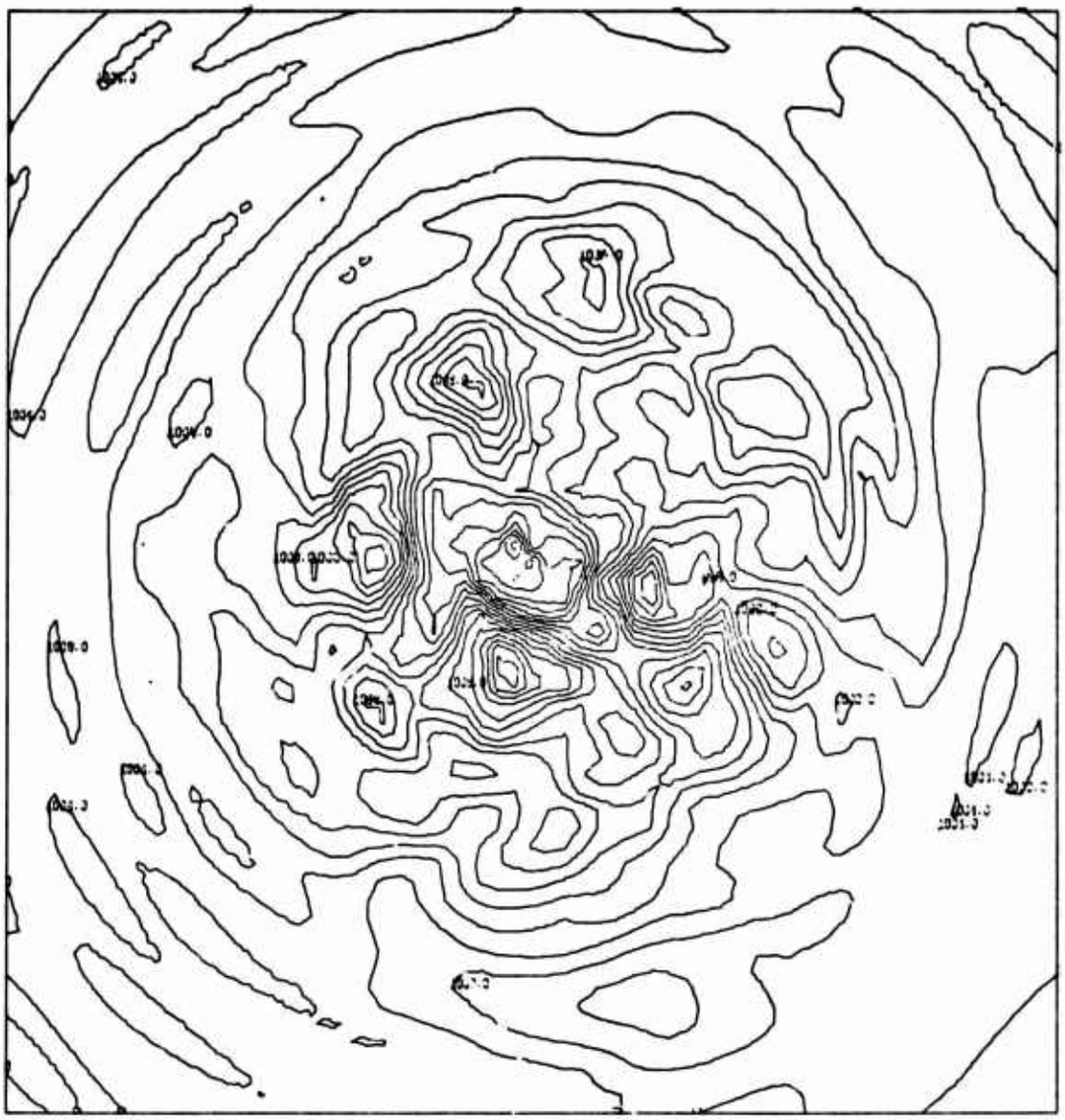

CHART Z. 72-Hour Surface Pressure Forecast Without Terrain Using Sigma Surface Initialized Winds (Experiment V)

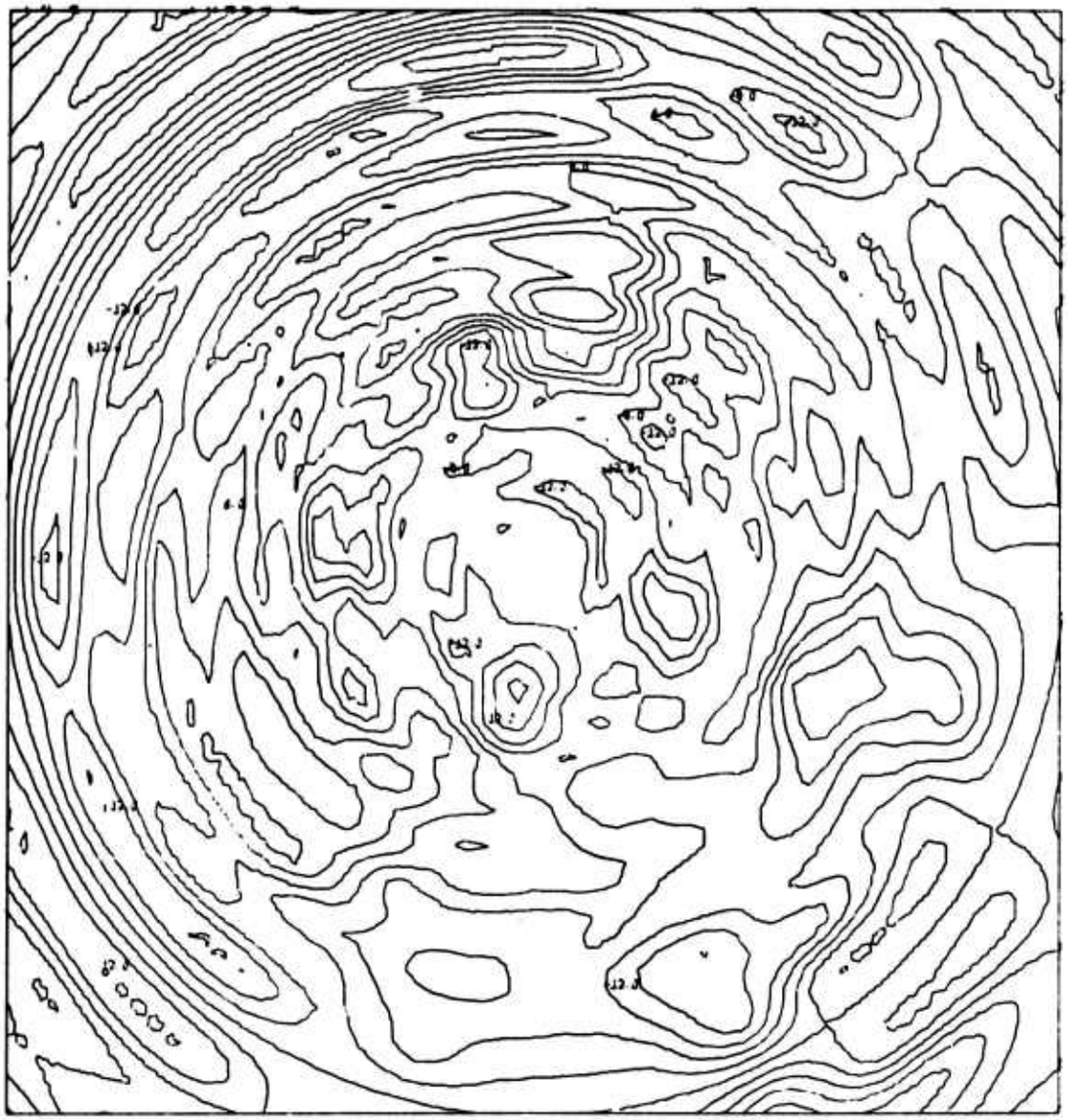

CHART AA. .9 Sigma Level Initial Guess Stream Function Field (Experiment VI)

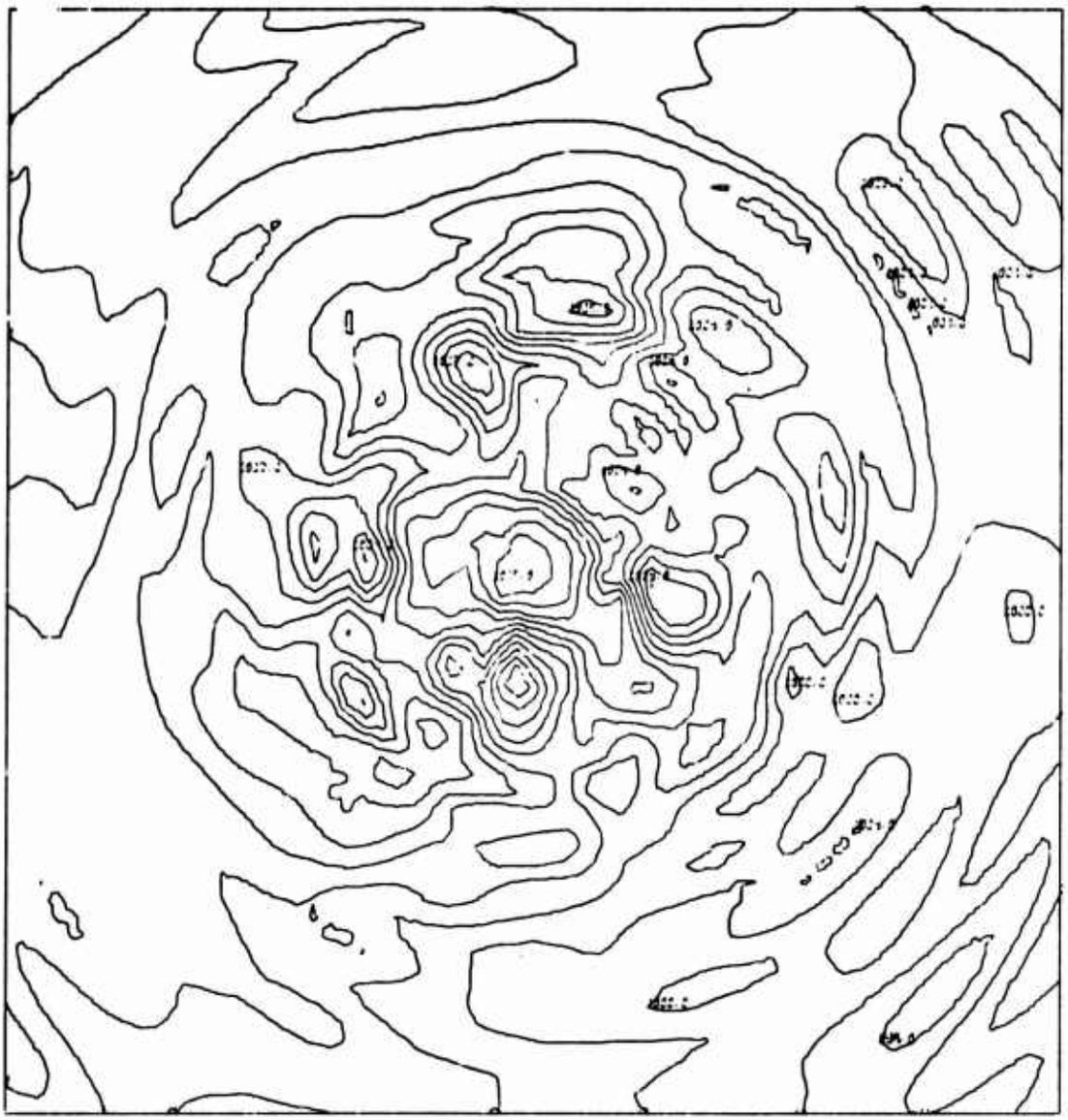

CHART BB. 12-Hour Surface Pressure Forecast Without Terrain Using Sigma Surface Initialized Winds VT 15 Z 10 May 73 (Experiment VI)

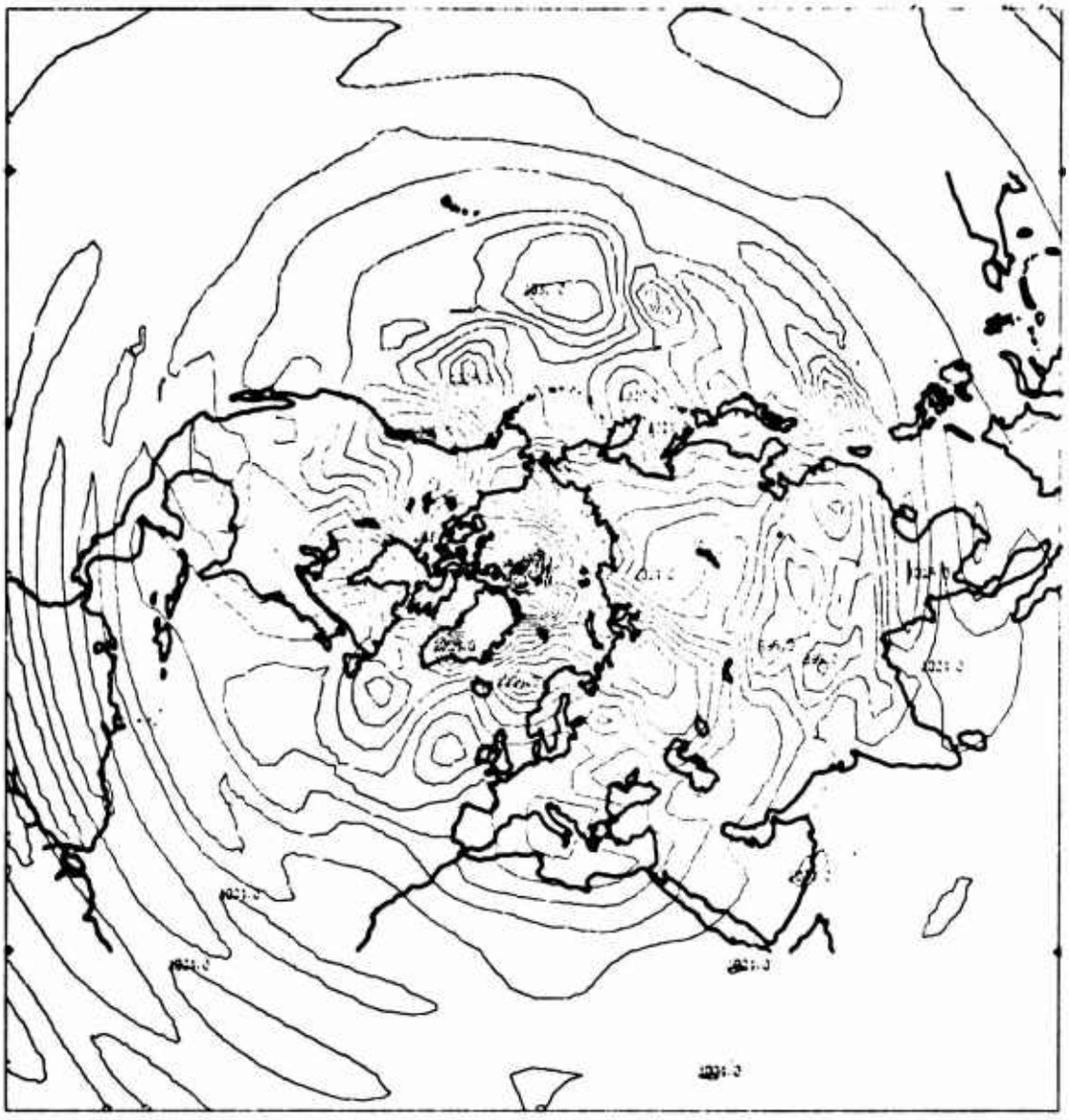

CHART CC. 72-Hour Surface Pressure Forecast
VT 12 Z 13 May 73 (Experiment VIII)

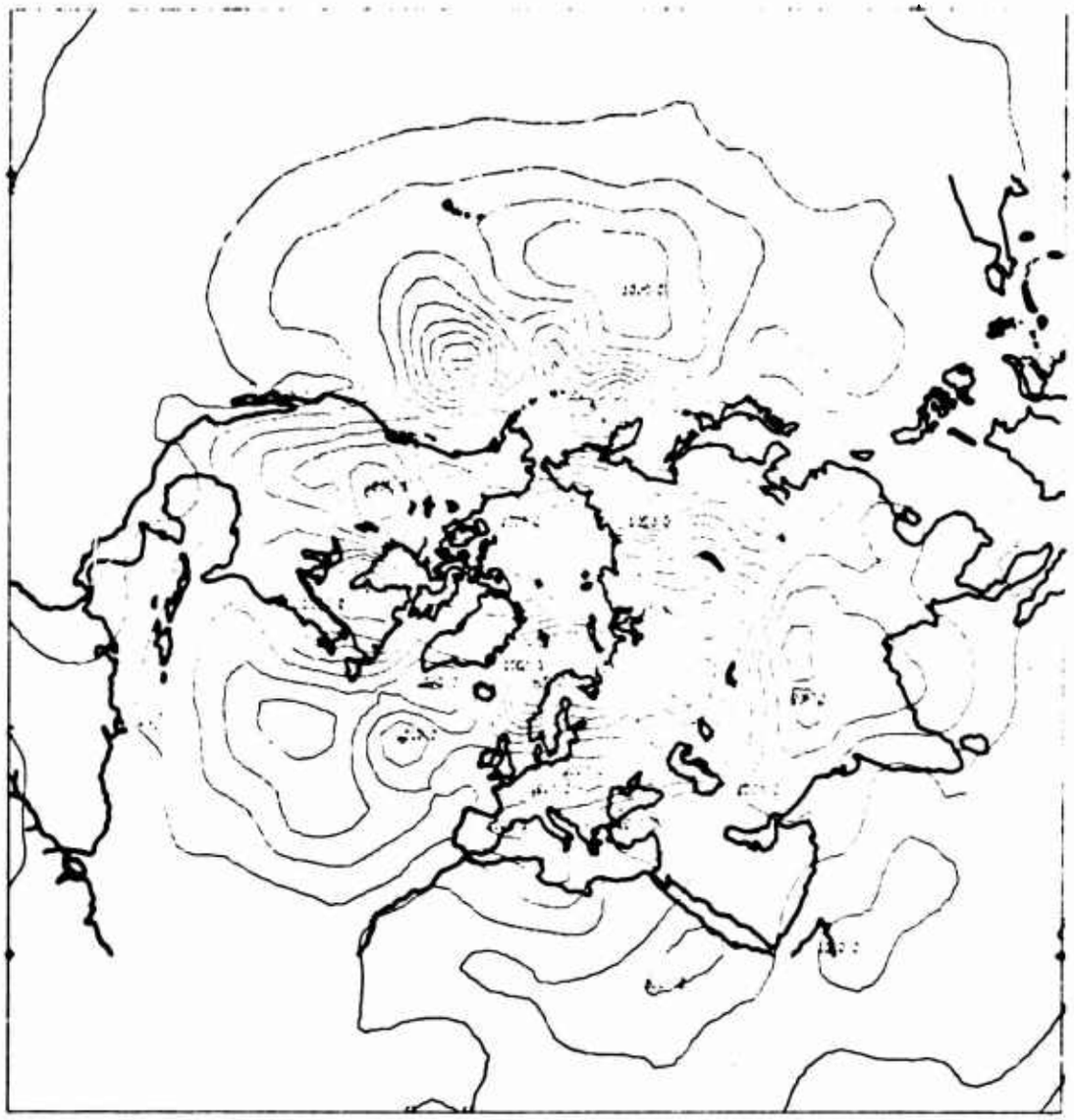

CHART DD. FNWC Objective Surface Pressure Analysis
12 Z 13 May 73 (Experiment VIII)

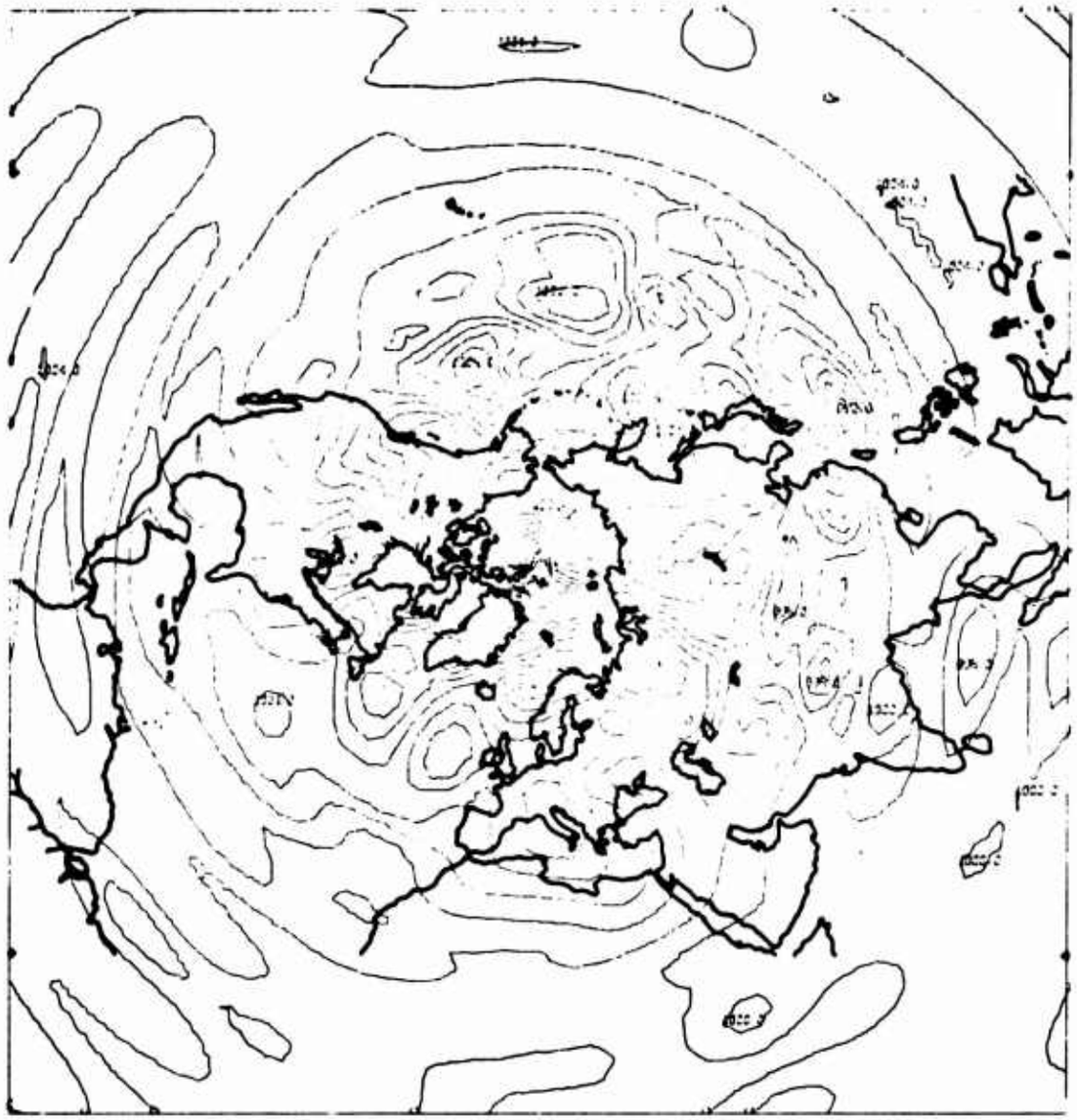

CHART EE. 84-Hour Surface Pressure Forecast
VT 00 Z 14 May 73 (Experiment VIII)

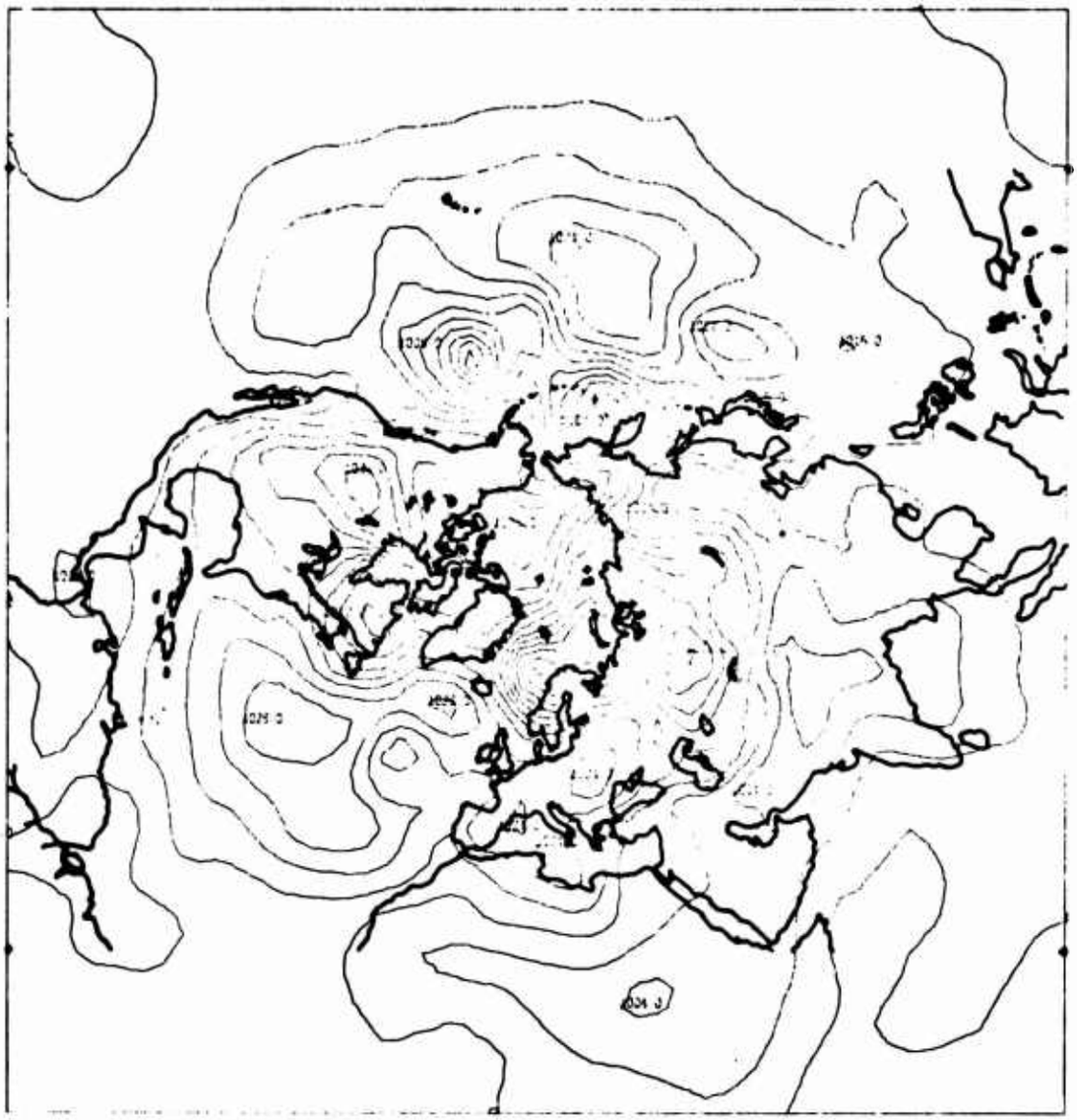

CHART FF. FNWC Objective Surface Pressure Analysis
00 Z 14 May 73 (Experiment VIII)

APPENDIX A

SIGMA COORDINATE - LINEAR BALANCE EQUATION IN FINITE DIFFERENCE FORM

$$\nabla^2\psi + \frac{\nabla\psi\cdot\nabla f}{f} = \frac{\pi\nabla^2\phi}{f} + \frac{\nabla\pi\cdot\nabla\phi}{f} + \frac{R}{f}\ (T\nabla^2\pi + \nabla T\cdot\nabla\pi)$$

(1) (2) (3) (4) (5) (6)

(1) $$\nabla^2\psi = (\psi_{ij+1} - 2\psi_{ij} + \psi_{ij-1}) - B_j(\psi_{ij+1} - \psi_{ij-1}) + A_j(\psi_{i+ij} - 2\psi_{ij} + \psi_{i-ij})$$

(2) $$\frac{\nabla\psi\nabla f}{f} = \frac{.25}{f_j}(f_{j+1} - f_{j-1})(\psi_{ij+1} - \psi_{ij-1})$$

(3) $$\frac{\pi\nabla^2\phi}{f} = \frac{\pi_{ij}}{f_j}[(\phi_{ij+1} - 2\phi_{ij} + \phi_{ij-1}) - B_j(\phi_{ij+1} - \phi_{ij-1}) + A_j(\phi_{i+ij} - 2\phi_{ij} + \phi_{i-ij})]$$

(4) $$\frac{\nabla\pi\cdot\nabla\phi}{f} = \frac{.25}{f_j}[(\pi_{ij+1} - \pi_{ij-1})(\phi_{ij+1} - \phi_{ij-1}) + A_j(\pi_{i+ij} - \pi_{i-ij})(\phi_{i+ij} - \phi_{i-ij})]$$

(5) $$\frac{R}{f}T\nabla^2\pi = \frac{RT_{ij}}{f_j}[(\pi_{ij+1} - 2\pi_{ij} + \pi_{ij-1}) - B_j(\pi_{ij+1} - \pi_{ij-1}) + A_j(\pi_{i+ij} - 2\pi_{ij} + \pi_{i-ij})]$$

$$(6)\qquad \frac{R}{\bar{T}}\,\nabla T\cdot\nabla\pi = \frac{.25R}{f_j}\left[(T_{ij+1} - T_{ij-1})(\pi_{ij+1} - \pi_{ij-1}) + A_j(T_{i+ij} - T_{i-ij})(\pi_{i+ij} - \pi_{i-ij})\right]$$

$$A_j = \frac{1}{\cos^2\theta} \qquad B_j = \frac{\Delta\theta \tan\theta}{2} \qquad F_j = 2\Omega \sin\theta$$

```
      SUBROUTINE BALSIG (PI,PHI,T,U,V,SI,FORCE,PIW,FORNEW)
      COMMON/H/ LEVEL
      DIMENSION PI(36,35),PHI(36,35),T(36,35),U(36,35),V(36,35)
      DIMENSION SI(36,35),FORCE(36,35),PIW(36,35),FORNEW(36,35)
      DIMENSION A(35),F(35),          DELTX(35),          B(35)
      DIMENSION IP(36),IM(36),IADD(36)
      DIMENSION AB(36,35)
      DIMENSION TITLE(24),R(5),FG(72,36),FL(63,63)
      DIMENSION FLD(3989)
      DIMENSION IPAR(3)
      EQUIVALENCE(FLD(21),FL(1,1))
      DATA IP
     1/2,3,4,5,6,7,8,9,10,11,12,13,14,15,16,17,18,19,20,21,22,23,24,25,
     226,27,28,29,30,31,32,33,34,35,36,1/
      DATA IM
     1/36,1,2,3,4,5,6,7,8,9,10,11,12,13,14,15,16,17,18,19,20,21,22,23,24
     2,25,26,27,28,29,30,31,32,33,34,35/
      DATA IADD
     1/19,20,21,22,23,24,25,26,27,28,29,30,31,32,33,34,35,36,1,2,3,4,5,6
     2,7,8,9,10,11,12,13,14,15,16,17,18/
C
C     SET UP CONSTANTS
      RD = 287.0
      RADIUS = 6.375E06
      OMEGA2 = 14.584E-05
      NI = 36
      NJ = 35
      NJM1 = NJ - 1
      NJM2 = NJ - 2
      ANGRAD = .01745329
      FBAR = OMEGA2 * SIN(40.0 * ANGRAD)
      FBARR = FBAR
      G = 9.81
      ALAT = 360.0/ FLOAT(NI)
      ALON = 360.0/ FLOAT(NJ+1)
      DELTY = (RADIUS*ALON*ANGRAD)
      SOR = 1.5
      R(1)=.1E09
      R(2)=.1E09
      R(3)=.1E10
      R(4)=.1E10
      R(5)=.1E10
C
CC    LEVEL IS SET IN MAIN AT 0. RESIDUAL VECTOR IS .9 TO .1 SIGMA SURFACES.
C
      LEVEL = LEVEL +1
      EPSILO = R(LEVEL)
C
```

```
C       A(J) = 1.0 /(COS(LAT))**2
C
        DO 10 J = 1,NJ
        A(J) = 1.0/(COS((-90.0 + J*5.0)*ANGRAD)) **2
   10 CONTINUE
C
CC      F(J) IS MODIFIED CORIOLIS PARAMETER
CCC
CCC     B(J) = DELTA LAT * TAN (LAT) / 2.0
C
        DO 20 JJ = 1,17
        J = NJ +1 - JJ
        ANG = -90.0 + J * 5.0
        S = SIN(ANG * ANGRAD)
        F(J) = OMEGA2 * S
        F(JJ) = - F(J)
        B(J)=.5*ALAT*TAN(ANG*ANGRAD)*ANGRAD
        B(JJ) = -B(J)
        DELTX(J) = DELTY*(COS((-90.0+5.0*J)*ANGRAD))
        DELTX(JJ) = DELTX(J)
   20 CONTINUE
        J=18
        B(J) = 0.0
        DELTX(J) = DELTY
        F(21)=F(22)
        F(20)=F(22)
        F(19)=F(22)
        F(18)=F(22)
        F(17)=F(14)
        F(16)=F(14)
        F(15)=F(14)
C
CC      AVERAGE PHI OVER GLOBE - COMPUTE DEVIATION PHI FIELD.
C
        PHIGLO = 0.
        DO 11 J=1,35
        DO 11 I=1,36
        PHIGLO = PHIGLO + PHI(I,J)
   11 CONTINUE
        PHIGLO = PHIGLO / 1260.
        DO 12 J = 1,35
        DO 12 I = 1,36
        PHI(I,J) = PHI(I,J) - PHIGLO
   12 CONTINUE
        CALL GRIDOU(PHI,FG)
        CALL LONGOU(FG,FL)
        CALL WRMSTX(FLD,IPAR)
        J = 1
```

```
      PIJM = 0.0
      PHIJM = 0.0
      TJM = 0.0
      DO 100 I =1,NI
   60 PIJM = PIJM +PI(I,J)/ FLOAT(NI)
   80 PHIJM = PHIJM + PHI(I,J)/ FLOAT(NI)
  100 TJM = TJM + T(I,J) / FLOAT(NI)
      J = NJ
      PHIJP = 0.0
      PIJP = 0.0
      TJP = 0.0
      DO 110 I =1,NI
   70 PIJP = PIJP + PI(I,J)/ FLOAT(NI)
   90 PHIJP = PHIJP + PHI(I,J)/ FLOAT(NI)
  110 TJP = TJP + T(I,J)/ FLOAT(NI)
C
CCC   CALCULATE PI AT THE WIND POINTS.
C
      DO 85 J= 3,NJM2,2
      JP1 = J + 1
      JM1 = J -1
      DO 86 I =1,NI
      IM1 = IM(I)
      PIW(I,J) = (PI(I,J)+PI(IM1,JP1)+PI(IM1,J)+PI(IM1,JM1))/4.0
   86 CONTINUE
   85 CONTINUE
      DO 87 J = 2,NJM1,2
      JP1 = J + 1
      JM1 = J - 1
      DO 88 I=1,NI
      IM1 = IM(I)
      PIW(I,J) = (PI(I,J)+PI(I,JP1)+PI(IM1,J)+PI(I,JM1))/ 4.0
   88 CONTINUE
   87 CONTINUE
      J=1
      JP1 = J+1
      DO 89 I = 1,NI
      IM1 = IM(I)
      PIW(I,J) = (PI(I,J)+PI(IM1,JP1)+PI(IM1,J)+PIJM) / 4.0
   89 CONTINUE
      J = NJ
      JM1 = J - 1
      DO 91 I = 1,NI
      PIW(I,J) = (PI(I,J)+PIJP+PI(IM1,J)+PI(IM1,JM1)) / 4.0
   91 CONTINUE
C
CCC   INITIALIZE PSI FIELD
C
```

```
      DO 30 J = 1,NJ
      FBARR = F(J)
      DO 40 I = 1,NI
      SI(I,J) = (PHI(I,J)/FBARR) * PI(I,J)
   40 CONTINUE
   30 CONTINUE
      CALL GRIDOU(SI,FG)
      CALL LONGOU(FG,FL)
      CALL WRMSTX(FLD,IPAR)
      SIJM = 0.0
      SIJP = 0.0
      GRADS = 0.
      GRADN = 0.
      DO 19 I= 1,NI
      GRADS = GRADS + (SI(I,1) - SI(I,3))
      GRADN = GRADN + (SI(I,35) - SI(I,33))
      SIJM = SIJM + SI(I,1) / 36.0
   19 SIJP = SIJP + SI(I,35)/ 36.0
      SIJM = SIJM + (GRADS/36.0)
      SIJP = SIJP + (GRADN/36.0)
C
C     CALCULATE FORCING FUNCTION - PHI PART
C
      DO 101 J = 3,NJM2
      FBAR=F(J)
      JM1 = J-2
      JP1 = J+2
      DO 111 I = 1,NI
      IM1 = IM(I)
      IP1 = IP(I)
      AB3 =PI(I,J)*(A(J)*(PHI(IM1,J)-2.0*PHI(I,J)+PHI(IP1,J))
     2                  +(PHI(I,JM1)-2.0*PHI(I,J)+PHI(I,JP1))
     2                  -(B(J)*(PHI(I,JP1)-PHI(I,JM1))))
      AB4 = .25*(A(J)*(PI(IP1,J)-PI(IM1,J))*(PHI(IP1,J)-PHI(IM1,J))
     2                 +(PI(I,JP1)-PI(I,JM1))*(PHI(I,JP1)-PHI(I,JM1)))
      AB5 =T(I,J)*(A(J)*(PI(IM1,J)-2.0*PI(I,J)+PI(IP1,J))
     2                  +(PI (I,JM1)-2.0*PI(I,J)+PI(I,JP1))
     2                  -(B(J)*(PI (I,JP1)-PI (I,JM1))))
      AB5 = AB5 * RD
      AB6 = .25*(A(J)*(T(IP1,J)-T(IM1,J))*(PI(IP1,J)-PI(IM1,J))
     2                +(T(I,JP1)-T(I,JM1))*(PI(I,JP1)-PI(I,JM1)))
      AB6 = AB6 * RD
      FORCE(I,J) =(AB3 + AB4 + AB5 + AB6)/FBAR
  111 CONTINUE
  101 CONTINUE
      J=2
      JP1 = J+2
      FBAR=F(J)
```

```
      DO 120 I=1,NI
      IM1 = IM(I)
      IP1 = IP(I)
      AB3 = PI(I,J)*(A(J)*(PHI(IM1,J)-2.0*PHI(I,J)+PHI(IP1,J))
     2                  +(PHIJM          -2.0*PHI(I,J)+PHI(I,JP1))
     2                   -(B(J)*(PHI(I,JP1)-PHIJM)))
      AB4 = .25*(A(J)*(PI(IP1,J)-PI(IM1,J))*(PHI(IP1,J)-PHI(IM1,J))
     2          +(PI(I,JP1)-PIJM     )*(PHI(I,JP1)-PHIJM      ))
      AB5 = T(I,J)*(A(J)*(PI(IM1,J)-2.0*PI(I,J)+PI(IP1,J))
     2                  +(PIJM     -2.0*PI(I,J)+PI(I,JP1))
     2                   -(B(J)*(PI (I,JP1)-PIJM )))
      AB5 = AB5 * RD
      AB6 = .25*(A(J)*(T(IP1,J)-T(IM1,J))*(PI(IP1,J)-PI(IM1,J))
     2          +(T(I,JP1)-TJM      )*(PI(I,JP1)-PIJM     ))
      AB6 = AB6 * RD
      FORCE(I,J) =(AB3 + AB4 + AB5 + AB6)/FBAR
  120 CONTINUE
      J =NJM1
      FBAR=F(J)
      JM1 = J - 2
      DO 130 I = 1,NI
      IM1 = IM(I)
      IP1 = IP(I)
      AB3 = PI(I,J)*(A(J)*(PHI(IM1,J)-2.0*PHI(I,J)+PHI(IP1,J))
     2                   +(PHI(I,JM1)-2.0*PHI(I,J) + PHIJP )
     2                   -(B(J)*(PHIJP-PHI(I,JM1))))
      AB4 = .25*(A(J)*(PI(IP1,J)-PI(IM1,J))*(PHI(IP1,J)-PHI(IM1,J))
     2          +(PIJP     -PI(I,JM1))*(PHIJP     -PHI(I,JM1)))
      AB5 = T(I,J)*(A(J)*(PI(IM1,J)-2.0*PI(I,J)+PI(IP1,J))
     2                   +(PI(I,JM1)-2.0*PI(I,J) + PIJP )
     2                   -(B(J)*(PIJP-PI(I,JM1))))
      AB5 = AB5 * RD
      AB6 = .25*(A(J)*(T(IP1,J)-T(IM1,J))*(PI(IP1,J)-PI(IM1,J))
     2          +(TJP     -T(I,JM1))*(PIJP     -PI(I,JM1)))
      AB6 = AB6 * RD
      FORCE(I,J) =(AB3 + AB4 + AB5 + AB6)/FBAR
  130 CONTINUE
      J = 1
      FBAR=F(J)
      JP1 = J + 2
      DO 300 I = 1,NI
      IM1 = IM(I)
      IP1 = IP(I)
      IJM = IADD(I)
      AB3 = PI(I,J) * (A(J)*(PHI(IM1,J)-2.0*PHI(I,J)+PHI(IP1,J))
     2                   +(PHI(IJM,J)-2.0*PHI(I,J)+PHI(I,JP1))
     2                   -(B(J)*(PHI(I,JP1)-PHI(IJM,J))))
      AB4 = .25*(A(J)*(PI(IP1,J)-PI(IM1,J))*(PHI(IP1,J)-PHI(IM1,J))
```

```
     2                    +(PI(I,JP1)-PI(IJM,J))*(PHI(I,JP1)-PHI(IJM,J)))
      AB5 = T(I,J)*(A(J)*(PI(IM1,J)-2.0*PI(I,J)+PI(IP1,J))
     2                    +(PI(IJM,J)-2.0*PI(I,J)+PI(I,JP1))
     2                    -(B(J)*(PI(I,JP1)-PI(IJM,J))))
      AB5 = AB5 * RD
      AB6 = .25*(A(J)*(T(IP1,J)-T(IM1,J))*(PI(IP1,J)-PI(IM1,J))
     2                    +(T(I,JP1)-T(IJM,J))*(PI(I,JP1)-PI(IJM,J)))
      AB6 = AB6 * RD
      FORCE(I,J) =(AB3 + AB4 + AB5 + AB6)/FBAR
  300 CONTINUE
      J = NJ
      FBAR=F(J)
      JM1 = J - 2
      DO 310 I = 1,NI
      IM1 = IM(I)
      IP1 = IP(I)
      IJP = IADD(I)
      AB3 = PI(I,J)*(A(J)*(PHI(IM1,J)-2.0*PHI(I,J)+PHI(IP1,J)
     2                    +(PHI(I,JM1)-2.0*PHI(I,J)+PHI(IJP,J))
     2                    -(B(J)*(PHI(IJP,J)-PHI(I,JM1))))
      AB4 = .25*(A(J)*(PI(IP1,J)-PI(IM1,J))*(PHI(IP1,J)-PHI(IM1,J))
     2                    +(PI(IJP,J)-PI(I,JM1))*(PHI(IJP,J)-PHI(I,JM1)))
      AB5 = T(I,J)*(A(J)*(PI(IM1,J)-2.0*PI(I,J)+PI(IP1,J))
     2                    +(PI(I,JM1)-2.0*PI(I,J)+PI(IJP,J))
     2                    -(B(J)*(PI(IJP,J)-PI(I,JM1))))
      AB5 = AB5 * RD
      AB6 = .25*(A(J)*(T(IP1,J)-T(IM1,J))*(PI(IP1,J)-PI(IM1,J))
     2                    +(T(IJP,J)-T(I,JM1))*(PI(IJP,J)-PI(I,JM1)))
      AB6 = AB6 * RD
      FORCE(I,J) =(AB3 + AB4 + AB5 + AB6)/FBAR
  310 CONTINUE
C
CC    CALCULATE FORCING FUNCTION - PSI PART
C
 1111 KPASS = 0
      DO 201 J=3,NJM2
      FBAR=F(J)
      JM1=J-2
      JP1=J+2
      DO 211 I=1,NI
      IM1=IM(I)
      IP1=IP(I)
      AB2=.25*(F(JP1)-F(JM1))*(SI(I,JP1)-SI(I,JM1))/FBAR
      FORNEW(I,J)= FORCE(I,J) - AB2
  211 CONTINUE
  201 CONTINUE
      J=2
      FBAR=F(J)
```

```
      JP1=J+2
      DO 220 I=1,NI
      IM1=IM(I)
      IP1=IP(I)
      AB2=.25*(F(JP1)+OMEGA2)*(SI(I,JP1)-SIJM)/FBAR
      FORNEW(I,J) = FORCE(I,J) - AB2
  220 CONTINUE
      J=NJM1
      FBAR=F(J)
      JM1=J-2
      DO 230 I=1,NI
      IM1=IM(I)
      IP1=IP(I)
      AB2=.25*(OMEGA2-F(JM1))*(SIJP-SI(I,JM1))/FBAR
      FORNEW(I,J) = FORCE(I,J) - AB2
  230 CONTINUE
      J=1
      FBAR=F(J)
      JP1=J+2
      DO 400 I=1,NI
      IM1=IM(I)
      IP1=IP(I)
      IJM=IADD(I)
      AB2=.25*(F(JP1) - F( J ))* (SI(I,JP1)-SI(IJM,J))/FBAR
      FORNEW(I,J) = FORCE(I,J) - AB2
  400 CONTINUE
      J=NJ
      FBAR=F(J)
      JM1 = J-2
      DO 410 I=1,NI
      IM1=IM(I)
      IP1=IP(I)
      IJP=IADD(I)
      AB2=.25*(F( J )-F(JM1))*(SI(IJP,J)-SI(I,JM1))/FBAR
      FORNEW(I,J) = FORCE(I,J) - AB2
  410 CONTINUE
C
CC    RELAX TO PSI
C
      SIJP = 0.0
      GRAD = 0.0
      DO 424 I=1,NI
      GRAD = GRAD + (SI(I,35) -SI(I,33))
      SIJP=SIJP + SI(I,35)/36.0
  424 CONTINUE
      SIJP = SIJP + (GRAD/36.0)
      SIJM=0.0
      DO 426 I=1,NI
```

```
      GRAD = GRAD + (SI(I,1) - SI(I,3))
      SIJM=SIJM+SI(I,1)/36.0
  426 CONTINUE
      SIJM = SIJM + (GRAD/36.0)
 1112 KOUNT = 0
      DO 420 J=3,17
      JP1 = J + 2
      JM1 = J - 2
      DO 421 I = 1,NI
      IM1 = IM(I)
      IP1 = IP(I)
      AB1 =       (A(J)*(SI(IM1,J) - 2.0*SI(I,J) + SI(IP1,J)))
     2                    +(SI(I,JM1)-2.0*SI(I,J) + SI(I,JP1))
     3                    -(B(J)*(SI(I,JP1)-SI(I,JM1)))
      AB(I,J)=AB1
      RESIDU = AB1 - FORNEW(I,J)
      RESID = ABS(RESIDU)
      IF (RESID.GT.EPSILO) KOUNT = KOUNT + 1
      CORREC = RESIDU / (2. + 2. * A (J))
      SI(I,J) = SI(I,J) + SOR * CORREC
  421 CONTINUE
  420 CONTINUE
CC
      EQUATOR VALUE IS AVERAGE OF 5 S AND 5 N PSI VALUES.
C
      J=18
      JP1=J+1
      JM1=J-1
      DO 1422 I = 1,36
      IP1=I
      IM1=IM(I)
      SI(I,J) = ( SI(IP1,JP1) + SI(IP1,JM1)
     2          + SI(IM1,JP1) + SI(IM1,JM1))/4.0
 1422 CONTINUE
      DO 1423 J=19,33
      JP1 = J + 2
      JM1 = J - 2
      DO 1424 I=1,36
      IM1 = IM(I)
      IP1 = IP(I)
      AB1 =       (A(J)*(SI(IM1,J) - 2.0*SI(I,J) + SI(IP1,J)))
     2                    +(SI(I,JM1)-2.0*SI(I,J) + SI(I,JP1))
     3                    -(B(J)*(SI(I,JP1)-SI(I,JM1)))
      AB(I,J)=AB1
      RESIDU = AB1 - FORNEW(I,J)
      RESID = ABS(RESIDU)
      IF (RESID.GT.EPSILO) KOUNT = KOUNT + 1
      CORREC = RESIDU / (2. + 2. * A (J))
```

```
      SI(I,J) = SI(I,J) + SOR * CORREC
 1424 CONTINUE
 1423 CONTINUE
      IF (KOUNT.EQ.0) GO TO 1113
      KPASS = KPASS + 1
      PRINT 450,KPASS,KOUNT
  450 FORMAT (' PASS ',I4,'     CORRECTIONS ',I4)
      IF(KPASS.EQ.200) GO TO 1111
      GO TO 1112
 1113 PRINT 450,KPASS,KOUNT
      IF (KPASS.EQ.0) GO TO 1115
      GO TO 1111
 1115 CONTINUE
 5000 FORMAT (' ',13E10.3)
      CALL GRIDOU(SI,FG)
      CALL LONGOU(FG,FL)
      CALL WRMSTX(FLD,IPAR)
      DO 27 J = 2,NJM1,2
      JP1 = J + 1
      JM1 = J - 1
      DO 28 I = 1,NI
      IP1 = IP(I)
      IM1 = IM(I)
      U(I,J) = -(SI(I,JP1) - SI(I,JM1)) / DELTY
      V(I,J) = (SI(I,J) - SI(IM1,J)) / DELTX(J)
   28 CONTINUE
   27 CONTINUE
      DO 32 J=3,NJM2,2
      JP1=J+1
      JM1=J-1
      DO 33 I=1,NI
      IP1=IP(I)
      IM1=IM(I)
      U(I,J) = -(SI(IP1,JP1)-SI(I,JM1))/DELTY
      V(I,J) = (SI(I,J)-SI(IM1,J))/DELTX(J)
   33 CONTINUE
   32 CONTINUE
      J = 1
      JP1 = J + 1
      DO 51 I = 1,NI
      IP1 = IP(I)
      IM1 = IM(I)
      U(I,J) =-(SI(IM1,JP1)-SIJM)/DELTY
      V(I,J) =  (SI(I,J)-SI(IM1,J))/DELTX(J)
   51 CONTINUE
      J = NJ
      JM1 = J - 1
      DO 52 I = 1,NI
```

```
      IP1 = IP(I)
      IM1 = IM(I)
      U(I,J) = -(SIJP - SI(IM1,JM1))/DELTY
      V(I,J) =  (SI(I,J)-SI(IM1,J)) / DELTX(J)
   52 CONTINUE
      DO 29 J = 1,NJ
      DO 31 I = 1,NI
      PIA = 1.0/ PIW(I,J)
      U(I,J) = PIA * U(I,J)
      V(I,J) = PIA * V(I,J)
   31 CONTINUE
   29 CONTINUE
      CALL GRIDOU(U,FG)
      CALL LONGOU(FG,FL)
      CALL WRMSTX(FLD,IPAR)
      CALL GRIDOU(V,FG)
      CALL LONGOU(FG,FL)
      CALL WRMSTX(FLD,IPAR)
      RETURN
      END
```

LIST OF REFERENCES

1. Arakawa, Akio, Katayama, Akira, and Mintz, "Numerical Simulation of the General Circulation of the Atmosphere," Proceedings of the WMO/IUGG Symposium on Numerical Weather Prediction, Tokyo, Japan, November 26 - December 4, 1968, Japan Meteorological Agency Tokyo, Mar. 1969, pp. IV-1 - IV-14.

2. Elias, T. E., Numerical Experiments with a Five-Level Global Atmospheric Prediction Model Using a Staggered, Spherical, Sigma Coordinate System, Master's Thesis, Naval Postgraduate School, Monterey, California, 1973.

3. Gates et al., A Documentation of the Mintz-Arakawa Two-Level Atmospheric General Circulation Model, RAND Corporation, December, 1971.

4. Institute of Meteorology Report DM-10, On Initialization for Models Using Sigma As Vertical Coordinate, by H. Sundquist, pp. 15, October 1973.

5. Kesel and Winninghoff, "The Fleet Numerical Weather Central Operational Primitive-Equation Model," Mon. Wea. Rev., V. 100, No. 5, p. 360-373, 1972.

6. Mihok, W.F., Fourth-Order Differencing in a Five-Layer Spherical Sigma Coordinate Global Weather Prediction Model, Master's Thesis, Naval Postgraduate School, Monterey, California, 1974.

7. Naval Postgraduate School Report NPS-51Wu71081A, Restorative-Iterative Initialization for a Global Prediction Model, by F. J. Winninghoff, September, 1971.

8. Robert, Andre, "The Behavior of Planetary Waves in an Atmospheric Model Based on Spherical Harmonics," Publication in Meteorology No. 77, Clearinghouse for Federal Scientific and Technical Information (CFSTI), Springfield, Va., June 1965, pp. 56-62.

9. Smagorinsky et al., "Numerical Results From a Nine-Level General Circulation Model of the Atmosphere," Monthly Weather Review, Vol. 93, No. 12, Dec. 1965, pp. 727-768.

10. Temperton, C., "Some Experiments in Dynamic Initialization for a Simple Primitive Equation Model," Quarterly Journal of the Royal Meteorological Society, v. 99, p. 303-319, April 1973.